Numerical Simulation and Customized DACM Based Design Optimization

A focus on performance improvement of micro cross-flow hydro turbine designs

by

Endashaw Tesfaye Woldemariam

Thesis submitted in fulfilment of
the requirements for the degree of
PHILOSOPHIAE DOCTOR
(PhD)

Faculty of Science and Technology
Department of Mechanical and Structural Engineering and Material Science
2018

University of Stavanger
NO-4036 Stavanger
NORWAY
www.uis.no

ISBN: 978-82-7644-762-0
ISSN: 1890-1387
PhD: Thesis UiS No. 386

Abstract

The diverse numerical modelling, analysis and simulation tools that have been developed and introduced to markets are intended to perform the virtual design and testing of products and systems without the construction of physical prototypes. Digital prototyping in the form of computer modelling and simulation are important means of numerical model predictions, i.e. design validation and verification. However, as the tools advance to more precise and diverse applications, the operation eventually becomes more complex, computationally expensive and error prone; this is particularly true for complex multi-disciplinary and multidimensional problems; for instance, in multi-body dynamics, Fluid-Structure Interaction (FSI) and high-dimensional numerical simulation problems. On the other hand, integrating design optimization operations into the product and system development processes, through the computer based applications, makes the process even more complex and highly expensive. This thesis analyses and discusses causes of complexity in numerical modelling, simulation and optimization operations and proposes new approaches/frameworks that would help significantly reduce the complexity and the associated computational costs. Proposed approaches mainly integrate, simplify and decompose or approximate complex numerical simulation based optimization problems into simpler, and to metamodel-based optimization problems.

Despite advancing computational technologies in continuum mechanics, the design and analysis tools have developed in separate directions with regard to ‘basis functions’ of the technologies until recent developments. Basis functions are the building blocks of every continuous function. Continuous functions in every computational tool are linear combinations of specific basis functions in the function space. Since first introduced, basis functions in the design and modelling tools have developed so rapidly that various complex physical problems can today be designed and modelled to the highest precision. On the other hand,

most analysis tools still utilize approximate models of the problems from the latter tools, particularly if the problem involves complex smooth geometric designs. The existing gap between the basis functions of the tools and the increasing precision of models for analysis introduce tremendous computational costs. Moreover, to transfer models from one form of basis function to another, additional effort is required. The variation of the basis functions also demands extra effort in numerical simulation based optimization processes. This thesis discusses the recently developed integrated modelling and analysis approach that utilizes the state-of-the-art basis function (NURBS function) for both design and analysis. A numerical simulation based shape optimization framework that utilizes the state-of-the-art basis function is also presented in a study in the thesis.

One of the common multidisciplinary problem that involves multiple models of domains in a single problem, fluid-structure interaction (FSI) problem, is studied in the thesis. As the name implies, the two models of domains involved in any FSI problems are fluid and structure domain models. In order to solve the FSI problems, usually three mathematical components are needed: namely, i) fluid dynamics model, ii) structural mechanics model and, iii) the FSI model. This thesis presents the challenges in FSI problems and discusses different FSI approaches in numerical analysis. A comparative analysis of computational methods, based on the coupling and temporal discretization schemes, is discussed using a benchmark problem, to give a better understanding of what a multidisciplinary problem is and the challenge for design optimizations that involve such problems.

Simplification and/or decomposition, approximation and replacing of complex models with simpler ones are some of the approaches to reduce the computational costs of various complex multidimensional and multidisciplinary computer-based problems. In the thesis a customized framework based on a known dimensional analysis conceptual modelling (DACM) framework is introduced. The latter is a conceptual

modelling and simulation tool in systems design. DACM is originally introduced to model various engineering problems. The well-known dimensional analysis (DA) theory, functional modelling and bond graph concepts are the bases of the framework. Moreover, the cause-effect relationships study between variables and functions in a problem is its fundamental process. Impact levels of variables are measured utilizing the concept of statistical Design of Experiment (DOE). Through customizing the DACM framework, a novel simplification and decomposition approach, which reduces the computational costs of complex optimization problems is introduced in this thesis. Apart from that, similar new optimization frameworks that utilize metamodelling approaches are developed and introduced. The metamodelling approach serves the optimization framework by either assisting to generate samples towards the optimum region or by approximating and completely replacing the original model. The proposed optimization frameworks are based on the later two separate metamodelling approaches. Moreover, another optimization framework without the metamodelling approaches is also introduced. The proposed frameworks and approaches are tested using case studies. The studies demonstrate that the results from the proposed optimization approaches outperform results from both the conventional approaches and the original models.

On the other hand, due to the dynamic rising in global population, the growing market economy and modernization, the global energy demand is increasing drastically. In fact, various studies project a large increase in global energy consumption in the coming decades. In order to meet this energy demand, a rise in production of alternative energy sources' is indispensable, which also has implications on global climate change. Among others, hydropower technology is one of the oldest and cheapest forms of renewable energy. Furthermore, in terms of current installed global renewable energy potential, hydropower constitutes the largest portion. However, more than half of the global hydropower potential has yet to be exploited. To best exploit the existing potential, in order to

satisfy the growing demand, utilizing efficient hydropower facilities is inevitable. Improving the performance of the critical parts of the facilities implies better performance of the facilities. In this thesis, case studies on performance optimization of micro cross-flow turbine designs, one of the critical components of hydropower facilities, are carried out deploying the proposed optimization approaches and frameworks. The micro- cross-flow turbine is one of the widely applied turbine designs in small and micro hydro facilities around the globe. The design is more compelling, particularly for run-of-the-river, off-grid applications in developing and less developed countries. Although the turbine design is flexible, relatively simple and less expensive compared to conventional turbines, the power generation efficiency of the turbine is not yet well optimized. The application results of the proposed optimization approaches and frameworks on the turbine designs are promising with regard to enhancing the performance as discussed in the thesis.

Keywords: Numerical Modelling and Simulation; Simulation-Based Design Optimization; Isogeometric Analysis; Customized DACM; NURBS Function; Shape Optimization; Micro Cross-Flow Turbine; Fluid-Structure Interaction

Acknowledgements

The research work in the thesis was carried out in the period from September 2014 to August 2017 in the Department of Mechanical and Structural Engineering and Materials Science at University of Stavanger. Part of the research work was conducted at Simon Frasor University in the Product Design and Optimization Laboratory, Surrey, Canada. The research work is fully financed and supported by the Norwegian Ministry of Education and the University of Stavanger. The support from both institutions is gratefully acknowledged.

First and foremost, I would like to express my greatest and deepest gratitude to my supervisor and my mentor Professor Hirpa G. Lemu for his limitless support and encouragement from the first day of my PhD period. His determination have kept me focused and motivated in the entire period. Beyond his scientific contributions to the research, his thoughtful and compassionate personality have made me to stay determined and to think bigger. Moreover, his simple characteristics and sense of humor in stressful situations have kept me feel at home while thousands of miles away from home. Thank you Professor!

I would also like to forward my deepest gratitude to Professor G. Gary Wang and his research team (particularly to Di Wu, Kambiz Haji Hajikolaei, and George Cheng) in the product design and optimization laboratory in Surrey, BC, Canada for their intellectual contributions and kind hospitality in the period of my research abroad stay. I also owe warmest gratitude to Professor Eric Coatanea, from Tampere Univesity of Technology, Tampere, Finland, for his valuable research contributions and friendly personality.

My deepest and special gratitude goes to my brothers and my sister-in-law, Semere (Kume), Leul and Eden. You have always kept your hearts wide open to me. You have special places in my heart especially Kumye and Leul. I am proud to have you as brothers and as best friends. You

have never let me down anytime I reached out to you looking for your advices or help. God bless you and your entire family! I would also like to thank my friend Jonny, my beautiful niece Delina and my mother-in-law Hirut, and Rahel for their warm welcoming and loving hospitality whenever I travel to their places for holidays. And I would like to thank all my brothers and sisters at home for their consistent encouragement and support. I love you all!

I would like to also extend my sincere regards to my department colleagues and friends, IKM employees, who showed their unwavering friendship and shared valuable ideas with since the beginning of the PhD period; especially Jithin Jose, Adekulne p. Armedo, Arvind Kapret, Adugna Deressa, Aboma Wagari and Ashish Aeren.

Last but not least, my deepest and unlimited gratitude goes to my parents (Ewaye and Aba). You crafted our journey in the best way one can imagine prioritizing our desires than yourselves. You have given us the best tools and lessons in life, you made us dream bigger regardless of what. Your limitless love and care, not just to us but to anyone who needs it, made us to stand still. Long live!

Praises to almighty God!

Table of Contents

Abstract ..... **i**

Acknowledgements ..... **v**

List of appended papers ..... **ix**

List of abbreviations ..... **xv**

Part I: Thesis Summary ..... **i**

1 Introduction **1**

1.1 General overview 1

1.2 Research objectives 5

1.3 Research gaps and questions 7

1.4 Limitations of the research 9

1.5 Thesis organization 10

2 Background review and state-of-the-art studies **11**

2.1 Finite element analysis vs. Isogeometric analysis 11

2.1.1 Non-uniform Rational B-spline function (NURBS) *12*

2.1.2 Knot refinement *14*

2.2 Fluid-Structure Interaction: Multi-discipline and high dimensionality 15

2.2.1 Introduction *15*

2.2.2 Computational and solution methods in FSI problems *15*

2.3 Customized DACM-based simplification and decomposition 17

2.4 Metamodelling in numerical simulation model approximation and design optimization 19

2.4.1 Introduction *19*

2.4.2 Metamodelling in optimization *20*

2.4.3 ANN metamodelling in optimization *22*

2.5 Case studies: Performance optimizations in two micro cross-flow hydro turbine designs 25

2.5.1 Introduction *25*

2.5.2 Hydropower *27*

2.5.3 Small- and micro-hydropower *30*

2.5.4 Cross-flow hydro turbine design 32

3 Research methodologies 37

3.1 General 37

3.2 Customized DACM based optimization framework 38

3.3 Metamodel assisted optimization (MMAO) framework 39

3.4 Direct GA-based optimization framework 41

3.5 Artificial Neural-Network Metamodel- GA-based optimization (ANN-MMBO) 42

4 Discussion of results 45

5 Concluding remarks and recommendations for future work 51

6 Scientific contributions 53

7 Summary of appended papers 55

References 69

Appendices 77

Appendix 1 – Design of experiment sample data 77

Part II: Appended Papers 87

List of appended papers

The thesis work is based on the following six appended papers. The papers are referred to in the thesis by the designated Roman numerals.

Paper I: Endashaw T. Woldemariam and Hirpa G. Lemu, (2015). "Nonlinear Isogeometric Analysis in Simulation Based Design Optimization: State-of-the-art analysis." *The 5th International Workshop of Advanced Manufacturing and Automation*, Shanghai, China, October 22-23, 2015; *WIT press*, ISBN: 978-1-78466-169-4

Paper II: Endashaw T. Woldemariam and Hirpa G. Lemu, (2016). "Comparative Analysis of Computational Methods in Fluid-Structure Interaction: Temporal discretization and coupling techniques." *The 6th International Workshop of Advanced Manufacturing and Automation*, Manchester, UK, November 10-11, 2016; *Atlantis press*, ISBN: 978-94-6252-243-5

Paper III: Endashaw T. Woldemariam, Eric Coatanea, G. Garry Wang, Hirpa G. Lemu and Di Wu, (2017). "Customized DACM Framework for Design Optimization (A Case Study on Cross-flow Micro Turbine Model)." *Journal of Engineering Optimization, Taylor & Francis publisher* (In review).

Paper IV: Endashaw T. Woldemariam, Hirpa G. Lemu and Gary G. Wang, (2017). "CFD-Driven Valve Shape Optimization for Performance Improvement of a Micro Cross-Flow Turbine." *Energies,* Vol. 11, 248; doi: 10.3390/en11010248

Paper V: Endashaw T. Woldemariam, Hirpa G. Lemu and G. Gary Wang, (2017). "Geometric Parameters' Effect Characterization and Design Optimization of a Micro Scale Cross-flow Turbine for an Improved Performance." *27th International Offshore and Polar Engineering Conference*, San Francisco, CA, June 25-30, 2017.

Paper VI: Endashaw T. Woldemariam and Hirpa G. Lemu, (2017). "Numerical Simulation Based Effect Characterization Study and Design Optimization of a Micro Cross-Flow Turbine to Improve its Performance". *Journal of Renewable Energy, Hindawi publisher* (In Review).

List of Figures

Figure 1.1 General Fluid-structure interaction domains representation..... 3
Figure 1.2. T15-300 micro cross-flow turbine design. 5
Figure 1.3. IAM micro cross-flow turbine design [3]..... 5
Figure 2.1 Steps in the customized DACM for simplification and decomposition of high-dimensional models 18
Figure 2.2. Metamodel utilizing optimization approaches (a) MMBO (b) MMAO..... 21
Figure 2.3. A feed-forward Artificial Neural Network architecture with multiple hidden layers..... 23
Figure 2.4. Flowchart of Artificial Neural Network metamodelling 24
Figure 2.5. Global energy consumption history and projection [37] 26
Figure 2.6. World energy consumption history and projection by energy sources [37]..... 26
Figure 2.7. Global total hydropower generation since 1980 [39] 28
Figure 2.8. Global share of renewable energy (%) [40]..... 31
Figure 2.9. Turbine efficiency curves for various small and micro hydro turbines [2] 33
Figure 2.10. Experimental setup for IAM turbine at NTNU [3]..... 34
Figure 2.11. Cross-flow turbine's rotor hydrodynamic details: (**a**) fluid jet trajectory and rotor's detail (**b**) velocity triangles at locations 1-4..... 35
Figure 3.1. Illustration of the research structure. 38
Figure 3.2. Two-stage optimization framework based on customized DACM framework 39
Figure 3.3. Metamodel assisted optimization frameworks: (a) utilize NURBS function; (b) direct-interface with ANSYS Workbench..... 41
Figure 3.4. Direct GA based optimization framework..... 42
Figure 3.5. ANN-MMBO metamodel-based optimization 43
Figure 4.1. Training, validation, test and all data graph in ANN metamodelling process..... 48
Figure 4.2. Total rotor moment responses comparison graph on the T15-300 cross-flow turbine model..... 49
Figure 7.1. HronTurek FSI benchmark channel configuration (a) entire model (b) magnified details of the structure model. 57

Figure 7.2. y-axis deformation responses in time at point A. 58
Figure 7.3. Causal network using the original theoretical models. 59
Figure 7.4. Causal network after the simplification. 60
Figure 7.5. NURBS curve of the valve profile 61
Figure 7.6. Boundaries configurations of T15-300 cross-flow turbine design; (a) full turbine model and (b) separate nozzle design. 62
Figure 7.7. Moment responses from the entire rotor blade surfaces. 63
Figure 7.8. Velocity streamline contour figures of steady analysis results from (a) original model, (b) direct GA based and (c) MMAO-based optimization models. 64
Figure 7.9. 2D model of IAM turbine design. 65
Figure 7.10. Sensitivity test viscous numerical model against experimental response. 66
Figure 7.11. Moment coefficient response comparison of the optimized model against 80% and 100% valve opening at 350 rpm rotor speed 67
Figure 7.12. Moment coefficient response comparison of the optimized model against 80% and 100% valve opening at 250 rpm rotor speed 68

List of Tables

Table 2.1: An overview of the unutilized hydropower potential of six selected countries [39, 45] 29
Table 4.1. Application results for three different optimization approaches..... 47
Table 4.2. Given conditions, stopping criteria and results of the ANN-MMBO application 48
Table 7.1. Geometric parametric values of the benchmark FSI channel configuration. 57
Table 7.2. Optimization results of the theoretical model 60

List of abbreviations

ANN	Artificial Neural Network
ANOVA	Analysis of Variance
BTU	British Thermal Unit
CAD	Computer Aided Design
CAE	Computer Aided Engineering
CFD	Computational Fluid Dynamics
DA	Dimensional Analysis
DACM	Dimensional Analysis Conceptual Modelling
DOE	Design of Experiment
FEA	Finite Element Analysis
FEM	Finite Element Method
FSI	Fluid-Structure Interaction
GA	Genetic Algorithm
IAM	International Assistance Mission
IGA	Isogeometric Analysis
MBDS	Multibody Dynamics Simulations
MHP	Micro-scale Hydropower
MMAO	Metamodel Assisted Optimization
MMBO	Metamodel Based Optimization
MOGO	Multi Objective Global Optimization
MPS	Mode Pursuing Sampling
MSE	Mean Square Error
OECD	Organization for Economic Cooperation and Development
NSBMAO	Numerical Simulation Based Metamodel Assisted Optimization
NURBS	Non Uniform Rational B-Spline
RBF	Radial Basis Function
SHP	Small-scale Hydropower
SOGO	Single Objective Global Optimization

Part I: Thesis Summary

1 Introduction

This thesis generally discusses the challenges in advancing computer-based design, analysis and optimization processes, particularly focusing on complex high-dimensional and multi-disciplinary problems. To address some of the challenges, new design optimization frameworks that utilize state-of-the-art approaches are introduced. The frameworks, in a nutshell, aim to reduce the computational costs associated with complex high-dimensional design optimization problems in computer-based applications. This particular section provides a general overview of the studies in the thesis work, presents the objectives of the thesis and the research questions answered by the studies. Finally, following a discussion on the limitations of the research, the overall thesis structure is presented.

1.1 General overview

In order to cope with the rapidly growing competitive market, diverse forms of computer-based supports in engineering and science have been introduced. Computer-aided design (CAD), multibody dynamics simulations (MBDS), computational fluid dynamics (CFD), finite element analysis (FEA) and other applications in solid mechanics, for instance in crack and fatigue analysis, are some of the tools and areas where advanced computer-based applications are introduced. These tools are intended to perform the virtual design and testing of products and systems at low cost and short lead time, without the construction of physical prototypes. Numerical model predictions, i.e. design validation and verification, are being carried out using such digital prototyping in the form of computer modelling and simulation. They are also more important, particularly in areas where conducting physical tests is hazardous, complex and/or technologically challenging, and where future forecasting is required. On the other hand, based on those numerical modelling and simulation tools, various digital algorithms are

also introduced to search for optimum design solutions that enable scientists and engineers to make better decisions in the design-development processes. However, as the interest in obtaining precise results through exact representation of the actual physical problem increases, and as the physical problem becomes complex and high-dimensional, the numerical modelling and simulation process eventually becomes more challenging and error prone. At the same time, this has a direct implication on the decision-making processes that are based on numerical models and simulations. Consequently, these lead us to deal with cumbersome data, that are complex and problematic to secure, process and sometimes to understand.

Comprehending the problem led various researchers from all fields of study to engage in looking for solutions in multiple perspectives. The state-of-the-art developments on approaches introduced to tackle these challenges in complex high-dimensional computer-based problems are categorized in, but not limited to, three broad perspectives. i.e. perspective that tend to:

- integrate the design modelling and simulation technologies. The two technologies have developed in two separate directions with respect to their building block functions, the 'basis functions'. Seamless integration of the technologies saves processing time and resources, enables to better visualize and understand the problem under consideration.
- further simplify/decompose, approximate and replace the original complex physical, numerical and/or simulation models with simpler surrogate models (metamodel).
- further enhance the accuracy and advance the processing capacity of computing machines. These enable to secure and process the cumbersome data in a shorter time and enable to better analyse the problem with an improved visualization (for instance, the recent quantum computing technology is one development in the area).

In this thesis, different approaches that lay under the first two perspectives are introduced and new frameworks are proposed and discussed aiming to tackle the aforementioned challenges particularly focusing on processes in design optimization problems. The later enable designers to make better decisions in system and product design processes. In relation to the first perspective, isogeometric analysis (IGA) which utilizes similar state-of-the-art basis functions for both modelling and analysis is introduced and discussed. IGA tool is a recent development in the area. In addition, the thesis discusses computational methods in fluid-structure interaction (FSI) problems, Figure 1.1, one of the widely applied multidisciplinary problems.

On the other hand, a study on the state-of-the-art metamodel-based optimization approach has been carried out, which addresses the second perspective. As demonstrated in the background study, in Section 2, the metamodel in the optimization approaches serve either as:

a) a surrogate model that approximate and then replace original complex models (after training, validating and testing using sample design of experiment data) or

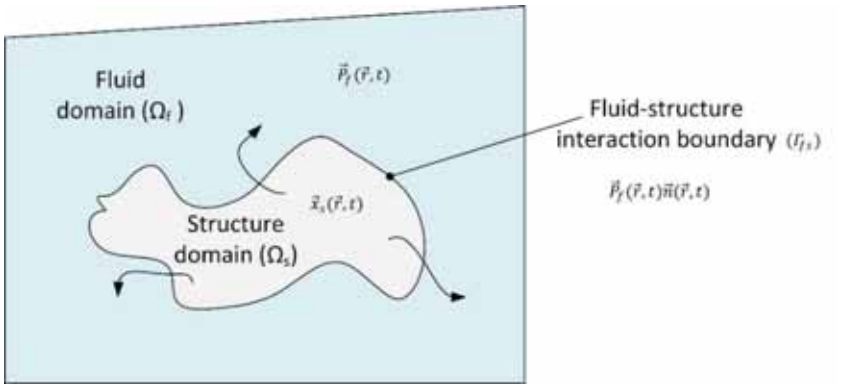

Figure 1.1 General Fluid-structure interaction domains representation

where: $\vec{P}_f(\vec{r},t)$, $\vec{x}_s(\vec{r},t)$ and $\vec{P}_f(\vec{r},t)\vec{n}(\vec{r},t)$ are the changes in pressure, deformation and boundary interaction at the fluid, solid and FSI domains as a function of displacement ($\vec{r}$) and time (t), respectively.

b) a tool to intelligently identify and locate global optimum regions in design spaces in optimization processes of complex high-dimensional problems.

The study proposes new design optimization frameworks, one of which utilizes the latest metamodelling approach for optimization; it also incorporates one of the state-of-the-art basis functions for shape representation.

On the other hand, an optimization framework based on a novel simplification and decomposition approach, which is based on a customized dimensional analysis conceptual modelling (DACM) framework, is developed and introduced which particularly aims to solve complex high-dimensional optimization problems. DACM is a framework originally developed for conceptual modelling and simulation of engineering systems [1].

Case studies are carried out employing the proposed approaches and frameworks introduced. Results obtained from optimization processes that employ the new approaches and frameworks introduced are compared against results obtained from optimization of original models employing genetic algorithm (GA) tool, the widely applied global optimization tool.

The case studies in the thesis employ the proposed optimization approaches and frameworks to improve the performance of two latest micro-cross-flow hydro turbine designs, see Figure 1.2 and 1.3. Cross-flow turbine is one of the most widely applied small and micro hydro turbine designs. The turbine is flexible, economical and favourable, particularly for run-of-the-river applications in remote areas, but its power generation efficiency is not yet well optimized [2]. Therefore, the case studies aim at enhancing the performance of the turbines' designs.

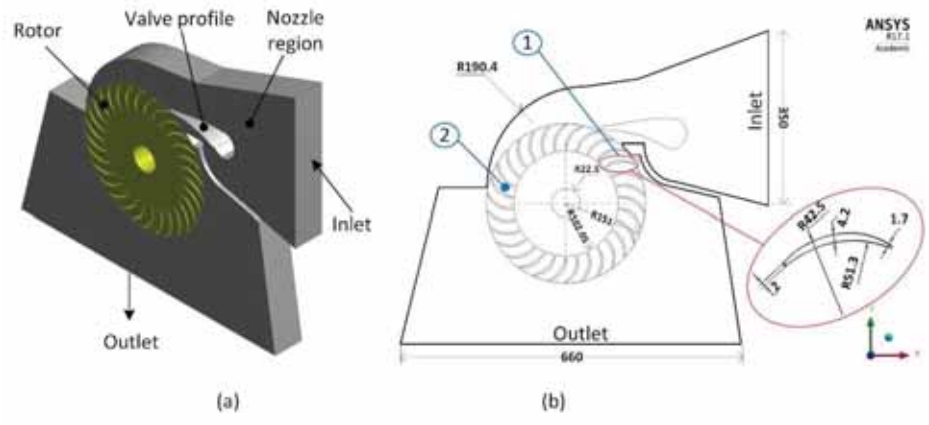

Figure 1.2. T15-300 micro cross-flow turbine design.

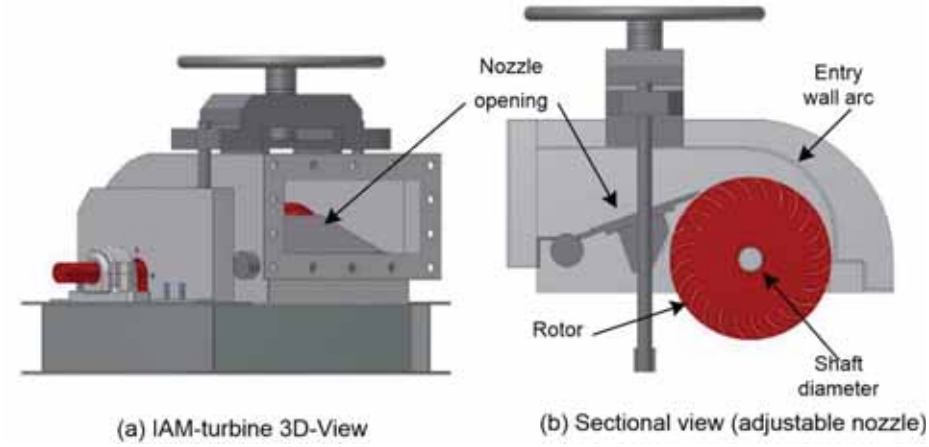

Figure 1.3. IAM micro cross-flow turbine design [3]

1.2 Research objectives

As discussed earlier in the current section, the studies in the thesis, in general terms, aim to investigate the challenges in computer-based modelling, analysis and optimization. It also aims to research on state-of-the-art techniques and approaches that best tackle the challenges and advance the application of computer aids in engineering. The thesis also discusses applications of computer-based approaches and frameworks

that aim to help curb the growing concern on climate-change, which is becoming a threat to the basic existence of humankind.

In general, the objectives of the thesis are:

- Identify the challenges in computer-based modelling, analysis, and simulation-based optimization processes, particularly focusing on processes that involve multidisciplinary and multi-dimensional problems.
- Survey available simplification, decomposition and approximation approaches/frameworks that are proposed and applied to tackle the identified challenges.
- Conceptualize, develop and propose new approaches/frameworks; validate them through comparative analysis.
- Utilize the proposed approaches and frameworks to enhance the performance of facilities that take part in the climate-change mitigations.

Based on the general objectives, the studies in the thesis focus on the following specific objectives:

- Investigate and study the state-of-the-art tools that integrate and simplify numerical modelling, analysis and optimization processes.
- Develop and propose novel approaches/frameworks to simplify, decompose and/or approximate multidisciplinary as well as high-dimensional optimization problems, aiming to reduce computational costs and shorten product-development life cycle.

- Identify a benchmark model or a case study in the renewable energy sector that has a significant impact, to address the current concerns on global climate change.

- Select important design parameters, valid numerical models and computational methods from existing systems/tools. Following the selections, conduct sensitivity tests and carry out the computation.

- Validate proposed approaches through application in case studies; conduct comparative analysis of the approaches with existing and/or state-of-the-art approaches and verify proposed frameworks and approaches employed.

1.3 Research gaps and questions

It is obvious that these days application of advanced numerical modelling and analysis tools, in almost every science and engineering fields, is becoming inevitable. The studies in the thesis fundamentally focus on identifying the specific challenges and addressing the growing research gaps in computer-based modelling, analysis and design optimization, with a particularly focus on complex multi-disciplinary and high-dimensional problems. Based on the later conception and background studies, the studies in the thesis try to answer the following formulated questions:

1. Although diverse computer-based tools are introduced to solve design and analysis problems, seamless integration of the tools remains a challenge. The integration believed to save huge computational time and resources that are otherwise wasted. What is the possible approach that exist that could seamlessly integrate the tools without utilizing approximate models and how does it benefit the numerical simulation-based optimization processes?

2. How could computational costs in computer based modelling, analysis and optimization of complex, multidiscipline and high-dimensional, problems be reduced? How could that be attained without significantly compromising technology developments toward accurate representation of problems? What are the latest developments in these regard?

3. Simplifying, and/or decomposing design parameters based on their importance level towards the objective of problems are some of the approaches being applied to tackle challenges in complex multidimensional and multidisciplinary optimization problems. What new developments could be achieved in this regard through utilizing the concepts under the DACM framework? How does the scientific community benefit from the customized DACM based optimization approach?

4. Approximation and replacing models of complex high-dimensional optimization problems with simpler models (metamodel) is one approach to reduce computational costs. What are the challenges and the latest developments in such approach? What are the pros and cons of tools that employ frameworks that incorporate the latest approaches, compared to the conventional approaches?

5. With the rising global energy demand as well as the growing concern about climate change, utilizing alternative energy sources is imperative. Hydropower is the major renewable energy source, with more than half of its global energy potential is yet unexploited. How do the diverse computer-based modelling, analysis and optimization tools benefit in harnessing the remaining potentials? How do optimization frameworks be utilized to enhance performance of micro-hydropower facilities?

1.4 Limitations of the research

Given the complexity and interdisciplinary nature of the focus research area and the subjects associated to it, developments of proposed approaches in more coordinated and integrated manner are limited. Apart from that, finding benchmark resources for fair comparison of results to help further advance the topics have been a challenge.

Despite the extra effort from the researcher and co-researchers involved in the course of the research period, it is only possible to address limited level of the scope of the research for various financial, time- and resource-related reasons. However, so to address the challenges critically, researchers (experts) from various fields of studies are advised to come together through collaborations.

In the case studies, it would have been more realistic if the 3D graphical models of the turbines' designs were developed and utilized in the analyses. However, on our workstation, the analyses would take hours before the single steady analysis converge if a 3D model is used. Which, therefore, might take days or, in some cases even weeks, if the optimization process is carried out using the 3D model. Therefore, in order to shorten the waiting time of the processes, without significantly compromising the accuracy of the analyses, approximated 2D or only selected sections of the 3D models are considered in the optimization studies. These approximations are therefore subjected to unnecessary errors in the process. However, the complete 3D models of the selected design optimization results are utilized in the validation processes. More on that, there were time limitations to testify all the proposed hypotheses and all Pareto-front design points in the analysis.

In addition, in order to further verify the numerical models and proposed approaches, finding real-time onsite or laboratory test results of the product designs utilized in the case studies was challenging. Therefore, only part of results of the models are verified using limited laboratory test results.

1.5 Thesis organization

The thesis is an article-based thesis and it constitutes two parts. Part I of the thesis summarizes the overall studies carried out in the articles appended in Part II. The introduction section of Part I presents a general overview of the works done, as well as discusses the research objectives, gaps and questions. In addition, the limitations of the research and the thesis organization are presented in the later section. Following the introduction section, state-of-the-art study of finite element based analyse methods and background review of computational methods in fluid-structure interaction problems and metamodelling processes are discussed in Section 2. Moreover, hydro turbine designs utilized in the case studies are presented in the later section. Section 3 discusses the general methodologies employed in the research, and the proposed optimization frameworks are demonstrated in detail. Discussion of the study results, conclusions drawn and recommendations for future works are presented in Sections 4 and 5, respectively. Section 4 includes also the results of unpublished work. Thereafter, the scientific contributions of the research are discussed in Section 6. Finally, summary of the articles appended in Part II is provided in Section 7.

2 Background review and state-of-the-art studies

Since the beginning of the digital world, computer-based design, analysis and simulation tools have developed immensely for diverse applications. Moreover, to help avoid risky decisions in product and system designs and enhance performances of systems and products, various computer-based optimization approaches have been introduced. In this section, the state-of-the-art computer-based modelling and analysis tools, and optimization approaches that have been utilized in our studies, are reviewed.

2.1 Finite element analysis vs. Isogeometric analysis

For decades, since first introduced, computer aided design and analysis technologies (particularly finite elements based analysis (FEA)) have developed in separate directions with regard to 'basis function' technologies they utilize. Basis functions are the building blocks of every continuous function as the latter is a linear combination of specific basis function in its function space. The design and modelling tools have advanced enormously, with respect to use of the latest basis functions, that various geometrically complex nonlinear physical problems can these days be designed and modelled to the highest precision. On the other hand, most finite element based analysis technologies still utilize approximate models of problems, especially if the problems involve complex, smooth nonlinear graphic designs. To narrow down the gaps between the technologies, various independent intermediate transfer technologies have been developed and standardized, such as STEP, IGES, STL and others, to approximate and transfer the models from one form of basis function to another. Although these data exchanges were intended to serve as a means of interfacing the available and isolated

engineering tools, most of them fail to properly define and transfer the accurate geometric properties of the original models.

The CAD tools utilize the state-of-the-art basis functions, such as T-spline and Non-uniform Rational B-spline (NURBS) functions, whereas most analysis tools still utilize polynomial interpolation functions. For this and other reasons, studies estimate that, on average, more than 80% of overall analysis time is wasted on approximating, transferring and mesh generation of models before the actual analysis [4]. Throughout the years, various researchers have expressed their concerns and proposed integration frameworks in various ways [4-6]. The recently developed Isogeometric Analysis (IGA) framework, first proposed by T. Hughes et al. in 2006 [4], which fully acknowledges the Isoparametric concept from the classical finite element method (FEM), realized the integration through utilizing the state-of-the-art basis functions, one of which is the NURBS function.

2.1.1 Non-uniform Rational B-spline function (NURBS)

The NURBS function is a B-spline-based recursive function that begins from a piecewise constant value (Eq. 2.1). For a polynomial of degree zero, *p=0*, the function begins as:

$$N_{i,0}(\xi) = \begin{cases} 1 & \xi_i \le \xi < \xi_{i+1} \\ 0 & otherwise \end{cases} \tag{2.1}$$

For $p \geq 1$, it is formulated as:

$$N_{i,p}(\xi) = \frac{\xi - \xi_i}{\xi_{i+p} - \xi_i} N_{i,p-1}(\xi) + \frac{\xi_{i+p+1} - \xi}{\xi_{i+p+1} - \xi_{i+1}} N_{i+1,p-1}(\xi) \tag{2.2}$$

where $N_{i,p}$ is the basis function with a degree *p*, *i* is the knot index ($i = 1,2, \dots, n$) and ξ is the knot value obtained from a given knot vector $\Xi = \{\xi_1, \xi_2, \xi_3, \dots \xi_{n+p+1}\}$.

Using the basis function, one-dimensional and multidimensional continuous functions can be obtained, as expressed in Eqs. 2.3 and 2.4:

$$C(\xi) = \sum_{i=1}^{n} N_{i,p}(\xi)\, B_i \tag{2.3}$$

$$S(\xi, \eta) = \sum_{j=1}^{l} \sum_{i=1}^{n} N_{j,p}(\eta) N_{i,p}(\xi)\, B_{ij} \tag{2.4}$$

where B_i and B_{ij} are the corresponding control points for the one-dimensional and two-dimensional continuous functions, $C(\xi)$ and $S(\xi, \eta)$, respectively.

The NURBS function is derived by introducing weighting values for each control point. The weighting values enable the function to be locally controlled when required. For a one-dimensional continuous function, the NURBS function is give as Eq. 2.5, where $R_{i,p}$ is the NURBS basis function, Eq. 2.6, and w_i is the corresponding weighting value.

$$C_n(\xi) = \sum_{i=1}^{n} \frac{N_{i,p}(\xi) w_i}{(\sum_{i=1}^{n} N_{i,p}(\xi) w_i)} B_i = \sum_{i=1}^{n} R_{i,p} B_i \tag{2.5}$$

$$R_{i,p} = \frac{N_{i,p}(\xi) w_i}{(\sum_{i=1}^{n} N_{i,p}(\xi) w_i)} \tag{2.6}$$

One of the most important technological aspects introduced within the IGA tool, apart from the *h*- and *p-refinement* common in the classical FEM, is the ability to mesh the exact CAD models using knot refinement technology, *K-refinement*. The latter is an important technology in the IGA tool.

2.1.2 Knot refinement

The *K-refinement* technique is used to mesh the CAD model, by inserting knots as well as generating the corresponding control points without changing the features of the geometry. By doing so, the technique increases the solution space of the problem.

For a given knot vector $\Xi = \{\xi_1, \xi_2, \xi_3, \dots \xi_k, \xi_{k+1} \dots \xi_{n+p+1}\}$, let us imagine that a new knot value $\bar{\xi} \in [\xi_k, \xi_{k+1}]$ is inserted to provide a new knot vector $\Xi = \{\xi_1, \xi_2, \xi_3, \dots \xi_k, \bar{\xi}, \xi_{k+1} \dots \xi_{n+p+1}\}$. The corresponding control point vector $\bar{B} = \{\overline{b_1}, \overline{b_2}, \overline{b_3}, \dots \dots \dots \overline{b_{n+1}}\}$ is obtained from the original vector $B_i = \{b_1, b_2, b_3, \dots \dots \dots, b_n\}$ using a parametric equation, Eq. 2.7:

$$\overline{b_\iota} = \alpha_i b_i + (1 - \alpha_i) b_{i-1} \tag{2.7}$$

where

$$\alpha_i = \begin{cases} 1, & 1 \le i \le k - p \\ \dfrac{\bar{\xi} - \xi_i}{\xi_{i+p} - \xi_i}, & k - p + 1 \le i \le k \\ o, & k + 1 \le i \le n + p + 2 \end{cases}$$

Since it was first developed and introduced, IGA has been applied in various fields of science and engineering, and the results of several studies demonstrate the power of the technology, especially in problems that involve nonlinearity, such as in plate and shell structural analysis and optimization problems [7-14], in multidisciplinary problems such as fluid-structure interaction problems [15-17] and others.

In this thesis, a state-of-the-art review of the IGA in nonlinear optimization problems is carried out in Paper **I**. In addition, the one-dimensional continuous function of one of the state-of-the-art basis function, NURBS, is utilized in one of the design optimization frameworks developed, in Paper **IV**, in which it represented a curve

function. The control points serve as optimization parameters while the weighting enabled local control, thereby providing smoothness to the curve. The process demonstrated the power of the function, as well the power of integrated approaches.

2.2 Fluid-Structure Interaction: Multi-discipline and high dimensionality

2.2.1 Introduction

The complexity and high-dimensionality of science and engineering problems arise from, among others, the multidisciplinary nature of problems. In a multidisciplinary problem, mostly each domain is represented with different mathematical or numerical model, based on the domain of the discipline in which it belongs. These characteristics of problems drive in the complexity and usually high-dimensionality of multidisciplinary problems. One of the most common multidisciplinary problem widely available in science and engineering is fluid-structure interaction problem (FSI). FSI problems occur, for instance, in medical science, in offshore technologies, in wind and hydropower technologies, and others. In this thesis work, the basic coupling and discretization techniques, and the computational methods used in FSI problems, are reviewed and discussed.

2.2.2 Computational and solution methods in FSI problems

As the name implies, two domains of different characteristics are involved in FSI problems, i.e. the fluid and structural domains, Figure 1.1. The structural domain is governed by principles in structural mechanics, whereas the fluid domain is based on the conservation laws of mass, momentum and energy in fluid dynamics. As a result, in solving FSI problems, the main challenge of the complexity is embedded with

handling the interface of the two domains. Based on the coupling behaviour and the time-dependent (temporal) discretization of the problems, the computational methods in FSI problems are classified [18-21] as:

a. One-way coupling method
b. Two-way coupling method
c. Monolithic method
d. Partitioned method.

The coupling of the domains is carried out, using – either separately or in combination – the well-known coupling conditions in FSI, the Neumann-Dirichlet coupling conditions [19], which are based on the:

i. Dirichlet and
ii. Neumann standard conditions.

The Neumann condition dictates that the nodal velocities of the two domains at the interface should be equal, Eq. 2.8, while, in the case of the Dirichlet condition, the static pressure of the fluid and the normal stress of the structure should be equivalent at the interface, Eq. 2.9.

$$\vec{\dot{x}}_i(x_i, t) = \vec{v}_i \tag{2.8}$$

$$\sigma_{ij}^{s}.\boldsymbol{n} = \sigma_{ij}^{f}.\boldsymbol{n} \tag{2.9}$$

$\vec{\dot{x}}_i(x_i, t)$ - is the structural velocity vector as a function of deformation (x_i) at nodal point *i* and time *t*; $\vec{v}_i$ – fluid velocity at nodal point *i*; $\sigma_{ij}^{s}.\boldsymbol{n}$ and $\sigma_{ij}^{f}.\boldsymbol{n}$ are stress and pressure vectors at *i* and *j* coordinates of the structural and fluid domain respectively.

A comparative analysis of computational methods on a benchmark problem, Paper **II**, revealed that a strongly coupled two-way partitioned approach demonstrates a more realistic result than the one-way coupled

partitioned approach. Moreover, from reviews, it is also found that the partitioned method requires an additional third interfacing component model to couple the two domain models, while the monolithic method follows a seamless integrated approach that does not require a third interfacing model; it is, however, demanding to apply the integrated approach for each and every specific problems.

2.3 Customized DACM-based simplification and decomposition

Customized dimensional analysis conceptual modelling (DACM) framework is a novel approach, intend to simplify and/or decompose system variables of an existing mathematical models of complex high-dimensional optimization problems. The decomposition of the variables is carried out based on their importance level towards the optimization objective of the problem. This approach is based on a DACM framework, initially introduced for conceptual modelling and simulation, life cycle analysis in product development and system engineering for qualitative analysis [1]. Both frameworks utilize the well-known dimensional analysis (DA) theories and bond graphing concepts, in order to carry out the cause-effect relations of system variables. The most important concepts of the frameworks that serve for the simplification and decomposition of the variables are the backward objective propagation that help search for contradictions, and computation of the level of importance using knowledge from the design of experiment (DOE). The frameworks require listing of all variables involved and categorize according to the variables' category to which they belong, with each category coded with a designated symbol or colour. The different variable category names and their description are given in Paper **III** appended. Following that, the importance levels of each variables towards the objective of the problem are computed. The overall activities of the customized framework are summarized in a few steps using a flowchart, as given in Figure 2.1.

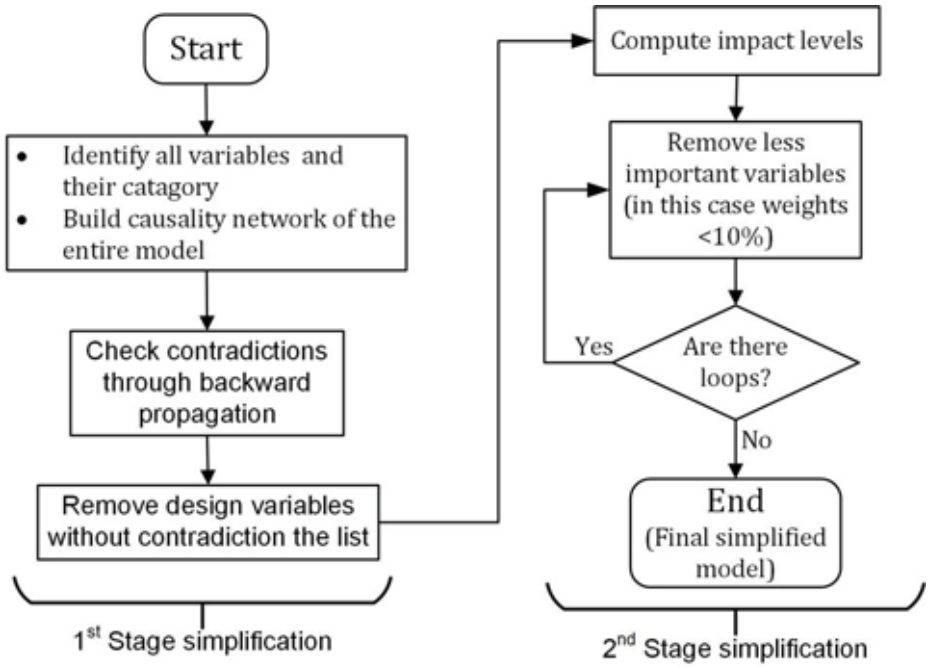

Figure 2.1 Steps in the customized DACM for simplification and decomposition of high-dimensional models

Once the variables are identified and the causal network is built based on the bond graph theory, the dimensional analysis concept comes into play, to find any contradictions within the variable regarding the objective/s.

The well-practised Vashy-Bukingham's Π-theorem and a mathematical machinery by Bhanskar and Nigam [22, 23] are utilized to determine relations between variables.

The other most important tool of the customized framework is the DOE. It generates samples to run virtual experiments and calculates the percentage effects of the variables. For the analysis and optimization work employing the current customized framework, the widely applied Box-Behnken and Latin Hypercube sampling and Taguchi analysis methods [24] are proposed to compute the importance levels of variables.

The two-stage simplification and decomposition method is enormously beneficial in the simplification and computational cost reduction of high-dimensional optimization problems. Optimization approaches are proposed based on the customized DACM framework, Paper **III**. A case study is carried out in the paper on the theoretical model of cross-flow turbine design, and the results demonstrate the powers of the customized DACM based optimization framework.

2.4 Metamodelling in numerical simulation model approximation and design optimization

2.4.1 Introduction

In simple terms, metamodelling is a process of approximating and/or replacing an existing model with a simplified model, called metamodel or surrogate model. Usually, existing or original models that are required to be approximated and/or replaced are models of complex implicit-problems. Such problems are computationally expensive to directly utilize them for subsequent analyses and optimization processes. Computational fluid dynamic (CFD) and finite element (FE) based analysis and optimization tools, among others, are the computer-based modelling and analysis tools that are considered for metamodelling-based analysis and optimization in order to reduce the computational costs, as they are some the computationally intensive applications that are rapidly expanding in various fields of study. For instance, as reported by Gu [25], one crash simulation at Ford Motor Company takes about 36-160 hrs. One can imagine how long it would take for the company to carry out crash simulation-based optimization for a couple of parameters using the model, assuming a few iterations. Hence, intervention of metamodelling is plays great role.

Metamodelling is fundamentally a combination of three basic processes [26]:

i. Sampling
ii. Metamodel selection
iii. Model fitting

Based on the chosen techniques at each step of the three processes, the metamodelling methods and their outcomes will vary. For instance, Kriging and Artificial Neural Network (ANN) methods are among the most widely applied metamodelling methods with different sampling, model and model fitting techniques [26]. The Kriging method utilizes the *D-Optimal experimental method, Realization of a Stochastic Process* and *Best Linear Unbiased Predictor* for sampling, modelling and model fitting, respectively. On the other hand, the ANN utilizes *Select by Hand sampling*, *Network of Neurons* and *Back-propagation techniques*, respectively. Once the techniques at each process are chosen, training and verification of the new model are required, so that it serves as a valid model that can replace the existing model. Training and verification of a model is carried out using list sample data from either physical or numerical experiments.

2.4.2 Metamodelling in optimization

There are various ways of utilizing metamodelling technique in model approximation and design optimization processes, particularly in numerical simulation-based optimization. Based on the reviews performed by Wang and Shan [27] and Simpson et al. [26], design optimization processes that comprise metamodelling techniques can simply be categorized in two broad groups:

a. metamodel based optimization (MMBO)
b. metamodel assisted optimization (MMAO)

The first category refers to those optimization techniques that utilize the metamodel to approximate and completely replace the original model with the newly generated metamodel. In this case, the original model will not be utilized anymore, and such MMBO approaches are referred to as

sequential approaches [25], as illustrated in Figure 2.2(a). Figure 2.2(b) illustrates the second category (i.e. MMAO), where the metamodel serves only to generate sample data towards the optimum in the design space. From various application reports, the second category provides the best trade-off between accuracy and computational costs; hence, state-of-the-art metamodelling-based optimization techniques reside in the second category [27-31]. Optimization frameworks in appended Papers **IV-VI**, integrate optimization tool that utilizes the approach in the second category, known as OASIS [32].

The OASIS tool in the papers utilizes the mode-pursuing sampling (MPS) method [28, 29, 31, 32], one of the metamodel assisted sampling method in the state-of-the-art optimization approach. The mode-pursuing sampling (MPS) method based optimization enables the tool to intelligently generate samples from the design space towards the optimum. In the MPS method, simple linear spline or radial basis functions (RBF) are used to represent the model [28].

In the thesis studies, optimization results from a framework that employ OASIS tool are compared against results from ANN metamodel-GA-based optimization framework, and results from direct GA-based optimization framework.

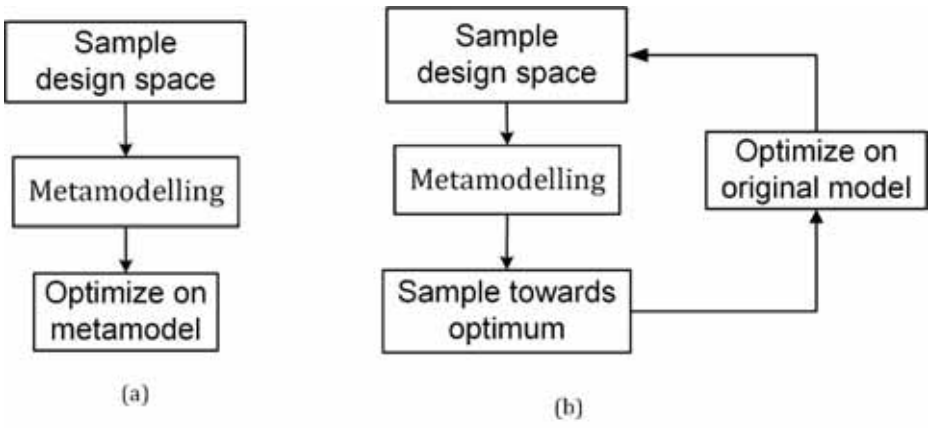

Figure 2.2. Metamodel utilizing optimization approaches (a) MMBO (b) MMAO

In the study, in the ANN metamodel-GA-based optimization framework the metamodel replaces the original model of the problem; hence the framework is categorized under the MMBO group. Whereas the GA-based optimization framework is applied on the original model. The next subsection discusses the ANN metamodelling technique that is utilized to approximate and replace the CFD model of section of one of the micro cross-flow turbine design considered in the case study in the thesis.

2.4.3 ANN metamodelling in optimization

ANN metamodelling is one of the artificial intelligence methods that comprises network of neurons, which fundamentally mimic how the human mind performs learning patterns of functions from experience [33]. The architecture of the network is constructed from neurons linked to each other (Figure 2.3), which are multiple linear regression models. Intermediate layers of neurons (hidden layers) between the input (***X***) and output (***Y***) enable the construction of multi-layer networks for better approximation.

Through the network, the typical nonlinear transformation function, i.e. the sigmoidal function, transforms the inputs to the output vectors. The sigmoidal transfer function for *i* number of inputs ***x*** and an output ***y*** in a network is expressed in simplified forms as in Eq. 2.10. The links of the network will then be represented by an approximate weighting value, w_i, in the model, and bias values can be used to adjust the returning output values. The feed-forward multi-layer architecture is the most common ANN metamodel [26]. For a detailed description of ANN, please refer to [33].

$$\boldsymbol{y} = \frac{1}{1 + e^{-\delta/m}} \qquad (2.10)$$

$$\delta = \sum w_i \boldsymbol{x}_i + \boldsymbol{b}_i$$

where $\boldsymbol{b}_i$ is a bias value of neurons, and *m* is the slope parameter of the sigmoid.

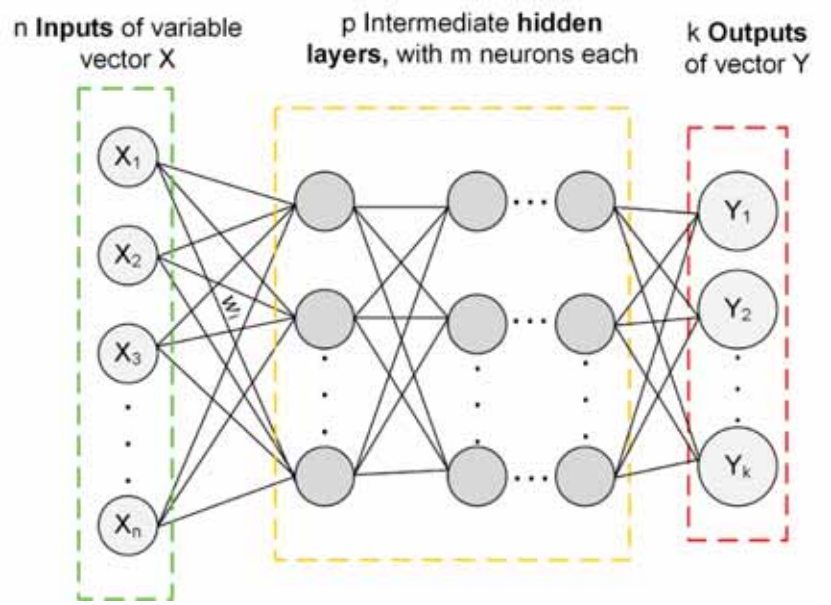

Figure 2.3. A feed-forward Artificial Neural Network architecture with multiple hidden layers

After building the architecture, the three basic processes in ANN are: (1) training, (2) validation and (3) testing of the model. Set of sample data from real-world experiments or computer analyses are used to train, verify and test models before replacing the original model. The overall ANN metamodeling process is summarised using flowchart as in Figure 2.4. Only fractions of the total data are selected and used for validating and testing in the model verification process. A back-propagation algorithm is applied to train the model until the approximation reaches an acceptable performance. In order to measure the performances in the training, the mean square error (MSE) method, Eq. 2.10, is employed.

$$\boldsymbol{E} = \sum_{k} (\boldsymbol{y_k} - \boldsymbol{\hat{y}_k})^2 \tag{2.11}$$

where $\boldsymbol{\hat{y}_k}$ is the output from the new model for a given input $\boldsymbol{x_k}$, and $\boldsymbol{E}$ is the total error of the system.

As ANN metamodelling is efficient and well developed, it has been applied in various applications, for instance in power generation and turbine applications [34-36]. As discussed in Section 3 of the thesis work, in one of the case studies, a multi-layer ANN metamodel is generated and utilized to replace the micro cross-flow turbine's numerical model in the design optimization of the turbine to improve its performance. In the study, a network architecture with five-input design variables ($\boldsymbol{X_{1\text{-}5}}$) and two output values ($\boldsymbol{Y_{1\text{-}2}}$) with 10 hidden layers is utilized.

The design variables represent control points of a NURBS based shape function of a valve profile of the T15-300 cross-flow turbine, as in Paper **IV**. The outputs represent the two objective functions in the turbine's nozzle analysis.

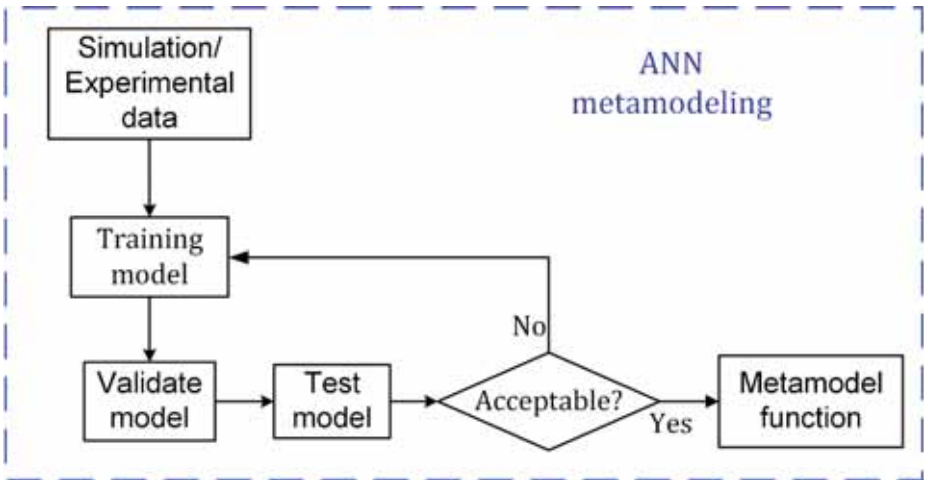

Figure 2.4. Flowchart of Artificial Neural Network metamodelling

2.5 Case studies: Performance optimizations in two micro cross-flow hydro turbine designs

2.5.1 Introduction

In this thesis, two micro cross-flow turbine designs are considered in the case studies, with the aim of enhancing their performance using the optimization frameworks developed. It is believed that enhancing the performance of the turbines will contribute to further increase the share of hydropower in the global energy market, which also has an implication for growing global energy consumption and climate-change concern.

Global energy consumption has revealed a consistent increase in the demand for energy in recent centuries, mainly because of the growing modernization, competitive market economy and increasing population, and it is likely to continue rising in the future. According to the projection in the 2017 International Energy Outlook report [37], Figure 2.5, the gross energy consumption, of both member and non-member nations of the Organization for Economic Cooperation and Development (OECD), is expected to increase. In order to satisfy this growing demand, nations should continue to rely on exploiting abundant energy sources and also enhance the efficiency and performance of existing technologies. As some of the major sources of energy are not renewable and thus diminishing in size, alternative energy sources are inevitable. Furthermore, nations throughout the world have come together and signed up to take collective action to curb the sources of energy we consume to a more climate friendly [38].

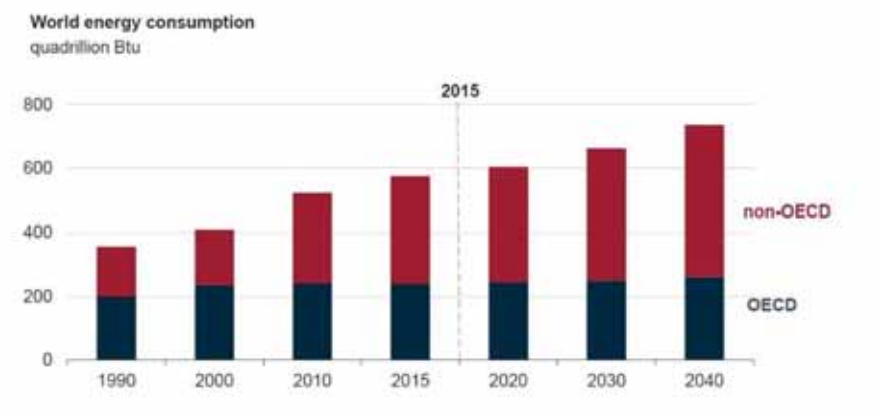

Figure 2.5. Global energy consumption history and projection [37]

The energy consumption projection by energy source, however, shows an increasing consumption of all, except for a slight fall in coal consumption, Figure 2.6. Despite fossil fuels and nuclear power sources continuing to contribute huge amounts to the energy demand, renewable energies have become the fastest growing energy sources. To date, of the total existing renewable energies, hydro accounts for the largest portion [39]; as of 2015, hydropower constituted 65% of the total global renewable energy source share.

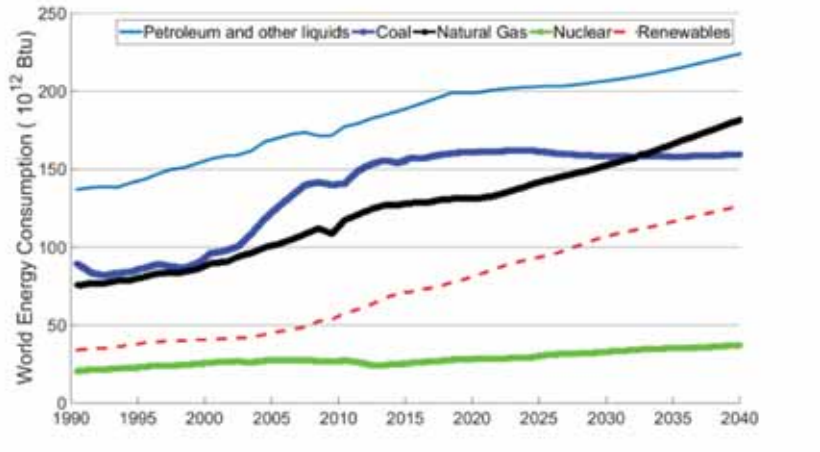

Figure 2.6. World energy consumption history and projection by energy sources [37]

2.5.2 Hydropower

Hydropower is, by definition, "the generation of power by harnessing energy from moving water" [39]. Despite the little attention paid by the research community to hydropower, compared with other renewable energy sources, hydropower still constitutes the largest portion of the world's renewable energy share [39, 40]. Moreover, in recent years, it has shown a growing development and a rise in consumption of the hydropower technologies. As can be seen in Figure 2.7, the total global installed capacity has grown by 39% in the period 2005 to 2015 alone [39], and it has shown a surge in increase in recent years. The World Energy Resources report indicates that, globally, hydropower supplies more than 61% of all the electricity generated from renewable energy sources and 16.4 % from all energy sources, with a total installed capacity reaching 1,064 GW as of 2016 [39, 41, 42].

The four most important factors in the energy sector that drive the development of hydropower technology are:

i. the increase in energy demand,

ii. the energy storage capability of the technology,

iii. its flexible generation capability, and

iv. contribution to climate-change mitigation.

In addition, hydropower infrastructure makes vast contributions in different areas, for instance in regional freshwater management; it also provides other valuable services and advantages.

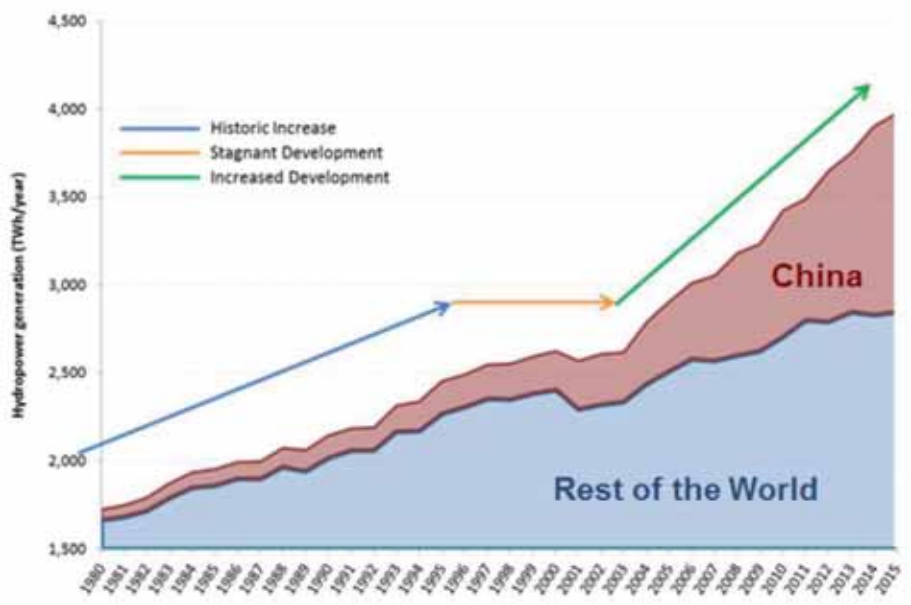

Figure 2.7. Global total hydropower generation since 1980 [39]

Based on the global energy utilization trend, regardless of the rise in consumption and the huge attention paid to other renewable energy sources, the demand for hydropower will continue to dominate the renewable electricity share, as a significant amount of undeveloped hydropower potential still exists across the globe. Norway, for instance, is one of the countries with the highest levels of hydropower consumption; however, it utilizes only 45% of its potential. In fact, Norway is one of the developed countries with 100% electrification rate, obtaining 99.95% of its electric energy from hydropower, while Iceland is a country almost exclusively powered by renewable energy, getting its power from hydro and geothermal resources [2]. In Africa (believed to be the future major market of hydropower), as of 2012, only an estimated 9% of the total potential has been developed, with average electrification rates of only 45% [42, 43].

The remaining untapped global hydropower potential, as of the beginning of the 21st century, was estimated at roughly twice the installed

capacity [44]. Current estimations indicate that the global available unutilized potential is approximately 10,000 TWh/year. To put this into perspective, Table 2.1 shows, for instance, samples of the total hydro potential and current utilization of selected countries. The first three are, globally, the top three countries in terms of total unutilized hydropower potential. At this point in time, unlike the rest of the world, only the USA has exploited over 50% of its hydro potential [45].

In addition to its abundant potential, hydropower is one of the lowest-cost [46] and most efficient sources of renewable energy, with most new hydro facilities currently achieving better efficiency in the conversion to electricity [39]. Companies like Statkraft and SN Power from Norway are investing in hydropower around the world, in order to benefit from its sustainability and future profit.

In the utilization of hydropower resources, the size of the hydropower facility and the performance of the technologies employed play important roles. Well-developed and cost-effective hydro technologies would realize an improved exploitation capacity of hydro resources across the globe.

Table 2.1: An overview of the unutilized hydropower potential of six selected countries [39, 45]

Country	Total potential (GWh/year)	Undeveloped (GWh/year)	Current Utilization (%)
Russian Federation	1 670 000	1 509 829	10%
China	2 140 000	1 013 600	41%
Canada	1 180 737	805 111	32%
Norway	300 000	161 000	45%
Angola	150 000	147 048	3%
Ethiopia	394 200	360 798	8.4%

In the current world status, the size of the installed hydropower facilities ranges from less than 100 kW to larger than 22 GW [39]. Based on their capacity, power generation facilities are classified as large-scale, medium-scale, small- and micro-scale. The latter two are usually run-of-the-river power-generation types that do not change the natural state of the river. They basically use canals or penstocks to channel flowing water from the river to the powerhouse. However, large-scale hydropower generation requires dam construction to store water from flowing river/s.

The recent advance in hydro development focusses on providing technologies with an improved flexibility for better grid stability and approaches to improve and develop efficient low-head turbine technologies that include small- and micro-scale hydropower facilities.

2.5.3 Small- and micro-hydropower

Hydropower facilities with an installed capacity below 100 kW are categorized as micro-scale hydropower (MHP), and those up to 10 MW are categorized as small-scale hydropower (SHP) [46, 47]. The small- and micro-hydropower technologies are economically feasible, with an insignificant impact on ecologies, particularly in less traditional sites with run-of-the-river applications. Moreover, they have relatively low investment costs, unlike large- and medium-scale hydropower facilities.

Small- and micro-scale hydropower are more feasible and reliable for remote villages that are far away from the main transmission zones. In addition, from all off-grid technologies, small- and micro-scale hydropower are the cheapest electricity generation methods, as they do not require expensive construction works and have lesser material and equipment costs [40, 48].

At the end of the 20th century, small hydropower represented the second largest share of the global renewable energy generation, by contributing

8.3% of the total [48]. However, despite the increase in its total capacity, in 2016, the total installed SHP constituted 7% of the total renewable energy, Figure 2.8. Note that wind and solar power are more expensive than large-scale hydropower, while small- and micro-scale hydropower are much cheaper than large-scale hydro facilities.

As of 2016, only about 36% of the global SHP potential is exploited, of which China constitutes the largest share. From Europe (the continent with the highest SHP development rate (48%)), Norway has the largest installed SHP capacity and also ranks 5th in the world, with total SHP potential [40].

Africa, the 4th highest in installed SHP, constitutes 1% of the global installed capacity, with less than 5% SHP development rate, while it has a total of around 12 GW potential. Of the total potential in the continent, East Africa constitutes the largest potential at around 6.7 GW. To date, East Africa has exploited 3% of its potential, with an overall installed SHP potential of only 216 MW. Kenya and Ethiopia have significant potentials of SHP, but they have very low installed potential of only 1% and 0.4%, respectively [40].

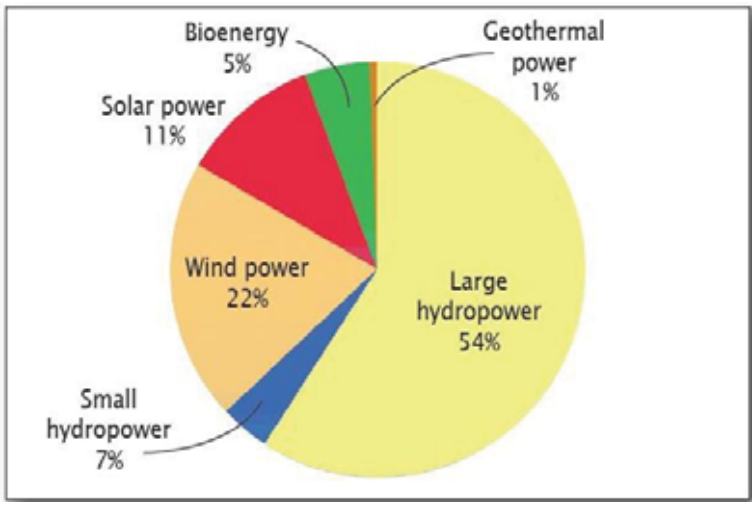

Figure 2.8. Global share of renewable energy (%) [40]

With the increasing global energy demand, reduction in fossil fuel reserves and growing concern regarding global climate change, it is inevitable to the exhaustive use of hydropower, in general, and SHP and MHP in particular. This is particularly important in developing and less developed countries.

In order to best harness the untapped small- and micro-scale hydropower potential, enhancing the performance of their facilities is important. Micro- and small-scale turbines are among the critical parts of the facilities that would enable to enhance their potential. Among others, the cross-flow turbine is one of the most widely applied micro- and small-scale turbines.

2.5.4 Cross-flow hydro turbine design

Compared to conventional small- and micro-scale hydro turbines, the cross-flow turbine is relatively less expensive and flexible in variable working conditions. In addition, the turbine design is simple in operation and uses hands-on technologies for its production and maintenance. The turbine design is more convenient for off-grid run-of-the-river applications in remote areas, particularly in developing and less-developed countries.

Despite the benefits of the turbine design and decades of developments in experimental and computer-based analysis and optimization approaches, the optimum efficiency of the cross-flow turbine remains below the optimum efficiencies of other conventional turbines, Figure 2.9. On the other hand, reports from various experimental and theoretical studies reveal huge inconsistencies in the optimum efficiency results [49-53].

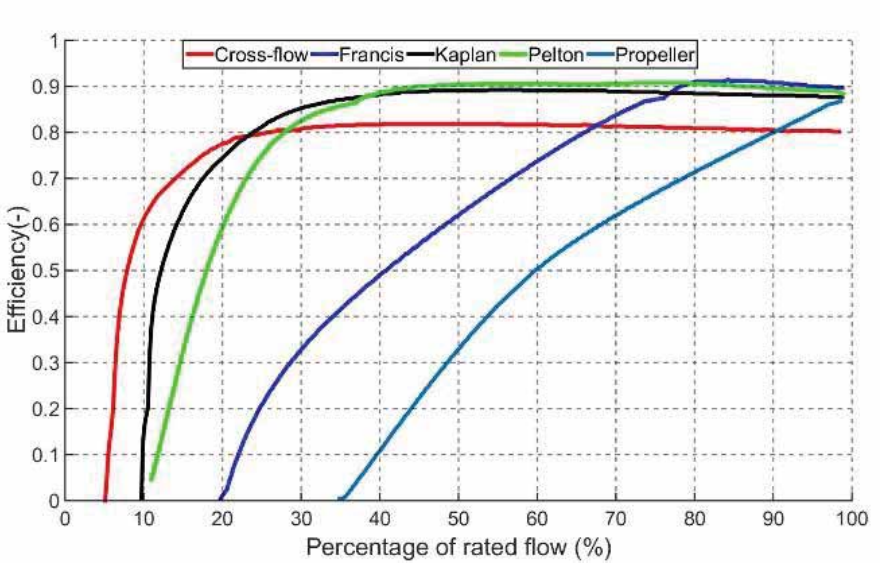

Figure 2.9. Turbine efficiency curves for various small and micro hydro turbines [2]

In this thesis, numerical simulation based optimization studies have been conducted on two different micro cross-flow turbine designs (the T15-300 (one of the T-series designs) and the IAM design, Figures 1.2 and 1.3), both developed and widely applied across the world (for instance in Indonesia, China, Ethiopia, Tanzania, South America and others). In the case studies, important geometric design parameters have been considered.

The shape parameters of the hydrodynamic shape of the guide vane design (guide valve profile, Figure 1.2) inside the nozzle region of the T15-300 turbine have been used in the CFD-based design optimization study (Paper **IV**). In this study, different optimization methods have been used, and performance results from the optimized models have been compared against the original model.

Similarly, the valve angle, the entry wall arc curvature and the rotor shaft diameter, Figure 1.3, are some of the important parameters considered from the IAM turbine design in the numerical simulation based studies

(Papers **V** and **VI**). Their design values are given in detail in the papers. These parameters are utilized in the numerical simulation based design optimization studies, aimed at obtaining the combined effect of the parameters to enhance the power-generation performance of the turbine. The latter two parameters, in particular, influence the second-stage power generation performance. The later power generation stage is the power conversion after the fluid jet crosses the shaft at the centre. Test results from an experimental study conducted at NTNU by Walseth [3] have been utilized for validation purposes. In the experimental setup, Figure 2.10, a strain gauge was attached to one of the rotor's blades to collect moment signals while operating. The reported moment response results were utilized in the studies for the validation and verification of the models and the proposed approaches.

Furthermore, the newly proposed customized DACM framework based design optimization has been carried out, using the theoretical models of cross-flow turbine designs, to improve the theoretical performance of the turbine.

Figure 2.10. Experimental setup for IAM turbine at NTNU [3]

The theoretical performance model of the turbine is based on the hydraulic and geometric parameters, Figure 2.11, developed based on Euler's turbomachinery equation and proposed constraints from onsite tests and experiments.

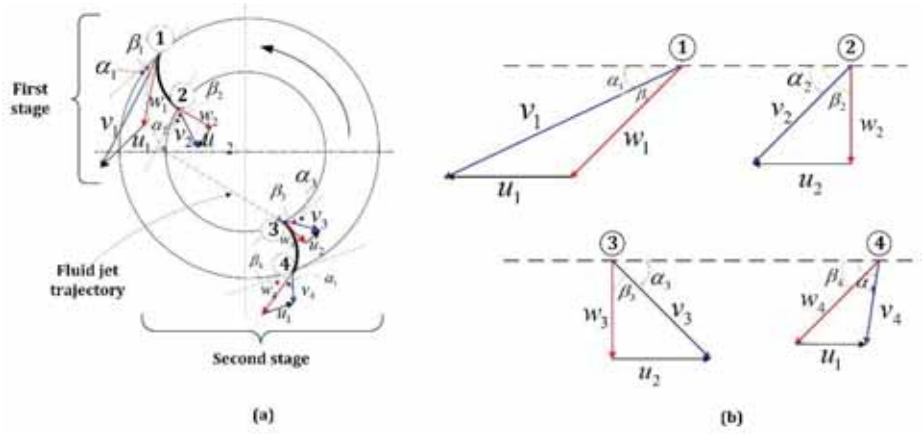

where: w_{1-4} - refer to relative velocities at Points 1-4; u_1 and u_2 - refer to peripheral velocities tangent to the outer and inner diameters respectively. v_{1-4} - refer to actual fluid velocities at Points 1 - 4. α_{1-4} and β_{1-4}- refer to the angles the actual fluid velocities and relative velocities make with the tangent, respectively.

Figure 2.11. Cross-flow turbine's rotor hydrodynamic details: (**a**) fluid jet trajectory and rotor's detail (**b**) velocity triangles at locations 1-4.

3 Research methodologies

3.1 General

In order to achieve the objectives of the research, important methodologies have been devised and followed throughout the course of the study. It is generally started by studying the operational and business values of computer-based computational approaches, with a particular focus on applications in complex and computationally expensive problems. Technical challenges in the implementation of case studies were identified and frameworks are proposed to address the challenges. Based on the scope of the current research, and taking into account conventional procedures in scientific researching, each article appended to the thesis has adhered to the following fundamental procedures.

i. Identify research gaps and challenges.

ii. Conduct background studies and state-of-the-art analyses of the subjects that they are dealing with.

iii. Conceptualize, develop and propose new frameworks and/or approaches to tackle the challenges where required and possible.

iv. Validate and verify the approaches.

v. Select benchmark problems/case studies and applying the proposed frameworks/approaches.

vi. Analyse results, conduct comparative analyses and then report.

Based on the studies conducted following the above fundamental methodological procedures, four optimization frameworks/approaches have been proposed, and their corresponding application results are presented in the appended articles. In the proposed optimization frameworks/approaches, the design variables are identified, the importance level of the variables are studied, and comparative analyses

of computational methods and model validations are conducted whenever required. The connection of the studies in the articles throughout the research period and the proposed frameworks and approaches followed are illustrated in the research structure, Figure 3.1. The proposed frameworks/approaches are briefly summarized in Sub-sections 3.2-3.5, together with flowcharts. The full descriptions can be referred to in the corresponding appended articles.

3.2 Customized DACM based optimization framework

Based on the simplification process of the customized DACM framework, the design variables in high-dimensional problems are categorized as very important (*Xu*) and less important (*Xr*) variables. Once the simplification is completed, as discussed in sub Section 2.3, the optimization process follows in two stages, depending on the designer's preference. The two-stage optimization process is summarized using a flow chart in Figure 3.2.

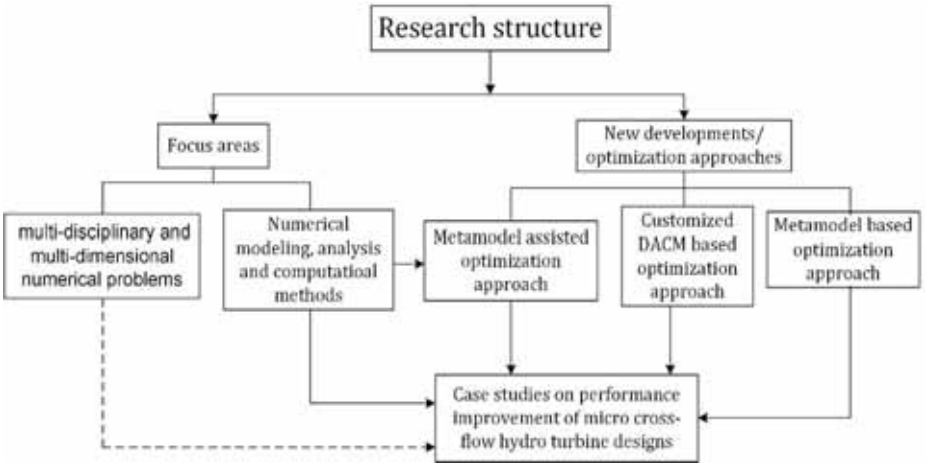

Figure 3.1. Illustration of the research structure.

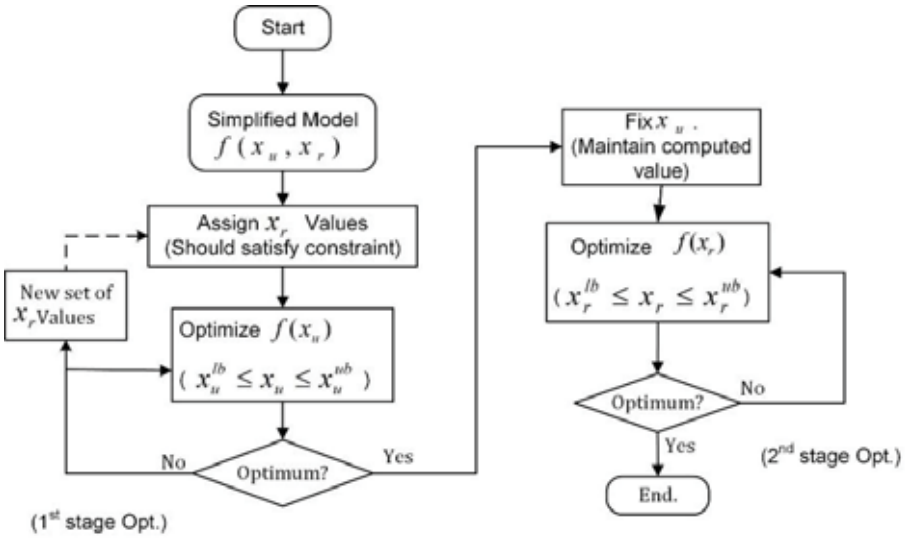

Figure 3.2. Two-stage optimization framework based on customized DACM framework

In the initial process of the first stage, the values of the less important variables should be qualitatively determined. On the other hand, if the designer is satisfied or only interested in the first-stage optimization, the optimization process terminates there. Thus, it is called a single-stage optimization; otherwise, it is a two-stage optimization.

3.3 Metamodel assisted optimization (MMAO) framework

In this category, two separate optimization approaches have been followed. In both cases, the latest MMAO approach based optimization tool (OASIS tool, V1.3) and a commercial modelling and analysis workbench (ANSYS Workbench, ANSYS, Inc., V17.1 [54]) have been utilized; see Figure 3.3(a) and 3.3(b). However, in the first approach, the state-of-the-art basis function (NURBS function) is utilized to model the shape of a geometry, as in the case study in Paper **IV**. In the study, the control points from the NURBS function have served as optimization parameters; a MATLAB script (using MATLAB programming tool,

MathWorks, Inc., R2016b) is used to generate the function. Meanwhile, in the second approach, the optimization tool is directly interfaced to the modelling and analysis workbench. Unlike the first approach, in the second approach, selected geometric parameters from the cases study's model are used as optimization parameters (Papers **V** and **VI**).

The optimization tool used in both approaches utilizes a metamodel that assists the optimization process by generating design points towards the optimum. Radial basis function and Kriging models are used in the metamodelling in the tool. Moreover, intelligent sampling schemes (such as MPS) are used in generating design points. On the other hand, ANSYS Modeller and ANSYS Fluent tools from ANSYS Workbench are used for modelling and analysis. The objective functions are results from the analysis tool. Geometric constraints are also employed, based on the configuration of the case study.

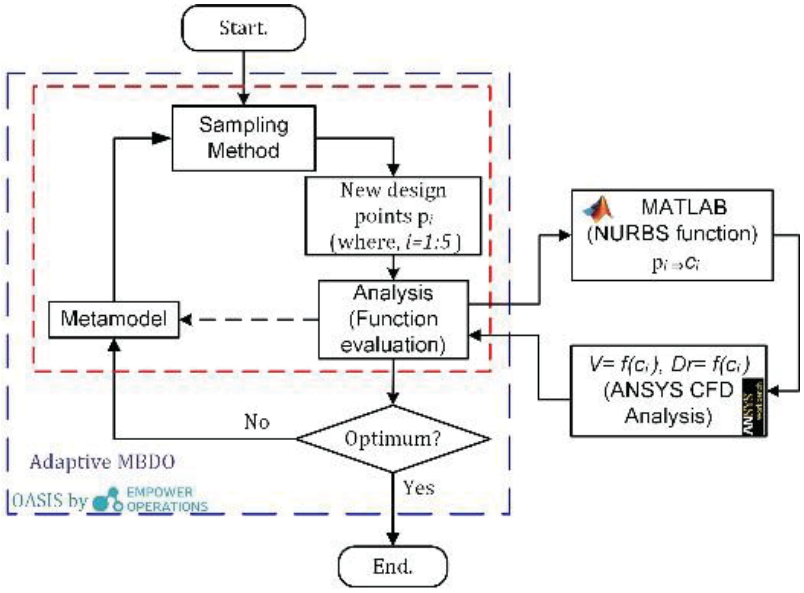

(a)

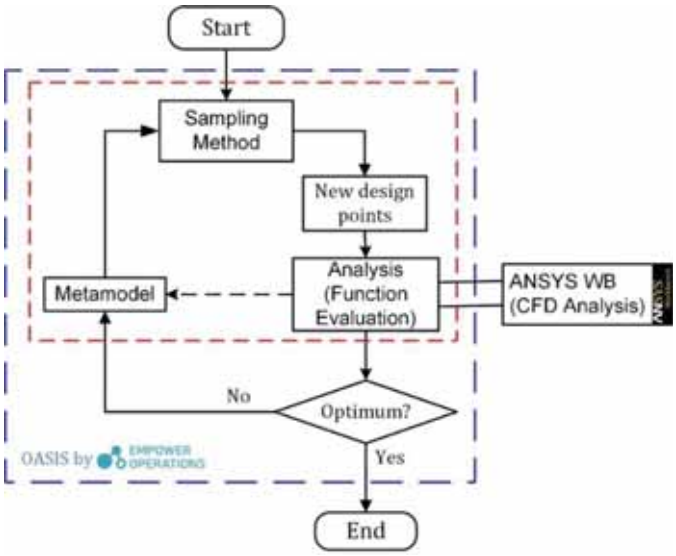

(b)

Figure 3.3. Metamodel assisted optimization frameworks: (a) utilize NURBS function; (b) direct-interface with ANSYS Workbench

3.4 Direct GA-based optimization framework

Similar to the first approach in Section 3.3 above, this framework has employed the state-of-the-art basis function and the ANSYS Workbench. The latter is used for modelling as well as analysis. However, the widely applied metaheuristic global optimization tool, Genetic Algorithm (GA), is utilized for the design optimization process, Figure 3.4. The GA is one of the nature-inspired optimization algorithms. The optimization algorithm imitates the theory of natural evolution. It employs the principle of breeding (crossover) and mutation to generate new design points (generations) from the selected best sample points (parents). MATLAB scripts are developed and used for the GA, as well as NURBS function. The total number of generations and stall generations are used as stopping criteria in the optimization process, in addition to the convergence tolerances.

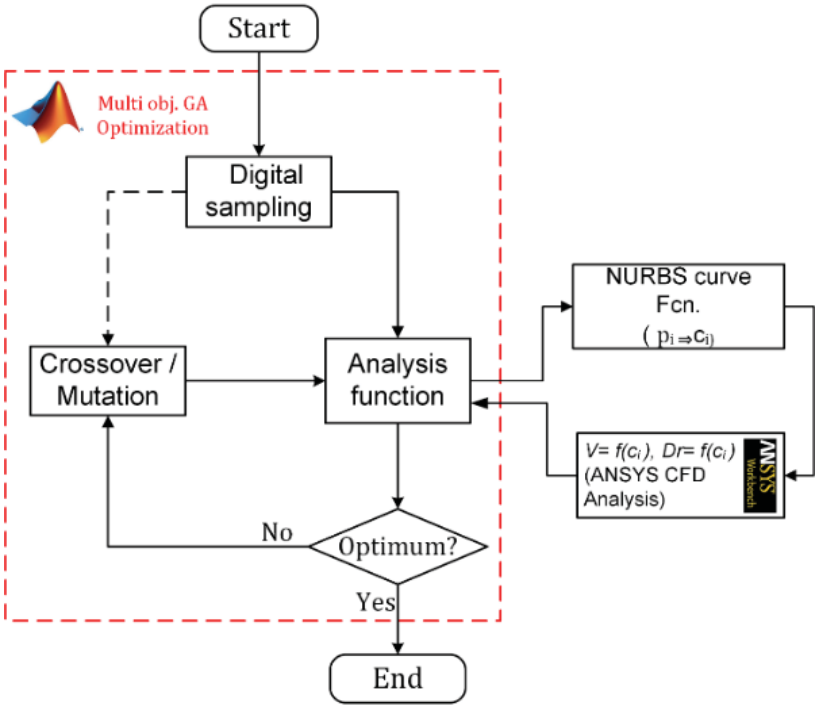

Figure 3.4. Direct GA based optimization framework

3.5 Artificial Neural-Network Metamodel- GA-based optimization (ANN-MMBO)

Unlike any of the above frameworks, this approach utilizes a metamodel to approximate and completely replace the original model. The machine-learning tool, the ANN model, is used for metamodelling; see Figure 3.5. The ANN requires experimental samples, generated using design point sample data in the design space, to train, validate and test the model to approximate and replace the original model. In the application, a full-factorial DOE method is used to generate the sample data in the metamodelling process. The DOE method is used to obtain an efficient design of the experiment from the digital simulation using the analysis tool; in the case study, 243 sample, ***Appendix 1***, of digital experimental data are generated and used in general to train (70% of the sample),

validate (15% of the sample) and test (15% of the sample) the model. On the other hand, the GA algorithm is used to optimize the design, using the final ANN metamodel as the objective function of the problem.

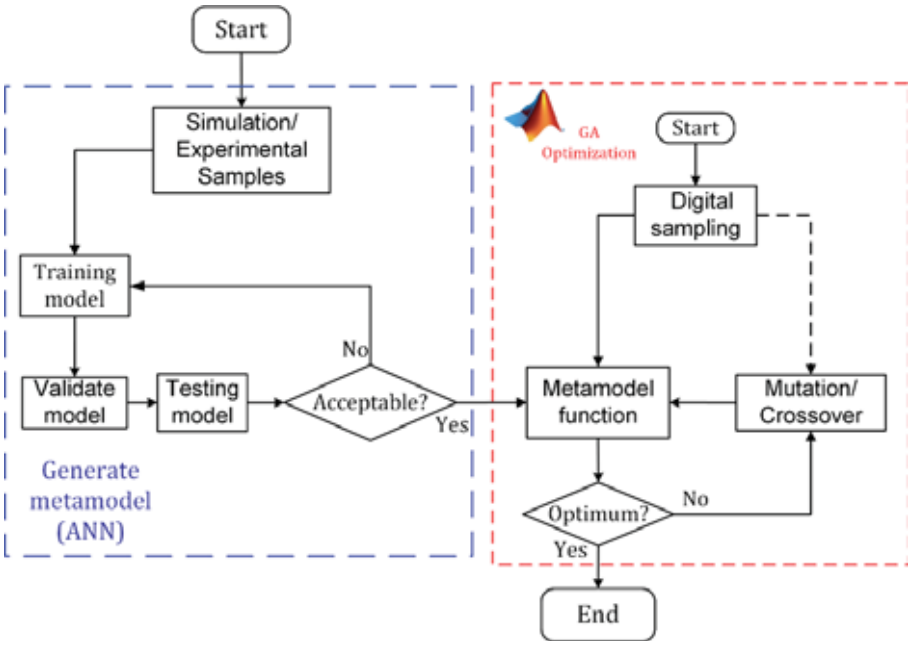

Figure 3.5. ANN-MMBO metamodel-based optimization

4 Discussion of results

As computer-based modelling, analysis and simulation tools advance to more precise and diverse applications, the operation eventually become more complex and expensive. Apart from that, in complex multidiscipline and multidimensional problems, proper modelling, analysing and processing is often demanding that the process requires relatively longer computational time, large storage resource to secure the data and skilled manpower. Moreover, integrating design optimization operation to the product and system development process through numerical modelling and simulation makes the process even more complex and expensive. The studies in this thesis, therefore, identifies some of the challenges, as well as review the state-of-the-art tools proposed to tackle the challenges. In addition, four new optimization approaches/frameworks are proposed aiming to tackle the challenges associated with complex computationally expensive optimization problems; their applications, case studies, on cross-flow hydro turbine designs (one of the widely applied micro hydro turbine) are presented.

One of the identified challenge that create computational complexity in both CAD modelling and finite element based simulation, and optimization based on the simulation is the separate development of the advanced computer-based modelling and analysis tools technologies in the market; separate development with regard to their building block function, basis function. An isogeometric analysis method, the latest analysis method, which utilizes same state-of-the-art basis function, such as NURBS or T-Spline function, for both modelling and analysis, is introduced and discussed. This method has been reported, in various studies and applications, to simplify problems and reduce their computational costs. Moreover, in this thesis, one of the state-of-the-art basis functions, NURBS function, is used in one of the newly proposed metamodel-based optimization frameworks.

The fluid-structure interaction (FSI) problem, a multidisciplinary problem, is one of the widely occurring problems in diverse applications. For instance, in aircraft design, offshore structures, ship designs, medical sciences and so many others. Understanding the specific challenges involved in such problems is a way to solve them. Hence, in this thesis, numerical FSI techniques and various computational methods are discussed. The comparative analysis of computational methods on a benchmark problem revealed that the result from the strongly coupled two-way partitioned approach is more realistic than its counterpart, the simpler one-way coupled approach.

The customized DACM based optimization framework, a novel simplification/decomposition approach-based optimization, is proposed to reduce the computational costs of complex high-dimensional optimization problems. The numerical approach is applied and tested on the theoretical mathematical models of a cross-flow hydro turbine. The result from the proposed single-stage optimization framework demonstrates that the approach is more effective and efficient. It returned a better objective value, and reduced the function evaluation to one-fifth of the original, thus largely reduces the computational cost.

Moreover, the other optimization approaches/frameworks proposed utilize metamodel in the numerical simulation based optimization processes. In the two MMAO frameworks, the metamodel is used to generate samples towards the optimum region. The first MMAO framework was used in shape optimization, which constitutes NURBS function. This framework was applied and tested on a widely applied cross-flow turbine model (T15-300) to optimize the shape of its guide valve aiming to enhance its performance. The case study result from applying this framework is compared with the result from the original model and from applying the direct GA based optimization approach. The result from the first MMAO approach estimated a 5.33% improvement on the performance, while the direct GA based approach estimated 4.73% improvement, Table 4.1. However, the first MMAO

approach converged much faster than its counterpart. The second MMAO framework also demonstrated an interesting performance on another case study application, in Papers **V** and **VI**.

The third metamodel-based optimization framework (ANN-MMBO), on the other hand, utilizes a metamodel to approximate as well as completely replace the original model. The GA optimization algorithm and the ANN metamodelling are used in the framework. The ANN-MMBO framework is also applied in a case study on the T15-300 cross-flow hydro turbine. Two hundred and forty-three (243) numerical experiment design samples were generated, and a 10-hidden-layer ANN architecture is used to train, validate and test the metamodel generated for the five-parameter numerical problem. The three operations were continued until the acceptable mean square error, the stopping criteria, to the metamodelling process was reached (where the regression (***R***) should be above 0.95 for the model to converge, as seen in Figure 4.1.) A *Random Data Division* and *Levenberg-Marquardt* training algorithms are selected in ANN MATLAB programming tool script.

Table 4.1. Application results for three different optimization approaches

Turbine Model	P_1 **(m)**	P_2 **(m)**	P_3**(m)**	P_4**(m)**	P_5**(m)**	**Power Output (Watt)**	**% increase of output power**
Original	0.151600	0.16092	0.2450	0.2500	0.1370	4841.83	
Direct GA	0.143077	0.16730	0.23089	0.2458	0.1331	5070.89	4.73
MMAO (OASIS)	0.142430	0.15588	0.23567	0.2406	0.1209	5099.85	5.33
ANN-MMBO	0.145377	0.163163	0.22554	0.2519	0.1317	5035.71	4.0

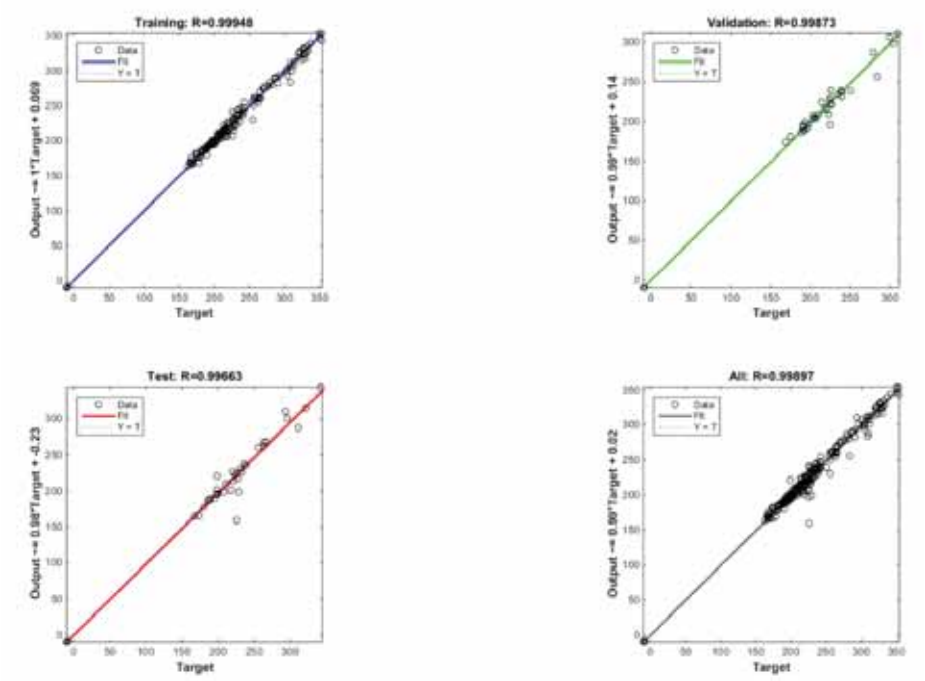

Figure 4.1. Training, validation, test and all data graph in ANN metamodelling process

The ANN-MMBO approach converged within less than two minutes for the conditions and stopping criteria given in Table 4.2, which is much faster than the first MMAO approach and the direct GA approach. The best selected optimum design from the Pareto fronts also returned an estimated 4% performance improvement. However, it took more than a day and a half to obtain the numerical design of experiment samples used to generate the metamodel.

Table 4.2. Given conditions, stopping criteria and results of the ANN-MMBO application

Population	Generation	Stall generation	Total function Evaluation	Total generation	Stopping time (s)
500	1000	50	201,001	401	113.031

Figure 4.2 illustrates the total moment responses from the rotor walls of the original and optimized models; i.e. from the direct GA based, the first MMAO and the ANN-MMBO approaches.

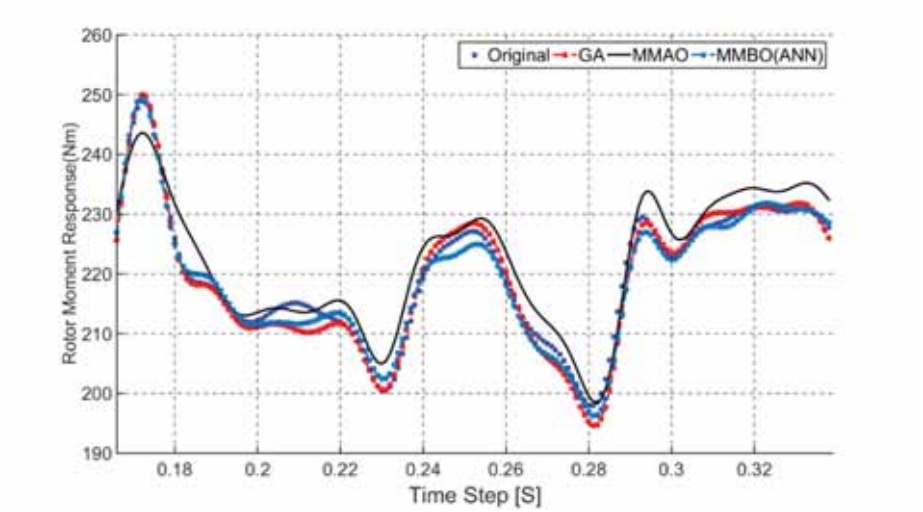

Figure 4.2. Total rotor moment responses comparison graph on the T15-300 cross-flow turbine model

5 Concluding remarks and recommendations for future work

The study conducted in this research revealed that utilization of the same basis function, such as NURBS function, for both modelling and analysis in the finite element based analysis approach, is a milestone in precise representation of the models in the analysis process. This, in addition, facilitates the realization of simpler simulation-based design optimization process. This fundamental integration approach saves significant amount of computational time that could be wasted otherwise.

The customized DACM approach based optimization framework is a novel framework proposed in this research. The simplification and decomposition methods have given the framework remarkable power to considerably reduce the computational cost in optimization processes. The case study deploying the framework, using one of the methods, demonstrates its simplifying capability by reducing the total function evaluation to 1/5, without compromising the objective value.

In order to enhance the performance of micro cross-flow hydro turbines through design optimization, as in the case studies, the proposed MMAO and MMBO frameworks were deployed. In the case studies presented in the thesis, results from the newly proposed design optimization frameworks that employ the metamodelling approach demonstrated better estimated performance than results from the original models as well as from the framework employing conventional approach.

In the conclusion, the MMAO-based optimization framework demonstrated comparatively better performance; hence, its application in other similar high-dimensional numerical simulation based optimization problems is recommended. On the other hand, the ANN-MMBO based optimization framework is suggested preferably for

problems with available experimental sample data as the effort of obtaining new data might be costly; depends on the case under consideration.

Finally, further development on the customized DACM based optimization approach is recommended to better automate the processes in the framework, as well as for general applications in different fields of study.

Based on the acquired knowledge from the current studies in the thesis, the author suggests future application of the MMAO and MMBO frameworks on the turbine designs considering the FSI between the valve structure and the fluid; in that case, any structural deformation due to the fluid pressure will be included. Moreover, verification of the optimized models and the frameworks, using physical tests, are also recommended.

6 Scientific contributions

Contrary to the growing benefits from the advancing computer-based modelling, analysis and optimization operations, the processes are becoming more complex, expensive and error prone, particularly when dealing with complex multidisciplinary and multidimensional problems. Simplifying the complexity and reducing associated computational costs without significantly compromising the accuracy is the way forward. On the other hand, with the growing energy demand, the intervention of the computer-based operations plays greater role in contributing to the climate-change mitigation. Based on the objectives conceived at the beginning of the research, the studies in the thesis contributed the following scientific achievements:

i. A novel simplification and decomposition approach based framework is developed and introduced. An optimization framework is developed, employing the approach to tackle multidimensional optimization problems.

ii. New frameworks, with architectures to integrate two widely applied tools (ANSYS Workbench and MATLAB) and optimization tools (MMAO (OASIS) and GA from MATLAB) are developed and introduced.

iii. Optimization frameworks that utilize state-of-the-art metamodel-assisted optimization approach are developed, introduced and employed in case studies.

iv. An optimization framework that utilizes metamodel-based approximation approach deploying the well-known machine-learning tool is introduced and employed in a case study.

v. An important development in performance enhancement of cross-flow turbines through design optimization is achieved.

vi. A new design optimization approach, focusing only on critical parts of reaction turbine designs in general and cross-flow turbine in particular, is developed and introduced.

7 Summary of appended papers

In this section, the six research articles appended to the thesis are summarized. Important results from the papers are discussed in order to highlight the focus areas of each article.

Paper I.

Paper **I** conducts state-of-the-art analysis on the IGA method, particularly focusing its application on nonlinear simulation based optimization problems. It reviews various studies and identifies some of the challenges of its application in simulation-based optimization operations of nonlinear problems. At the outset, the fundamental motivation behind the utilization of the IGA method in most applications is its seamless integration of numerical modelling and analysis operations, and its flexibility and robustness in both operations. In addition, the method utilizes the state-of-the-art basis functions in both modelling and analysis that enable accurate representation of problems. NURBS and T-splines are two of the B-spline-based basis functions that the IGA method utilize. Algorithms developed in IGA to solve nonlinear simulation-based problems are presented. The study indicates that, in different areas of application, simulation-based design optimization based on the IGA method outperformed the conventional FEM method. However, only limited researches have been conducted in the area so far. In the survey, some of the studies reported patch mismatching problems at domain interfaces due to the irregular parameterization problems at boundaries and due to the independent control points manipulation capability of the method. However, techniques to avoid the encountered problems were introduced. The study also presents a preliminary comparison between CAD-, FEM- and IGA-based optimization frameworks.

Paper II.

The second appended paper, Paper **II**, carries out comparative analysis of computational methods in FSI problem, which is one of the widely occurring multidisciplinary problem in science and engineering. The multidisciplinary nature of the problem mostly brings complexity to the analysis process. The article discusses the most common techniques employed in solving FSI problems. It is indicated that part of the computational complexity in such problems arise principally from the modelling and analysis of the interfaces. The interfaces of FSI problems are usually treated as independent parts. Computational approaches and techniques based on spatial and temporal discretization schemes in various studies have been reviewed and their basic principles are discussed in the article. Monolithic, partitioned, one-way and two-way coupled approaches are the four basic numerical analysis method classifications in FSI problems. The standard FSI coupling conditions, the Dirichlet and Neumann conditions, are also discussed in the article.

Moreover, a case study on the widely applied FSI benchmark configuration, known as the HronTurek configuration, Figure 7.1 and Table 7.1 has been conducted for the comparison of two commonly used FSI computational methods. The benchmark configuration is the configuration of a channel flow of incompressible laminar fluid over an elastic structure attached to a cylinder. A parabolic fluid velocity profile is applied at the inlet (left side) of the channel. In the study on the benchmark, comparisons between computational responses from application of different solution methods and different material property magnitudes are also studied.

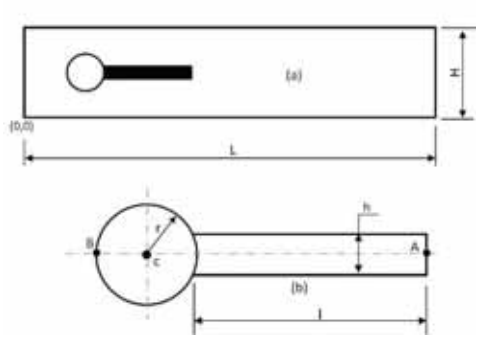

Figure 7.1. HronTurek FSI benchmark channel configuration (a) entire model (b) magnified details of the structure model.

Deformation responses at selected location, point A, on the benchmark configuration, are utilized for comparison. Responses from a strongly coupled two-way partitioned approach, employing an open source code, known as OpenFoam, and a one-way coupled partitioned approach, employing a commercial modelling and analysis tool, ANSYS Workbench are compared. The results demonstrate that the strongly coupled portioned approach return a more realistic result than that of its counterpart; see Figure 7.2.

Table 7.1. Geometric parametric values of the benchmark FSI channel configuration.

Geometric parameters		**Value [m]**
Channel length	L	2.5
Channel width	H	0.41
Cylinder center position	C	(0.2, 0.2)
Cylinder radius	r	0.05
Elastic structure length	l	0.35
Elastic structure thickness	h	0.02
Reference point (at t=0)	A	(0.6, 0.2)
Reference point	B	(0.15, 0.2)

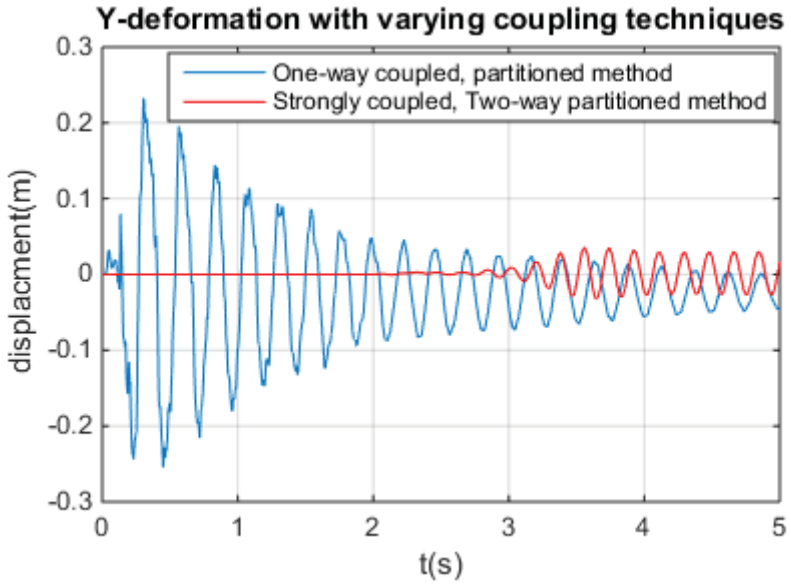

Figure 7.2. y-axis deformation responses in time at point A.

Paper III.

This paper introduces a novel simplification and decomposition approach that is used in solving expensive high-dimensional optimization problems. The approach is based on customized dimensional analysis conceptual modelling (DACM) framework. The DACM framework is a modelling and simulation framework originally developed for conceptual modelling and simulation in systems design. The fundamental theory from the well-practised dimensional analysis (DA), concepts from functional modelling and bond graphing are utilized in the framework. Cause-effect relations analysis between variables and functions in a problem is the other basic principle in the framework. The original DACM framework is customized to serve in the simplification and decomposition of models in high-dimensional optimization problems. In the customized framework, statistical design of experiment tools are utilized to measure the impact levels of variables in the decomposition stage. Simplifying, as well as decomposing, followed by optimization of high-dimensional expensive problems, to

lower the computational cost without compromising the objective function results, are the focuses of the approach.

To illustrate the approach, a case study using theoretical mathematical models of cross-flow turbine design was employed in the paper. The design configuration of a T15-300 cross-flow turbine design with initial conditions of 10 m head and 350-rpm rotational speed of the rotor are considered. Important geometric and hydraulic parameters are identified and utilized. The presented case study in the article aimed to improve the theoretical performance of the micro hydro-turbine design. In the case study, different shapes and colours are used to separate different categories of variables. Figure 7.3 illustrates the causal network of the original model after propagating the qualitative objectives, whereas Figure 7.4 illustrates the simplified causal network of the models. For detailed analysis of the network and the parameters in it, please refer to appended article, Paper **III**.

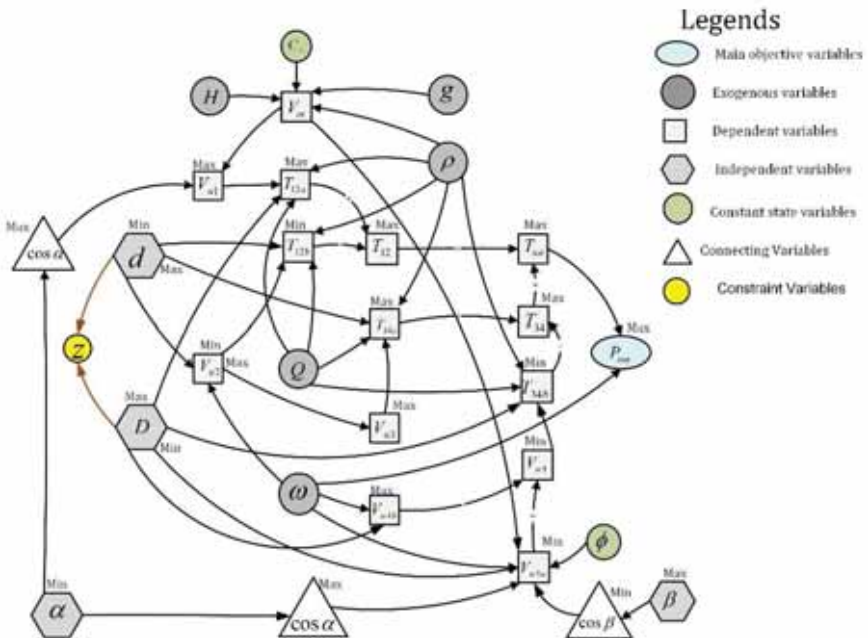

Figure 7.3. Causal network using the original theoretical models.

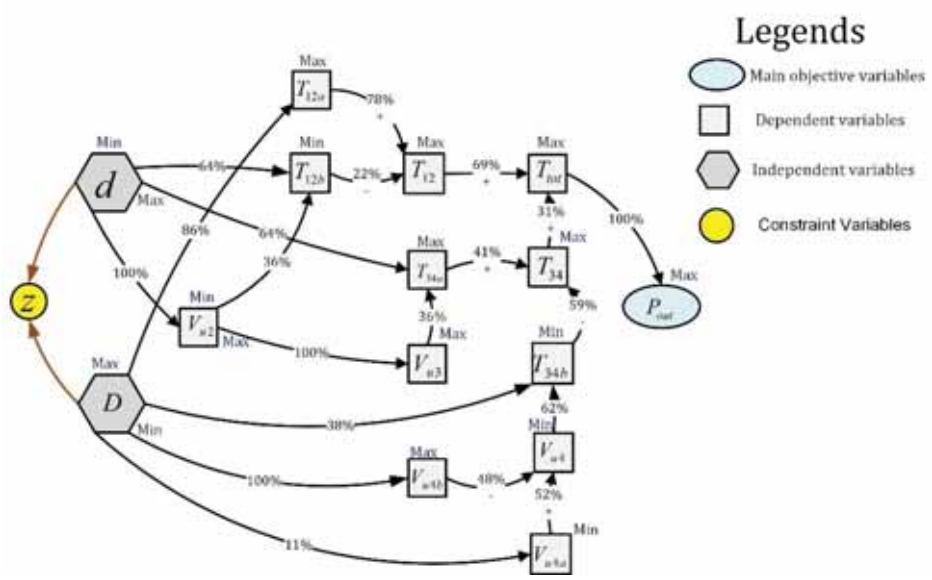

Figure 7.4. Causal network after the simplification.

An optimization framework based on the customized DACM and GA tool was developed in MATLAB and applied in the case study. From the two proposed approaches, the single-step optimization framework was employed in the case study. The simplified model, based on the proposed approach, converged faster and returned better results than the original un-simplified model, Table 7.2. The function evaluation was reduced to 1/5 of that of the application on the original model.

Table 7.2. Optimization results of the theoretical model

Model	Design Variables				Target value	*Pout*	# of Function Evaluations
	α	β	D	d			
Original	15	25.232	0.3020	0.2423	57891	57891.0	10971.8
Single step	15	30	0.3009	0.2139	57891	63660.1	2132.8

Paper IV.

Paper **IV** introduces a CFD-driven design optimization method which utilizes metamodelling in the optimization framework (MMAO) to assist the optimization process, Figure 3.3(a). On the other hand, as turbines are critical parts in hydropower facilities, the framework is applied on the T15-300 turbine model, aiming to enhance its performance. The T15-300 turbine design, Figure 1.2, is one of the widely applied cross-flow turbine designs in small- and micro-hydro facilities.

In the study, the optimization approach in the framework is applied to one of the critical parts of the turbine, the valve, which controls the fluid flow as well as determines the velocity and pressure magnitudes of the fluid jet leaving the nozzle region in the turbine. NURBS function in MATLAB tool is used to design the valve profile, Figure 7.5. The function generates construction points for the valve profile curve design in the modelling and analysis tool, in ANSYS Workbench.

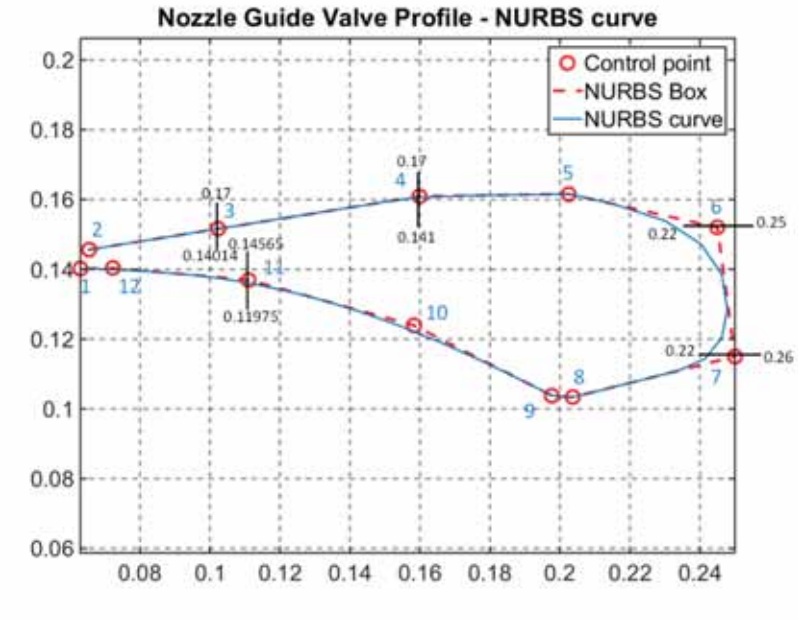

Figure 7.5. NURBS curve of the valve profile

Of the twelve control points (as indicated in the figure), coordinates of the five that are highly sensitive to the output power are selected as parameters for design optimization. In the study, the curve function serves to generate a total of 50 construction points that are used in the modeling of the valve profile in the modeling tool. Which implies that, utilizing the NURBS function saves computational time by reducing the total number of optimization parameters by at least 45 if polynomial function was used to generate the same curve for the valve profile.

Apart from the optimization approach, the other most important approach followed in the study of this paper is the utilization of the separate nozzle design in the design optimization, Figure 7.6. The approach is followed assuming the turbine is an impulse type turbine, and understanding that the nozzle region plays a significant role in the performance of such turbine. Correlation study is carried out between performance parameters from the separate nozzle and full turbine model to validate the assumptions. Drag force on the valve wall and y-axis component of the fluid outlet velocity at the Outlet (2), Figure 7.6(b), are the objective functions in the multi-objective optimization processes.

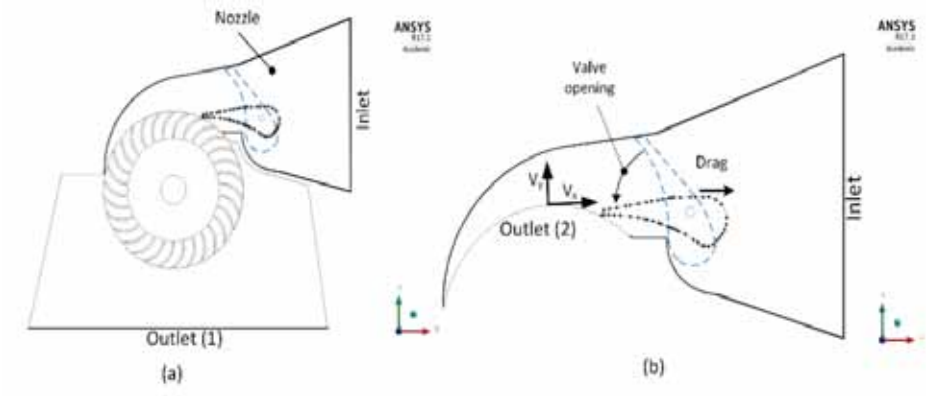

Figure 7.6. Boundaries configurations of T15-300 cross-flow turbine design; (a) full turbine model and (b) separate nozzle design.

In addition to the MMAO, the direct GA based optimization framework is also applied in this study for comparison.

The numerical study result, using initial conditions of a 12.5 m head and 360 rpm rotor speed demonstrated that the optimized models from both optimization frameworks, the MMAO and direct GA based, have better estimated performance than the original model. In fact, they have showed 5.53% and 4.73% improvement on the output numerical performance, respectively. Moment responses from the entire rotor walls are also collected and compared, as shown in Figure 7.7.

Moreover, for visual evaluation, the velocity streamline contour comparison figures of the steady analyses results of the selected optimum models are presented in the study, see Figure 7.8(a-c). The figures demonstrated that, the optimized models have lesser fluid-band width at the first quarter than the original model. Lower fluid-band width implies lower ineffective fluid volume as it hits the back side of the blade at the second-stage.

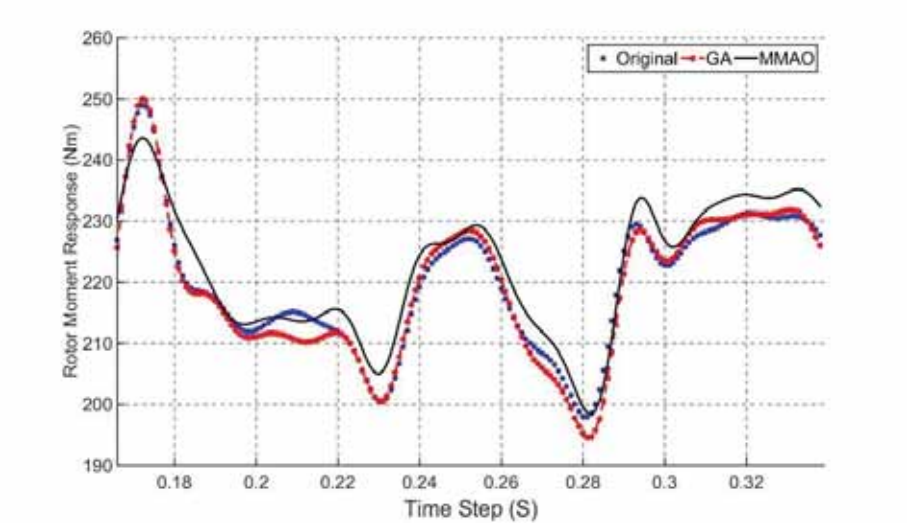

Figure 7.7. Moment responses from the entire rotor blade surfaces.

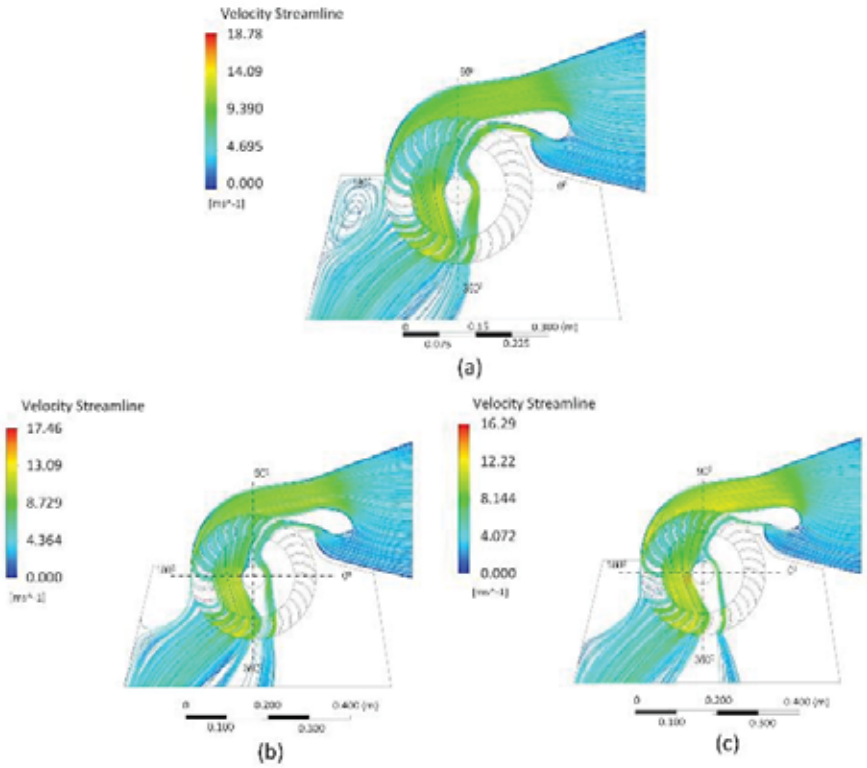

Figure 7.8. Velocity streamline contour figures of steady analysis results from (a) original model, (b) direct GA based and (c) MMAO-based optimization models.

Paper V.

This paper conducts effect characterization of selected geometric parameters on the IAM design, Figure 1.3, the other widely applied cross-flow turbine design. Following on that, numerical simulation-based design optimization is conducted using selected geometric design parameters aiming to improve the turbine's performance. Three important geometric parameters (i.e. the valve angle, the entry arc curvature and the shaft diameters) are chosen, see Figure 7.9.

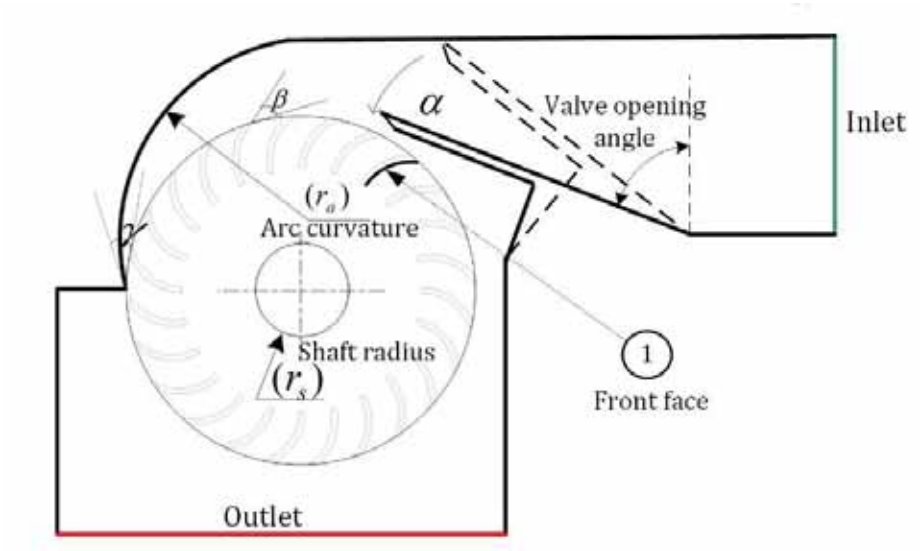

Figure 7.9. 2D model of IAM turbine design.

In order to reduce the computational time and the associated cost, 2D model of the turbine is utilized in the design optimization process of the study. Change trend of (effect on) the output power due to change in valve angle from the experimental test are compared against results from the numerical models. The study is using initial conditions of 5 m head and 360-rpm rotational speed.

Based on the qualitative and quantitative studies, it is demonstrated in the article that the valve angle has a greater effect on the output power than the other two parameters.

The optimization tool is directly interfaced with the modelling and analysis tool. The MMAO tool is utilized in the design optimization process using the 2D model. The indicators of the results from the optimum model from the optimization, demonstrates a better performance of the model compared to the original. However, it needs subsequent studies to verify the result.

Paper VI.

Paper **VI** is an extended work of the later paper, Paper **V**. The study in the paper conducts a numerical simulation-driven effect characterization on the IAM turbine design. Unlike the study in Paper **V**, this paper carries out the effect analysis on the 3D numerical model of the turbine. Apart from that, the change trends of moment coefficient responses collected from walls of the entire rotor blades are compared against experimental test result to conduct sensitivity analysis on the numerical models, Figure 7.10. Moreover, the analysis on the moment coefficient responses enable to visualize the characteristics of the two power generation stages.

Similar to Paper **V**, the MMAO based optimization framework, Figure 3.3(b), is employed in this study.

Based on the comparative and qualitative studies on the numerical moment coefficient responses and output performances, the report on the paper shows that the optimized model returns better results than both original models at 80% and 100% valve opening positions at both 350 and 250 rpm of the rotor; see Figure 7.11 and 7.12.

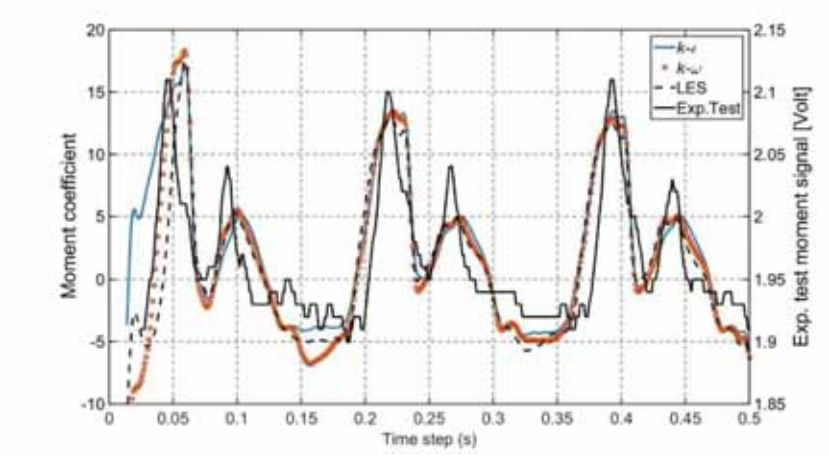

Figure 7.10. Sensitivity test viscous numerical model against experimental response.

The study indicates that based on the numerical study on the optimized and original models, the optimized model demonstrates 17.88% improvement in efficiency than the original at 250-rpm rotational speed the rotor at which the experimental study referred reports the optimum. However, the authors suggest subsequent numerical and experimental studies to verify the results.

On the other hand, the paper discusses the computational benefits and outcomes of the optimization framework based on the observed optimization results in the paper.

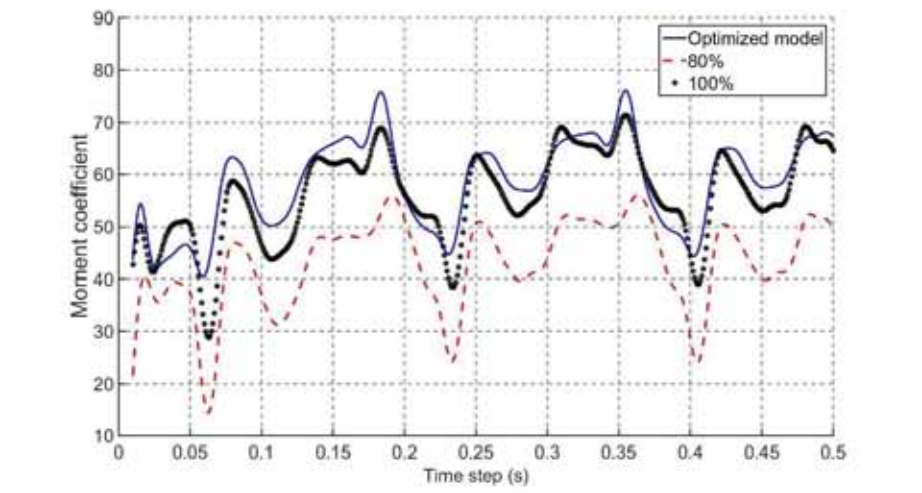

Figure 7.11. Moment coefficient response comparison of the optimized model against 80% and 100% valve opening at 350 rpm rotor speed.

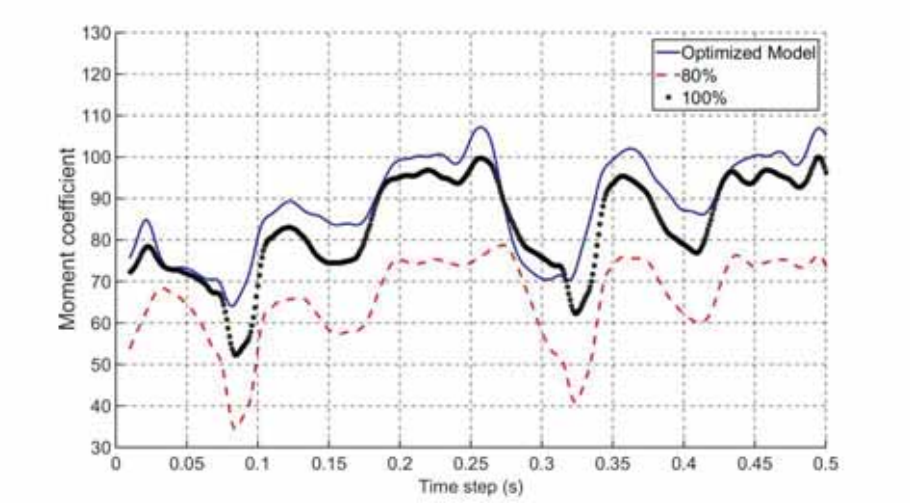

Figure 7.12. Moment coefficient response comparison of the optimized model against 80% and 100% valve opening at 250 rpm rotor speed

References

[1] E. Coatanéa, R. Roca, H. Mokhtarian, F. Mokammel, and K. Ikkala, "A conceptual modeling and simulation framework for system design," *Computing in Science & Engineering*, vol. 18, no. 4, pp. 42-52, 2016.

[2] J. A. Tuhtan, "Cost Optimization of Small Hydropower," Master of Science Water Resources Engineering and Management, Universität Stuttgart, 2007.

[3] E. C. Walseth, "Investigation of the Flow through the Runner of a Cross-Flow Turbine," Institutt for energi-og prosessteknikk, 2009.

[4] J. A. Cottrell, T. J. Hughes, and Y. Bazilevs, *Isogeometric analysis: toward integration of CAD and FEA*. John Wiley & Sons, 2009.

[5] S. Arabshahi, D. C. Barton, and N. K. Shaw, "Steps towards CAD-FEA integration," *Engineering with Computers*, journal article vol. 9, no. 1, pp. 17-26, 1993.

[6] D. Rypl and B. Patzák, "From the finite element analysis to the isogeometric analysis in an object oriented computing environment," *Advances in Engineering Software*, vol. 44, no. 1, pp. 116-125, 2012.

[7] L. V. Tran, A. Ferreira, and H. Nguyen-Xuan, "Isogeometric analysis of functionally graded plates using higher-order shear deformation theory," *Composites Part B: Engineering*, vol. 51, pp. 368-383, 2013.

[8] H. Nguyen-Xuan, C. H. Thai, and T. Nguyen-Thoi, "Isogeometric finite element analysis of composite sandwich plates using a higher order shear deformation theory," *Composites Part B: Engineering,* vol. 55, pp. 558-574, 2013.

[9] H. Kapoor and R. Kapania, "Geometrically nonlinear NURBS isogeometric finite element analysis of laminated composite plates," *Composite Structures,* vol. 94, no. 12, pp. 3434-3447, 2012.

[10] A. P. Nagy, S. T. IJsselmuiden, and M. M. Abdalla, "Isogeometric design of anisotropic shells: optimal form and material distribution," *Computer Methods in Applied Mechanics and Engineering,* vol. 264, pp. 145-162, 2013.

[11] S.-g. ZHANG, Y.-w. WANG, and Z.-d. HUANG, "Isogeometric shell analysis and shape optimization," *Chinese Journal of Computational Mechanics,* vol. 31, no. 1, pp. 115-119, 2014.

[12] D. Benson, Y. Bazilevs, M.-C. Hsu, and T. Hughes, "A large deformation, rotation-free, isogeometric shell," *Computer Methods in Applied Mechanics and Engineering,* vol. 200, no. 13, pp. 1367-1378, 2011.

[13] J. M. Kiendl, *Isogeometric analysis and shape optimal design of shell structures*. Shaker, 2011.

[14] S. Hosseini, J. J. Remmers, C. V. Verhoosel, and R. De Borst, "An isogeometric continuum shell element for non-linear analysis,"

Computer Methods in Applied Mechanics and Engineering, vol. 271, pp. 1-22, 2014.

[15] Y. Bazilevs, V. M. Calo, Y. Zhang, and T. J. Hughes, "Isogeometric fluid–structure interaction analysis with applications to arterial blood flow," *Computational Mechanics,* vol. 38, no. 4-5, pp. 310-322, 2006.

[16] Y. Bazilevs, M.-C. Hsu, and M. Scott, "Isogeometric fluid–structure interaction analysis with emphasis on non-matching discretizations, and with application to wind turbines," *Computer Methods in Applied Mechanics and Engineering,* vol. 249, pp. 28-41, 2012.

[17] C. Heinrich, R. Duvigneau, and L. Blanchard, "Isogeometric shape optimization in fluid-structure interaction," Research Report, RR 7639, INRIA, 2011.

[18] F.-K. Benra, H. J. Dohmen, J. Pei, S. Schuster, and B. Wan, "A comparison of one-way and two-way coupling methods for numerical analysis of fluid-structure interactions," *Journal of applied mathematics,* vol. 20, 2011.

[19] G. Hou, J. Wang, and A. Layton, "Numerical methods for fluid-structure interaction—a review," *Communications in Computational Physics,* vol. 12, no. 2, pp. 337-377, 2012.

[20] J. Degroote, "Partitioned simulation of fluid-structure interaction," *Archives of Computational Methods in Engineering,* vol. 20, no. 3, pp. 185-238, 2013.

[21] T. Richter, "Numerical methods for fluid-structure interaction problems," *Institute for Applied Mathematics, University of Heidelberg, Germany*, 2010.

[22] G. I. Barenblatt, Scaling, Self-similarity, and Intermediate Asymptotics: dimensional analysis and intermediate asymptotics. Cambridge University Press. ISBN: 0521435226, 1996.

[23] R. Bhaskar and A. Nigam, "Qualitative physics using dimensional analysis," *Artificial Intelligence*, vol. 45, no. 1, pp. 73-111, 1990.

[24] P. Goos and B. Jones, *Optimal design of experiments: a case study approach*. John Wiley & Sons, 2011.

[25] L. Gu, "A comparison of polynomial based regression models in vehicle safety analysis," in *ASME Design Engineering Technical Conferences - Design Automation Conference*, Pittsburgh, PA, 2001, vol. 2, pp. 509-514.

[26] T. W. Simpson, J. Poplinski, P. N. Koch, and J. K. Allen, "Metamodels for computer-based engineering design: survey and recommendations," *Engineering with computers*, vol. 17, no. 2, pp. 129-150, 2001.

[27] G. G. Wang and S. Shan, "Review of metamodeling techniques in support of engineering design optimization," *Journal of Mechanical design*, vol. 129, no. 4, pp. 370-380, 2007.

[28] L. Wang, S. Shan, and G. G. Wang, "Mode-pursuing sampling method for global optimization on expensive black-box functions," *Engineering Optimization*, vol. 36, no. 4, pp. 419-438, 2004.

[29] G. H. Cheng, A. Younis, K. H. Hajikolaei, and G. G. Wang, "Trust region based mode pursuing sampling method for global optimization of high dimensional design problems," *Journal of Mechanical Design*, vol. 137, no. 2, p. 021407, 2015.

[30] K. H. Hajikolaei, G. H. Cheng, and G. G. Wang, "Optimization on Metamodeling-Supported Iterative Decomposition," *Journal of Mechanical Design*, vol. 138, no. 2, p. 021401, 2016.

[31] B. Sharif, G. G. Wang, and T. Y. ElMekkawy, "Mode pursuing sampling method for discrete variable optimization on expensive black-box functions," *Journal of Mechanical Design*, vol. 130, no. 2, p. 021402, 2008.

[32] E. O. Corp. (2016, January 6). *Integrate and Optimize*. Available at: https://empoweroperations.com/en/oasis/

[33] S. S. Haykin, *Neural networks and learning machines*. Pearson Upper Saddle River, NJ, USA:, 2009.

[34] J. Smrekar, D. Pandit, M. Fast, M. Assadi, and S. De, "Prediction of power output of a coal-fired power plant by artificial neural network," *Neural Computing and Applications*, journal article vol. 19, no. 5, pp. 725-740, July 01 2010.

[35] S. De, M. Kaiadi, M. Fast, and M. Assadi, "Development of an artificial neural network model for the steam process of a coal biomass cofired combined heat and power (CHP) plant in Sweden," *Energy*, vol. 32, no. 11, pp. 2099-2109, 2007.

[36] A. T. Hammid, M. H. B. Sulaiman, and A. N. Abdalla, "Prediction of small hydropower plant power production in Himreen Lake dam (HLD) using artificial neural network," *Alexandria Engineering Journal*, 2017/01/07/ 2017.

[37] U.S. EIA, "International Engergy Outlook 2017," in "International Engergy Outlook," U.S. Engergy Information Adminstration Report September, 2017 2017, Available at: https://www.eia.gov/outlooks/ieo/.

[38] UNFCCC. (2014, February 02). *The Paris Agreement*. Available at: http://unfccc.int/paris_agreement/items/9444.php

[39] WEC, "World Energy Resources 2016," in "World Energy Resources," World Energy Council, Strategic Occtober 2016 2016, vol. 80 Available at: https://www.worldenergy.org/publications/2016/world-energy-resources-2016/, Accessed on: August 2017.

[40] UNIDO, "World Small Hydropower Development Report 2016," United Nations Industrial Development Organization 2016, Available at: https://open.unido.org/publications/.

[41] REN21. (2016, August 2017). *Renewables 2016 Global Status Report* [Electronic]. Available at: hhttp://www.ren21.net/status-of-renewables/global-status-report/renewables-2016-global-status-report/

[42] IHA, "2016 Hydropower Status Report," International Hydropower Association Anual Report 2016, Available at:

https://www.hydropower.org/2016-hydropower-status-report, Accessed on: August 2017.

[43] IEA, "African Energy Outlook," International Energy Agency, Report 2014, Available at: https://www.iea.org/publications/freepublications/publication/weo-2014-special-report-africa-energy-outlook.html, Accessed on: August 2017.

[44] F. H. Koch, "Hydropower—the politics of water and energy: Introduction and overview," *Energy Policy*, vol. 30, no. 14, pp. 1207-1213, 2002.

[45] IHA, "2017 Hydropower Status Report," in "Hydropower Status Report," International Hydropower Association Report 2017 2017, Available at: https://www.hydropower.org/2017-hydropower-status-report, Accessed on: September 2017.

[46] IRENA, "Renewable Power Generation Costs in 2014," in "Renewable Power Generation Costs," International Renewable Energy Agency, Report January 2015, Available at: http://www.irena.org/menu/index.aspx?mnu=Subcat&PriMenuID=36&CatID=141&SubcatID=494, Accessed on: August 2017.

[47] ICSHP, *WHAT IS SHP?* Available at: http://www.inshp.org/detail.asp?RID=8&BID=80, Accessed on: August 2017

[48] C. Dragu, T. Sels, and R. Belmans, "Small Hydro Power: State of the art and applications," in *Power generation and sustainable development. International conference*, 2001, pp. 265-270.

[49] V. Sammartano, C. Aricò, A. Carravetta, O. Fecarotta, and T. Tucciarelli, "Banki-michell optimal design by computational fluid dynamics testing and hydrodynamic analysis," *Energies*, vol. 6, no. 5, pp. 2362-2385, 2013.

[50] N. H. Pereira and J. Borges, "A Study on the Efficiency of a Cross-Flow Turbine Based on Experimental Measurements," in *Proceedings of the 5th International Conference on Fluid Mechanics and Heat & Mass Transfer (FLUIDSHEAT'14), Lisbon, Portugal*, 2014, pp. 63-72.

[51] W. Durgin and W. Fay, "Some fluid flow characteristics of a cross-flow type hydraulic turbine," *Small Hydro Power Fluid Machinery*, pp. p77-83, 1984.

[52] C. A. Mockmore and F. Merryfield, "The Banki water turbine," Bulletin Series No. 25, Engineering Experimental Station, Oregon State System of Higher Education, Oregon State College, NY, 1949.

[53] N. C. Pereira and J. Borges, "Study of the nozzle flow in a cross-flow turbine," *International journal of mechanical sciences*, vol. 38, no. 3, pp. 283-302, 1996.

[54] ANSYS Inc., *Engineering Simulation Platform*. Available t: http://www.ansys.com/products/platform, Accessed on: June 2017.

Appendices

Appendix 1 – Design of experiment sample data

#	P1 (*m*)	P2 (*m*)	P3 (*m*)	P4 (*m*)	P5 (*m*)	V_X[1] (*m/s*)	Drag force (*N*)
1	0.14565	0.17	0.25	0.25	0.14014	-9.2794636	225.17262
2	0.14565	0.16092	0.22	0.22	0.14014	-9.3836756	185.99548
3	0.14014	0.141	0.25	0.22	0.11975	-9.6295444	208.89504
4	0.141	0.17	0.22	0.22	0.137	-9.3016012	208.45792
5	0.16092	0.17	0.245	0.25	0.137	-9.179816	277.18751
6	0.14565	0.17	0.245	0.25	0.14014	-9.4596925	227.22919
7	0.16092	0.17	0.25	0.22	0.11975	-9.8223791	301.94948
8	0.1516	0.17	0.25	0.22	0.137	-9.3909381	242.47285
9	0.16092	0.17	0.245	0.26	0.137	-9.2389645	279.76664
10	0.16092	0.17	0.25	0.22	0.137	-9.4413697	310.6452
11	0.17	0.17	0.22	0.26	0.137	-9.1313218	313.82579
12	0.1516	0.17	0.22	0.22	0.137	-9.4523258	228.77509
13	0.141	0.14565	0.22	0.22	0.14014	-9.0715836	228.83031
14	0.17	0.17	0.25	0.26	0.14565	-9.0362839	328.75468
15	0.141	0.17	0.25	0.25	0.14565	-9.346496	202.95384
16	0.141	0.17	0.245	0.22	0.137	-9.3377636	209.72329
17	0.16092	0.17	0.25	0.25	0.14565	-9.049567	271.86204
18	0.17	0.17	0.22	0.25	0.137	-9.1160294	312.7896
19	0.14014	0.16092	0.245	0.26	0.137	-9.4721584	181.80439
20	0.17	0.17	0.25	0.26	0.137	-9.0339125	332.73372
21	0.16092	0.17	0.22	0.25	0.14565	-9.2190326	254.65086
22	0.1516	0.17	0.245	0.25	0.137	-9.4240651	238.43522
23	0.14014	0.14014	0.25	0.22	0.11975	-9.565118	217.88123
24	0.141	0.1516	0.245	0.22	0.137	-9.3384831	174.9141

[1] V_X = X-component velocity

#	P1 (*m*)	P2 (*m*)	P3 (*m*)	P4 (*m*)	P5 (*m*)	V_X^1 (*m/s*)	Drag force (*N*)
25	0.14014	0.16092	0.245	0.25	0.11975	-9.8451096	223.75612
26	0.14014	0.17	0.25	0.22	0.137	-9.335498	214.99148
27	0.1516	0.17	0.25	0.26	0.11975	-9.9050529	265.76347
28	0.141	0.17	0.245	0.26	0.137	-9.4090418	212.85703
29	0.141	0.17	0.22	0.25	0.137	-9.4218125	198.86814
30	0.1516	0.16092	0.25	0.26	0.11975	-9.9237854	234.80789
31	0.1516	0.16092	0.25	0.26	0.137	-9.3644187	213.48489
32	0.16092	0.17	0.25	0.22	0.14565	-9.3262524	308.73044
33	0.14014	0.141	0.25	0.22	0.137	-9.2577039	188.26854
34	0.14014	0.17	0.25	0.26	0.11975	-9.8878375	240.95259
35	0.14565	0.17	0.22	0.25	0.14014	-9.3085712	208.06018
36	0.14565	0.16092	0.25	0.26	0.14014	-9.3839963	198.08159
37	0.14014	0.16092	0.25	0.26	0.11975	-9.9168411	220.82092
38	0.1516	0.16092	0.25	0.25	0.14565	-9.2289804	202.99649
39	0.1516	0.17	0.22	0.25	0.11975	-9.8347762	234.57709
40	0.141	0.1516	0.22	0.22	0.11975	-9.8181621	188.83136
41	0.14014	0.17	0.25	0.26	0.137	-9.3521292	214.13479
42	0.1516	0.17	0.25	0.25	0.11975	-9.8949681	266.32722
43	0.14565	0.16092	0.245	0.26	0.14014	-9.3980763	194.37594
44	0.16092	0.17	0.25	0.25	0.11975	-9.6355546	293.66706
45	0.141	0.1516	0.25	0.25	0.137	-9.4276366	178.35127
46	0.16092	0.17	0.22	0.26	0.137	-9.1568224	263.47904
47	0.17	0.17	0.25	0.25	0.14565	-8.9956304	320.7584
48	0.1516	0.17	0.245	0.26	0.137	-9.5136091	239.98978
49	0.1516	0.16092	0.25	0.22	0.11975	-9.9566652	232.72097
50	0.141	0.14565	0.25	0.25	0.14014	-9.2462635	166.8875
51	0.17	0.17	0.25	0.22	0.14565	-8.8990979	322.09868
52	0.141	0.17	0.22	0.22	0.14565	-9.4319623	224.61425
53	0.14014	0.17	0.25	0.25	0.11975	-9.7854001	225.82555
54	0.141	0.1516	0.22	0.25	0.14565	-9.7854001	225.82555

#	P1 (*m*)	P2 (*m*)	P3 (*m*)	P4 (*m*)	P5 (*m*)	V_X^1 (*m/s*)	Drag force (*N*)
55	0.17	0.17	0.25	0.25	0.11975	-9.509841	350.05094
56	0.1516	0.17	0.245	0.26	0.14565	-9.3213452	230.82028
57	0.14014	0.141	0.25	0.26	0.137	-9.2975796	170.27695
58	0.1516	0.16092	0.245	0.26	0.14565	-9.2190398	204.84378
59	0.14014	0.17	0.22	0.26	0.137	-9.4041781	198.06776
60	0.14014	0.17	0.25	0.22	0.11975	-9.7195209	236.13736
61	0.146	0.1516	0.245	0.26	0.14565	-9.2706216	169.81605
62	0.17	0.17	0.25	0.22	0.11975	-9.399634	350.02864
63	0.1516	0.16092	0.245	0.25	0.14565	-9.3141245	201.57479
64	0.16092	0.17	0.245	0.22	0.11975	-9.7121376	286.12593
65	0.16092	0.17	0.22	0.22	0.14565	-9.1594417	255.89678
66	0.14565	0.16092	0.22	0.26	0.14014	-9.4454004	181.28932
67	0.141	0.14565	0.245	0.25	0.14014	-9.3528334	162.72653
68	0.14565	0.17	0.22	0.26	0.14014	-9.3376795	215.53491
69	0.17	0.17	0.245	0.26	0.11975	-9.5662116	342.21705
70	0.141	0.17	0.25	0.22	0.137	-9.346186	214.85795
71	0.14565	0.17	0.25	0.26	0.14014	-9.4870778	255.79081
72	0.14014	0.16092	0.22	0.26	0.137	-9.3906735	175.91573
73	0.14565	0.16092	0.25	0.22	0.14014	-9.2295499	198.52231
74	0.14014	0.141	0.245	0.22	0.11975	-9.6270839	199.99764
75	0.1516	0.16092	0.22	0.22	0.11975	-9.6172526	236.0396
76	0.17	0.17	0.22	0.26	0.14565	-9.0063586	304.17736
77	0.1516	0.17	0.245	0.25	0.11975	-10.052853	261.99325
78	0.17	0.17	0.245	0.26	0.14565	-8.9504052	324.65402
79	0.17	0.17	0.245	0.26	0.137	-9.2095128	331.80805
80	0.1516	0.17	0.245	0.26	0.11975	-9.9046473	264.06475
81	0.1516	0.16092	0.22	0.26	0.14565	-9.256853	187.64581
82	0.17	0.17	0.245	0.25	0.14565	-8.9615508	321.46606
83	0.1516	0.17	0.25	0.26	0.137	-9.6551679	263.16333
84	0.141	0.1516	0.22	0.22	0.137	-9.2078066	190.13568

#	P1 (*m*)	P2 (*m*)	P3 (*m*)	P4 (*m*)	P5 (*m*)	V_X^1 (*m/s*)	Drag force (*N*)
85	0.14014	0.17	0.22	0.26	0.11975	-9.8058162	231.49035
86	0.14014	0.16092	0.245	0.22	0.137	-9.3314805	188.44185
87	0.1516	0.16092	0.245	0.26	0.137	-9.2618728	211.87102
88	0.141	0.1516	0.25	0.26	0.14065	-9.3668196	178.12925
89	0.14014	0.141	0.245	0.22	0.137	-9.1632985	192.25812
90	0.16092	0.17	0.22	0.26	0.14565	-9.0546753	257.15209
91	0.141	0.1516	0.25	0.22	0.14	-9.3362461	174.09898
92	0.1516	0.16092	0.245	0.25	0.11975	-9.7154645	219.57751
93	0.14014	0.141	0.245	0.26	0.137	-9.3661612	165.5106
94	0.1516	0.16092	0.25	0.22	0.14565	-9.1706027	205.98041
95	0.14014	0.141	0.25	0.26	0.11975	-9.9120463	199.38632
96	0.16092	0.17	0.22	0.22	0.137	-9.2145261	263.21427
97	0.14014	0.17	0.245	0.22	0.11975	-9.8018701	232.83215
98	0.14014	0.16092	0.245	0.22	0.137	-9.3297998	189.29571
99	0.16092	0.17	0.245	0.22	0.14565	-9.062959	271.31685
100	0.14014	0.141	0.22	0.25	0.11975	-9.521315	242.66505
101	0.1516	0.16092	0.22	0.22	0.14565	-9.2002223	196.87709
102	0.1516	0.16092	0.25	0.22	0.137	-9.3616459	214.53371
103	0.14014	0.141	0.245	0.22	0.137	-9.1631927	190.29703
104	0.1516	0.16092	0.25	0.25	0.137	-9.2660993	215.00663
105	0.16092	0.17	0.22	0.25	0.137	-9.1844601	258.61287
106	0.16092	0.17	0.25	0.25	0.137	-9.2789806	278.8008
107	0.14014	0.141	0.245	0.25	0.11975	-9.8897471	197.54518
108	0.14014	0.17	0.245	0.26	0.137	-9.3422565	211.35448
109	0.14014	0.141	0.22	0.25	0.137	-9.1156551	216.82172
110	0.141	0.17	0.25	0.26	0.137	-9.3399644	215.80258
111	0.1516	0.17	0.25	0.25	0.14565	-9.2588063	249.96445
112	0.16092	0.17	0.22	0.26	0.11975	-9.6468454	291.02564
113	0.14014	0.16092	0.25	0.25	0.11975	-9.8028209	226.88028
114	0.14014	0.16092	0.22	0.22	0.137	-9.3672108	182.20401

#	P1 (*m*)	P2 (*m*)	P3 (*m*)	P4 (*m*)	P5 (*m*)	V_X[1] (*m/s*)	Drag force (*N*)
115	0.1516	0.17	0.25	0.22	0.11975	-9.6230925	257.5792
116	0.14014	0.141	0.22	0.25	0.137	-9.1330038	216.65398
117	0.14014	0.16092	0.25	0.25	0.137	-9.3797952	190.18065
118	0.1516	0.17	0.245	0.22	0.14565	-9.1295738	230.02901
119	0.14014	0.16092	0.22	0.22	0.11975	-9.8229696	200.16746
120	0.14014	0.16092	0.25	0.25	0.137	-9.3533656	190.09637
121	0.1516	0.17	0.22	0.26	0.11975	-9.6294607	239.07562
122	0.14014	0.141	0.22	0.22	0.11975	-9.6474588	265.85327
123	0.1516	0.17	0.25	0.25	0.137	-9.2519779	243.60038
124	0.14014	0.17	0.245	0.22	0.137	-9.3837102	209.25928
125	0.14014	0.141	0.245	0.26	0.137	-9.3716499	166.7596
126	0.17	0.17	0.22	0.26	0.11975	-9.5550983	333.71271
127	0.141	0.17	0.22	0.26	0.11975	-9.8175466	214.15135
128	0.141	0.17	0.25	0.26	0.11975	-9.8690099	239.9548
129	0.141	0.1516	0.22	0.26	0.11975	-9.9157885	195.86017
130	0.1516	0.17	0.22	0.26	0.14565	-9.1975174	217.93926
131	0.16092	0.17	0.25	0.26	0.11975	-9.7869888	310.06103
132	0.16092	0.17	0.245	0.26	0.14565	-9.1900307	269.59989
133	0.141	0.17	0.25	0.25	0.137	-9.3513757	213.32151
134	0.146	0.1516	0.245	0.25	0.14565	-9.2739337	174.11106
135	0.1516	0.17	0.245	0.25	0.14565	-9.124684	231.59832
136	0.1465	0.17	0.245	0.26	0.14565	-9.3253461	223.78474
137	0.1516	0.17	0.25	0.22	0.14565	-9.182996	234.84494
138	0.14014	0.141	0.22	0.26	0.11975	-9.6747727	256.07855
139	0.1516	0.16092	0.245	0.25	0.137	-9.3023042	210.24403
140	0.14014	0.17	0.245	0.22	0.137	-9.3057675	209.21877
141	0.16	0.167	0.245	0.25	0.137	-9.1824135	263.38872
142	0.1516	0.16092	0.25	0.26	0.14565	-9.2776622	206.42382
143	0.14014	0.16092	0.245	0.25	0.137	-9.3480273	185.52869
144	0.17	0.17	0.22	0.25	0.11975	-9.4409728	325.94497

#	P1 (*m*)	P2 (*m*)	P3 (*m*)	P4 (*m*)	P5 (*m*)	V_X^1 (*m/s*)	Drag force (*N*)
145	0.14014	0.17	0.25	0.25	0.137	-9.4224869	205.44153
146	0.1516	0.152	0.245	0.22	0.11975	-9.8647869	223.74634
147	0.14014	0.16092	0.22	0.25	0.11975	-9.7797248	217.38763
148	0.165	0.168	0.245	0.25	0.14565	-9.0468231	282.52196
149	0.1516	0.17	0.25	0.26	0.14565	-9.3495476	236.87209
150	0.1516	0.152	0.22	0.25	0.11975	-9.8141114	198.73855
151	0.141	0.145	0.245	0.26	0.137	-9.3173276	167.35306
152	0.17	0.17	0.245	0.22	0.14565	-8.9448246	320.02605
153	0.156	0.1562	0.245	0.26	0.11975	-9.9181705	232.82866
154	0.167	0.1678	0.25	0.26	0.14565	-9.0874004	295.48443
155	0.1516	0.16092	0.245	0.26	0.11975	-9.9664981	219.20986
156	0.1516	0.158	0.22	0.25	0.137	-9.3813721	189.95002
157	0.165	0.1682	0.245	0.22	0.137	-9.1294609	289.62284
158	0.1516	0.156	0.22	0.22	0.14565	-9.2931922	183.20315
159	0.1516	0.16092	0.245	0.22	0.137	-9.3518062	208.99315
160	0.165	0.1678	0.22	0.25	0.11975	-9.6374938	304.28185
161	0.1516	0.152	0.245	0.26	0.11975	-9.9059252	218.11041
162	0.1516	0.16092	0.245	0.22	0.11975	-9.7473128	225.37085
163	0.1516	0.17	0.22	0.22	0.14565	-9.2403594	217.5304
164	0.14014	0.17	0.22	0.25	0.11975	-9.7575614	219.28999
165	0.14014	0.16092	0.25	0.26	0.137	-9.3698428	191.24919
166	0.145	0.148	0.22	0.22	0.11975	-9.7533427	219.84015
167	0.145	0.148	0.25	0.25	0.11975	-9.7443078	202.41451
168	0.14014	0.141	0.22	0.26	0.137	-9.0868976	217.74553
169	0.1516	0.152	0.22	0.26	0.14565	-9.1864479	167.6104
170	0.1516	0.16092	0.22	0.25	0.11975	-9.7233451	217.5126
171	0.165	0.16892	0.25	0.26	0.137	-9.1323173	299.82553
172	0.14014	0.16092	0.245	0.22	0.11975	-9.7068524	211.53297
173	0.14014	0.16092	0.245	0.26	0.11975	-9.9219285	220.70507
174	0.1516	0.1521	0.25	0.26	0.11975	-9.9095167	223.31925

#	P1 (*m*)	P2 (*m*)	P3 (*m*)	P4 (*m*)	P5 (*m*)	V_X[1] (*m/s*)	Drag force (*N*)
175	0.165	0.1692	0.22	0.25	0.11975	-9.8235458	311.05711
176	0.17	0.17	0.245	0.25	0.11975	-9.6047065	353.36608
177	0.165	0.1692	0.22	0.22	0.11975	-9.7965588	292.60554
178	0.165	0.169	0.245	0.22	0.14565	-9.1296731	286.52377
179	0.14014	0.17	0.22	0.22	0.11975	-10.010836	223.22471
180	0.1516	0.16092	0.245	0.22	0.14565	-9.2143603	203.33877
181	0.1516	0.17	0.22	0.22	0.11975	-9.8363491	254.69386
182	0.14014	0.16092	0.245	0.25	0.137	-9.3362569	186.38623
183	0.1516	0.1541	0.22	0.26	0.137	-9.2667928	182.72305
184	0.165	0.1692	0.245	0.26	0.11975	-9.6360048	329.66818
185	0.15	0.16	0.245	0.25	0.11975	-9.9153095	228.32125
186	0.17	0.17	0.25	0.26	0.11975	-9.5015583	352.9945
187	0.14014	0.17	0.22	0.22	0.137	-9.4028658	205.56426
188	0.14014	0.17	0.245	0.25	0.11975	-9.8921725	238.91939
189	0.14014	0.141	0.25	0.25	0.137	-9.3252076	169.99807
190	0.152	0.1561	0.25	0.22	0.14565	-9.2266106	197.34154
191	0.152	0.1561	0.22	0.25	0.14565	-9.2417737	180.80498
192	0.14014	0.17	0.245	0.25	0.137	-9.4066659	207.30229
193	0.152	0.1561	0.245	0.22	0.11975	-9.8870818	220.42418
194	0.17	0.17	0.25	0.22	0.137	-9.1231069	327.15717
195	0.14014	0.16092	0.22	0.25	0.137	-9.4736548	173.87306
196	0.152	0.1561	0.25	0.26	0.14565	-9.1936733	198.83378
197	0.14014	0.16092	0.25	0.22	0.137	-9.3623064	191.90566
198	0.14014	0.141	0.245	0.25	0.137	-9.3902725	169.11533
199	0.1516	0.16092	0.22	0.25	0.137	-9.2398985	201.78222
200	0.1516	0.17	0.22	0.26	0.137	-9.3471518	227.34749
201	0.1516	0.17	0.245	0.22	0.137	-9.3471518	227.34749
202	0.1516	0.16092	0.22	0.25	0.14565	-9.2934666	188.28782
203	0.14014	0.17	0.22	0.25	0.137	-9.4013412	190.9631
204	0.1516	0.1561	0.25	0.22	0.11975	-9.7184344	220.77485

#	P1 (*m*)	P2 (*m*)	P3 (*m*)	P4 (*m*)	P5 (*m*)	V_X[1] (*m/s*)	Drag force (*N*)
205	0.14014	0.141	0.25	0.22	0.137	-9.2513942	188.24175
206	0.17	0.17	0.22	0.22	0.14565	-8.8838343	308.35437
207	0.14014	0.17	0.245	0.26	0.11975	-9.9051182	239.28341
208	0.17	0.17	0.22	0.22	0.137	-9.1252048	308.42319
209	0.1516	0.17	0.22	0.25	0.14565	-9.3372847	216.66413
210	0.156	0.16092	0.245	0.25	0.14565	-9.2490934	218.02865
211	0.156	0.16092	0.245	0.25	0.11975	-9.8750115	226.20767
212	0.17	0.17	0.25	0.25	0.137	-9.0034185	327.9973
213	0.1516	0.1561	0.25	0.25	0.11975	-9.9078796	227.51861
214	0.1516	0.1561	0.25	0.22	0.137	-9.3384403	204.46398
215	0.17	0.17	0.245	0.22	0.137	-9.0961886	320.19876
216	0.1516	0.1561	0.245	0.22	0.14565	-9.350685	195.01838
217	0.152	0.1561	0.25	0.22	0.11975	-9.8047232	224.14878
218	0.1516	0.1561	0.245	0.25	0.137	-9.3503936	197.17391
219	0.1516	0.1561	0.25	0.25	0.14565	-9.2476195	193.20316
220	0.1516	0.1561	0.25	0.26	0.137	-9.5334317	226.09326
221	0.14014	0.17	0.245	0.26	0.137	-9.3784636	210.96458
222	0.1516	0.16092	0.22	0.22	0.137	-9.2720946	201.54089
223	0.14014	0.17	0.22	0.22	0.137	-9.4391282	205.1236
224	0.1516	0.16092	0.25	0.25	0.11975	-9.7214999	228.82564
225	0.156	0.1562	0.22	0.26	0.137	-9.3226074	199.16942
226	0.156	0.1562	0.22	0.26	0.14565	-9.2174461	190.85209
227	0.14014	0.17	0.25	0.22	0.137	-9.344418	215.01329
228	0.14014	0.141	0.25	0.26	0.137	-9.3354571	167.92095
229	0.17	0.17	0.245	0.22	0.11975	-9.6505277	337.13582
230	0.14014	0.16092	0.22	0.25	0.137	-9.3497692	174.57847
231	0.14014	0.141	0.22	0.22	0.137	-9.0823266	235.70792
232	0.17	0.17	0.22	0.22	0.11975	-9.5740122	327.11634
233	0.17	0.17	0.245	0.25	0.137	-9.201961	328.1166
234	0.1516	0.16092	0.22	0.26	0.11975	-9.904558	205.45799

#	P1 (*m*)	P2 (*m*)	P3 (*m*)	P4 (*m*)	P5 (*m*)	V_X^1 (*m/s*)	Drag force (*N*)
235	0.1516	0.16092	0.22	0.26	0.137	-9.3764854	197.78091
236	0.1516	0.17	0.245	0.22	0.11975	-9.7398794	283.92733
237	0.17	0.17	0.22	0.25	0.14565	-8.9325391	304.12772
238	0.14014	0.141	0.22	0.26	0.137	-9.0534994	218.25481
239	0.1516	0.1561	0.245	0.25	0.11975	-9.7450468	218.39108
240	0.14014	0.141	0.245	0.26	0.11975	-9.6395481	201.54828
241	0.1516	0.17	0.22	0.25	0.137	-9.240172	225.88521
242	0.14014	0.16092	0.22	0.26	0.11975	-9.484695	202.11792
243	0.14014	0.141	0.25	0.25	0.11975	-9.7370264	193.51296

Part II: Appended Papers

Paper IV

CFD-Driven Valve Shape Optimization for Performance Improvement of a Micro Cross-Flow Turbine

Endashaw T. Woldemariam, Hirpa G. Lemu and Gary G. Wang

In: Energies, MDPI publisher; doi: 10.3390/en11010248

energies

MDPI

Article

CFD-Driven Valve Shape Optimization for Performance Improvement of a Micro Cross-Flow Turbine

Endashaw Tesfaye Woldemariam [1], Hirpa G. Lemu [1,*] and G. Gary Wang [2]

[1] Department of Mechanical and Structural Engineering and Materials Science, University of Stavanger, 4036 Stavanger, Norway; endashaw.t.woldemariam@uis.no
[2] School of Mechatronics System Engineering, Simon Fraser University, Surrey, BC V5A 1S6, Canada; gary_wang@sfu.ca
* Correspondence: hirp.g.lemu@uis.no

Received: 13 December 2017; Accepted: 16 January 2018; Published: 19 January 2018

Abstract: Turbines are critical parts in hydropower facilities, and the cross-flow turbine is one of the widely applied turbine designs in small- and micro-hydro facilities. Cross-flow turbines are relatively simple, flexible and less expensive, compared to other conventional hydro-turbines. However, the power generation efficiency of cross-flow turbines is not yet well optimized compared to conventional hydro-turbines. In this article, a Computational Fluid Dynamics (CFD)-driven design optimization approach is applied to one of the critical parts of the turbine, the valve. The valve controls the fluid flow, as well as determines the velocity and pressure magnitudes of the fluid jet leaving the nozzle region in the turbine. The Non-Uniform Rational B-Spline (NURBS) function is employed to generate construction points for the valve profile curve. Control points from the function that are highly sensitive to the output power are selected as optimization parameters, leading to the generation of construction points. Metamodel-assisted and metaheuristic optimization tools are used in the optimization. Optimized turbine designs from both optimization methods outperformed the original design with regard to performance of the turbine. Moreover, the metamodel-assisted optimization approach reduced the computational cost, compared to its counterpart.

Keywords: CFD-driven optimization; NURBS function; micro-hydropower; cross-flow turbine; metamodel-assisted optimization; turbine performance

1. Introduction

Due to the dynamically increasing population, competitive market economy and modernization, the global demand for energy is increasing dramatically. Projections from various studies indicate a large increase in energy consumption in the coming decades, especially in developing countries [1]. In the last two decades, the increased consumption of renewable energy sources has shown a surge (Figure 1). In fact, the studies project that this trend will also continue in the future. Among others, hydropower is the major source of renewable energy.

As of 2015, hydropower sources constitute around 61% of the total global renewable energy share. Of these, micro- and small-hydropower constitute around 4.5% and 7% (Figure 2), respectively. Hydropower facilities with an installed capacity between 100 kW and 10 MW are categorized under small-hydropower, while those below 100 kW are categorized under micro-hydropower [2,3]. Hydropower is one of the least expensive forms of renewable energy [2]. Moreover, despite its long history in global civilization and the increasing energy demand, more than half of the global hydropower potential still remains unexploited [4,5].

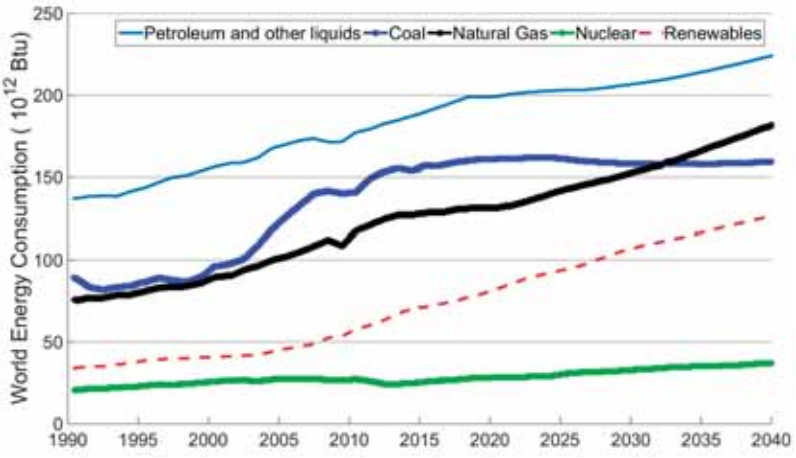

Figure 1. World energy consumption history and projection by energy sources [1].

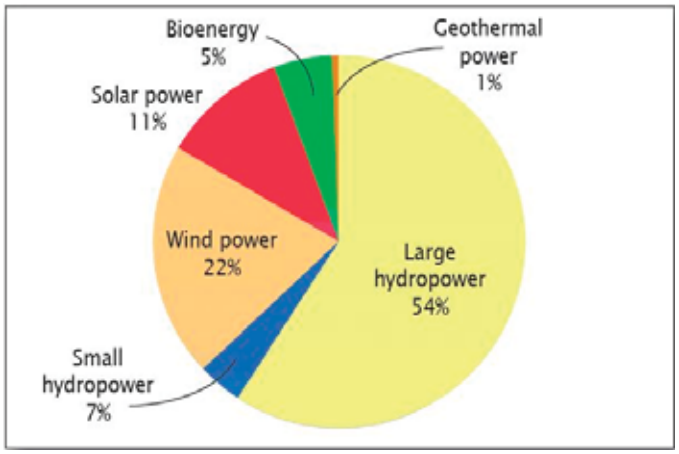

Figure 2. Global share of renewable energy (%) [6].

In the existing global hydro potential, small- and micro-hydropower constitute significant portions, and they play a significant role in exploiting the remaining potential, particularly in remote areas in developing and less developed countries. These hydropower sources play an important role in off-grid rural-area electrification with insignificant impact on the surrounding ecosystem [7]. Moreover, of all off-grid technologies, they constitute the least expensive form of electricity generation [6,8].

In order to best exploit the existing small- and micro-hydro potential, with the ultimate goal of meeting the growing energy demand, deploying efficient equipment to the hydropower facilities is required. The hydro-turbine is one of the most critical parts in hydropower facilities, and among other turbine designs, the cross-flow turbine is one of the most widely-applied designs in small- and micro-hydropower facilities around the globe, particularly for off-grid run-of-the-river applications.

The cross-flow hydro-turbine is relatively simple, flexible and less expensive, compared to the conventional hydro-turbines. Contrary to the developments in various computer and experiment-based optimization approaches within the last few decades, the power generation efficiency of cross-flow turbines is not yet well optimized, and insignificant research attention is given

to this area. Obviously, the design methodology used to develop the turbine has a significant impact on the performance. Such a design methodology should account for not only the efficient conversion of fluid flow to mechanical energy, but also define, among others, the exact geometry of the blades, the rotational speed of the turbine and the upstream velocity that should be sustained under severe cyclic loading [9]. In this regard, some simulation-based design optimization approaches are proposed in the literature. Signagra et al. [10] investigated the reasons for the reduction of turbine efficiency and proposed a design methodology based on Computational Fluid Dynamics (CFD) simulation. The study reported by Soenoko [11] reviewed cross-flow turbine developments and suggested, among others, optimization of the nozzle construction to improve the performance of the turbine. Sammartano et al. [12] carried out computer-based tests utilizing numerical CFD and hydrodynamic analysis to obtain an optimum design aimed to come up with a theoretical framework for the turbine sequential design. However, the study was limited only to turbine configurations without a guide valve and mainly on parameters embedded in the rotor design. Anagnostopoulos and Papantonis [13], on the other hand, conducted size optimization of small hydropower plants using a then newly-developed evaluation algorithm. However, their focus was on the overall plant performance using basic plant size parameters to optimize project cost. Apart from that, there is considerable inconsistency, as regards the optimum efficiency of cross-flow turbines, in the analysis study results of various reports, both theoretical and experimental [12,14–17].

This paper has followed a new approach, in which a CFD-driven metamodel-assisted and metaheuristic design optimization tools are employed to optimize the shape of the valve profile of a T15-300 micro-cross-flow turbine design. This is one of the T-series turbine designs widely applied around the globe. The profile of the valve is generated using the NURBS (Non-Uniform Rational B-Spline) function. The main objective of the research is to improve the performance of the turbine design at the optimum valve angle. Moreover, the study aims to promote the simulation-based optimization approach for further applications on similar turbines.

The paper is organized as follows. The next section discusses in detail the turbine type employed in the research. Section 3 then discusses the NURBS function utilized to represent the valve profile. The methodologies followed in the paper are discussed in Section 4, and the numerical modeling of a case study is presented in Section 5. Thereafter, correlation studies between important hydraulic parameters in the nozzle and the entire turbine model are discussed in Section 6. Section 7 presents the sensitivity analyses' results of the optimization parameters, while the results of the research work are discussed in Section 8. Finally, conclusions drawn from the study and recommendations are presented in Section 9.

2. Cross-Flow Turbine

Cross-flow hydro-turbines, also known as Michell-Banki's turbines, have been in development for decades since they were first patented by Donat-Banki in Budapest in the 1920s [16]. The benefits of the turbine, in addition to those mentioned in Section 1, are that most of cross-flow turbine parts can be manufactured with hands-on technologies [13]. Moreover, they have better power generation capability at part load conditions and favorable run-of-the-river application. Figure 3 shows the efficiency curves of various turbine designs per percentage rated flow. Despite the benefits, the figure shows that, the optimum efficiency of cross-flow turbines is lower compared to the other turbines.

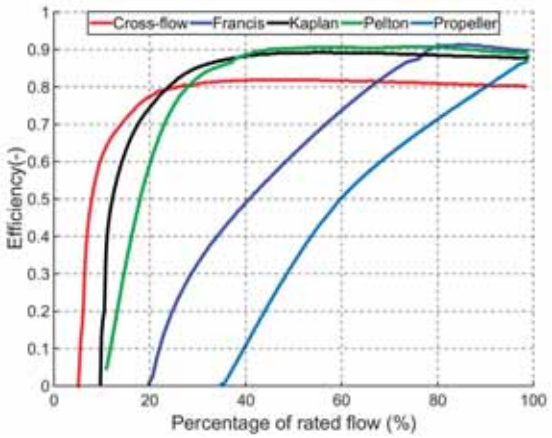

Figure 3. Efficiency curve of various turbine designs per percentage of rated flow [18].

In recent cross-flow turbine design developments, nozzles, along with guide vanes or valves, are being utilized in order to control the flow and improve the turbine's power-generating capacity [19,20]. Since the turbine is categorized as an impulse turbine, the valve is the critical part. Along with other design parameters [12], the valve design determines the magnitude of some of the important hydraulic parameters that in turn determine the power-generating capacity of the turbine. Among others, the T-series cross-flow turbine designs are the most widely-applied turbine designs that contain guide valves in their nozzles (see Figure 4). The T15-300 is one of the latest T-series models designed and has been supplied by a well-known Switzerland/Indonesia-based company called ENTEC ag, St. (Gallen, Switzerland) [21]. For this study, we used the single-compartment design of the T15-300 turbine model, which has a width of 68 mm. As can be understood from Figure 4a, the fluid flow starts from the inlet, passes through the nozzle and then crosses the rotor before leaving through the outlet.

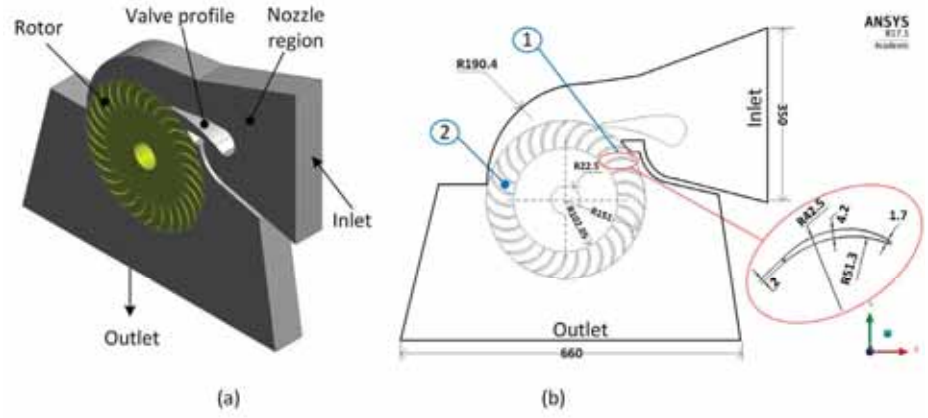

Figure 4. T15-300 cross-flow turbine design: (**a**) 3D geometry, (**b**) front view with detailed blade geometry.

According to experimental investigations and numerical analysis results reported by Costa Pereira et al. [17], cross-flow turbines with a guide valve inside the nozzle have better performance as compared to those without a guide valve. Various numerical studies also concluded that the nozzle region and guide valves highly impact the fluid characteristics inside the turbine, which thus determines the performance of the turbine [11,22,23]. Fluid jet velocity components (Figure 5) at

different locations of the cross-flow turbine rotor are some of the important parameters in the power conversion of the impulse type cross-flow turbines. In impulse turbines, the theoretical power conversion computation is calculated using Euler's turbomachinery equation. The angles α_1–α_4 and β_1–β_4 (Figure 5), the angles that the actual velocity and relative velocities make with the horizontal, respectively, play important roles in transferring hydraulic and mechanical powers. The guide valve shape and rotor blades' profile determine the magnitudes of the transferred power.

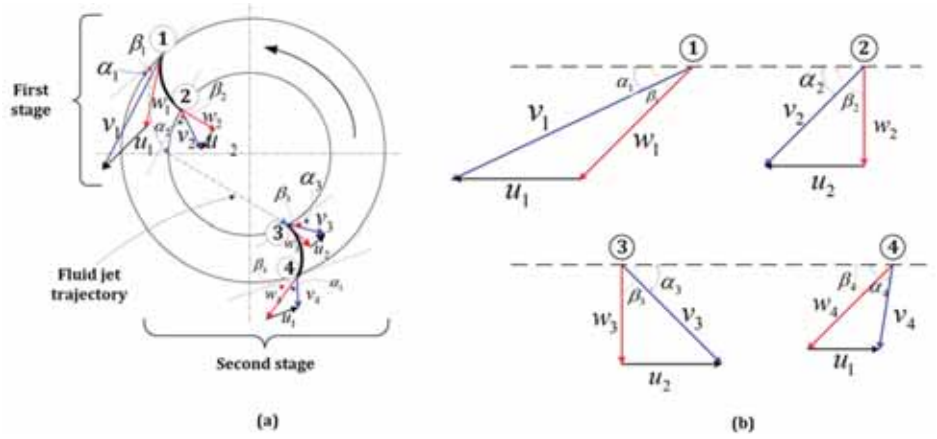

Figure 5. Cross-flow turbine rotor: (**a**) fluid jet trajectory at different locations and (**b**) velocity triangles at Locations 1–4. w_{1-4} refer to relative velocities at Points 1–4; u_1 and u_2 refer to peripheral velocities tangent to the outer and inner diameters respectively; v_{1-4} refer to actual fluid velocities at Points 1–4.

3. NURBS Function

Most Computer-Aided Design (CAD) tools utilize basis functions that are based on B-spline functions. Among others, the NURBS function is one of the state-of-the-art design basis functions applied in the latest CAD tools. NURBS can be used to describe arbitrarily-shaped curves, surfaces or bodies, have a high level of continuity and allow refinement ability on the CAD geometries [24].

The basis function is based on a parameterized recursive function, which begins from a piecewise constant value at a polynomial degree of $p = 0$. For a single dimensional problem, for example, the function is formulated as:

$$N_{i,0}(\xi) = \begin{cases} 1 & \xi_i \le \xi < \xi_{i+1} \\ 0 & otherwise \end{cases} \quad (1)$$

For polynomial functions of a higher degrees, $p \ge 1$, the function can be recursively obtained using Equation (2),

$$N_{i,p}(\xi) = \frac{\xi - \xi_i}{\xi_{i+p} - \xi_i} N_{i,p-1}(\xi) + \frac{\xi_{i+p+1} - \xi}{\xi_{i+p+1} - \xi_{i+1}} N_{i+1,p-1}(\xi) \quad (2)$$

where: $N_{i,p}$ is the basis function of the polynomial degree p with knot index $i = 1,2,\dots,n$. ξ determines knot values from a given knot vector $\Xi = \{\xi_1, \xi_2, \xi_3, \dots, \xi_{n+p+1}\}$. The B-Spline basis curve function, $C_b(\xi)$, is given by Equation (3).

$$C_b(\xi) = \sum_{i=1}^{n} N_{i,p}(\xi)\, B_i \quad (3)$$

where $B_i = \{b_1, b_2, b_3, \dots, b_n\}$ are the corresponding control points.

NURBS differs from B-spline in such a way that it introduces a weighting value for the corresponding control points to enable local control of the design variables. The NURBS curve equation is given as,

$$C_n(\xi) = \sum_{i=1}^{n} \frac{N_{i,p}(\xi)w_i}{(\sum_{i=1}^{n} N_{i,p}(\xi)w_i)} B_i = \sum_{i=1}^{n} R_{i,p}B_i \quad (4)$$

$$R_{i,p} = \frac{N_{i,p}(\xi)w_i}{(\sum_{i=1}^{n} N_{i,p}(\xi)w_i)} \quad (5)$$

where $R_{i,p}$ is the NURBS basis function and w_i are the given weighted values for the control points.

4. Methodology and Approaches

In this study, a new optimization approach has been employed to optimize the design of the valve profile in the nozzle of the cross-flow turbine under consideration. The optimization approach, illustrated in Figure 6, interconnects an optimization tool, a curve function and a modeling and analysis tool. In this approach, two optimization methods have been utilized. The first method, a Multi-Objective Metamodel-Assisted Optimization Method (MO-MMAO), uses the Optimization Assisted System Integrated Software (OASIS) optimization tool. The optimization tool, OASIS [25], has been developed for the optimization of computationally-expensive implicit problems. It was originated from the Product Design and Optimization Laboratory (PDOL) at Simon Fraser University, Canada, and developed and marketed by Empower Operation Corp (V1.3, Surrey, BC, Canada). OASIS incorporates various optimization algorithms, which are assisted by various metamodels, machine learning, statistical analysis and other tools. The optimization tool follows a direct sampling strategy, where the metamodel adaptively updates itself during the optimization process [26]. For this study, the Multi-Objective Global Optimization (MOGO) algorithm of the tool has been used. The second optimization tool is the well-known metaheuristic optimization tool, Genetic Algorithm (GA). It is a population-based optimization tool motivated by the evolutionary concept of survival of the fittest [27].

In the general approach, which employs either of the two optimization tools, a MATLAB (MathWorks, Inc., Natick, MA, USA) script is used to generate construction points from a NURBS function with the construction points being used to generate the profile of the valves of the cross-flow turbine in the modeling and analysis tool, i.e., ANSYS Workbench (ANSYS, Inc., V17.1, Canonsburg, PA, USA) [28].

The MATLAB script uses a total of twelve (12) control points (see Figure 7) to generate a second-order polynomial NURBS curve equation [29]. Of the 12 control points, *x* or *y*-coordinates of only five selected control points are selected as optimization parameters: the *y*-coordinates of Control Points 3, 4 and 11 and the *x*-coordinates of Control Points 6 and 7 are the parameters chosen. These parameters are represented by P_i (where i = 1–5). The remaining control points maintain their original design values as they are assumed to be less important in the optimization, but critical for the overall valve operation. For instance, Control Points 1, 2, 8 and 9 are at critical locations of the valve and are used for proper sealing when the valve is in a closing position (Figure 8a), while Point 5 maintains the gap between the valve profile and the shaft outer diameter, which is used to maneuver the valve. A total of fifty (50) construction points is generated from the NURBS curve equation. The *x*- and *y*-axis components of the 50 construction points are mapped to 100 design parameters in the ANSYS Workbench CAD modeling tool. The construction point parameters are represented by C_i (where i = 1–100). Based on the sensitivity to the objectives (see Section 7), the five optimization parameters are given different weighting values in the NURBS function.

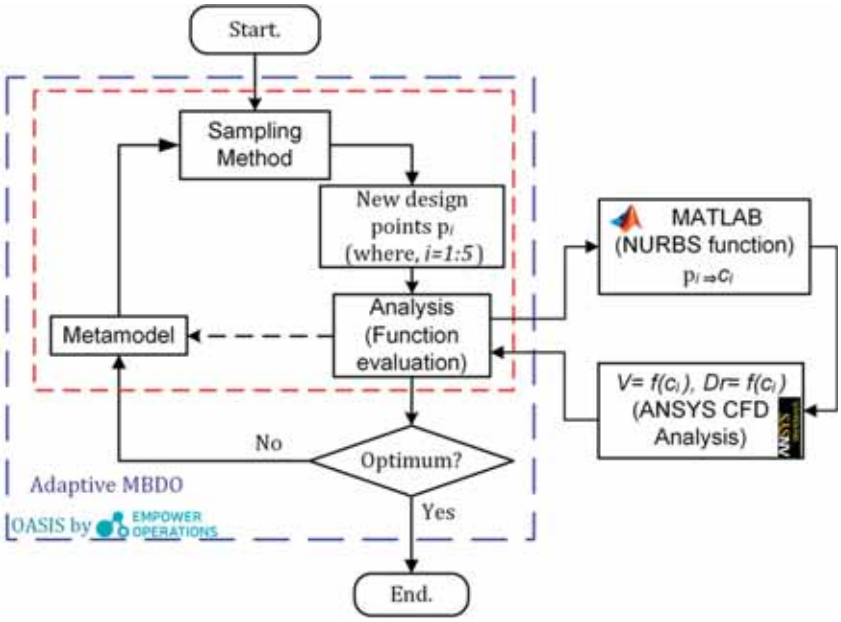

Figure 6. Optimization approach flowchart: inter-connection of OASIS, MATLAB and ANSYS Workbench tools.

The other important concept in the optimization approach is to separately optimize the nozzle region (Figure 8b). We have followed this concept for three important reasons:

(i). Since the turbine is assumed as the impulse turbine, this part of the turbine plays a critical role in the entire power generation;
(ii). It enables us to easily identify and control the important hydraulic parameters at the nozzle that are important in the entire power transfer and are mainly affected by the shape of the guide valve;
(iii). It reduces the computational cost in the optimization process.

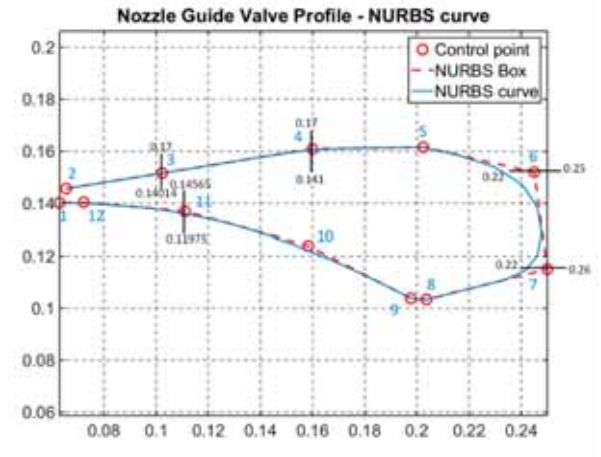

Figure 7. NURBS curve generated from 12 control points.

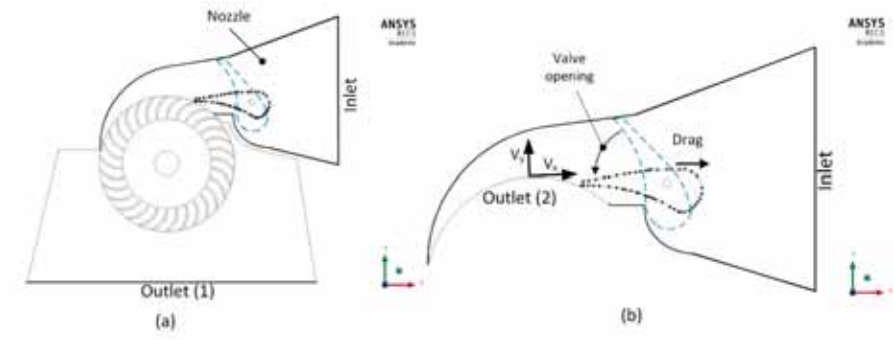

Figure 8. The nozzle region and boundaries of T15-300 cross-flow turbine model: (**a**) the full cross-flow turbine model and (**b**) separate nozzle region with both the inlet and outlet boundaries.

It is important to note that the change in the trends of the output parameters from the separate nozzle design are initially correlated with the change in the trends of the important output parameters of the full turbine design due to the change of valve angle (with respect to the turbine's performance), which is discussed in Section 6. After the optimization process, a comparison of the optimized valve designs with the original design is carried out using the full turbine model.

The multi-objective optimization problem has two objectives and two constraint functions. The two objectives of the optimization, based on the correlation studies are (1) minimizing the *x*-component (maximizing the magnitude) of the area-weighted average velocity (V_x) of the nozzle outlet fluid and (2) minimizing the drag force (Drag) on the valve profile. The general formulation of the problem is given in Equation (6). Both objective functions are obtained after the CFD computation of the turbulent numerical model using the implicit analysis tool, ANSYS Fluent tool:

$$\begin{aligned} &\text{Minimize} && V_x = f(P_i) \text{ and } Dr = f(P_i); (i = 1, 2, \ldots 5) \\ &\text{Constraints} && C(P_i) \leq 0, (P_1 - P_2 \leq 0, \text{and } P_5 - P_1 \leq 0) \\ & && P_i \in [P_{iL}, P_{iU}] \end{aligned} \quad (6)$$

where V_x and Dr represent the *x*-component of the area-weighted average velocity at the nozzle outlet and drag force functions; where both are functions of the optimization parameters (P_i); $C(P_i)$ represents the constraint functions respectively; and P_{iL} and P_{iU} are the lower and upper bounds of the optimization parameters, respectively.

The lower and upper bounds of the parameters are obtained from the design configuration of the original turbine design so that they should not create any irregular valve profile and unacceptable nozzle region; see Table 1. Therefore, the parameters are bounded inside the nozzle region. The same principle is followed when the constraints on the design variables are determined from the turbine configuration.

Table 1. Design points, lower and upper bound values of the optimization parameters.

Name of points	P_1 (m)	P_2 (m)	P_3 (m)	P_4 (m)	P_5 (m)
Design point	0.15160	0.16092	0.24500	0.25000	0.13700
Lower bound	0.14014	0.14100	0.22000	0.22000	0.11972
Upper bound	0.17000	0.17000	0.25000	0.26000	0.14565

5. Numerical Modeling

Based on our experience of comparative studies of the applications of different numerical models on similar problems and various other numerical studies, the standard *K*-ε numerical model [30,31] is found to best represent the fluid flow inside the cross-flow turbine. According to

studies and user guides of simulation tools, this model is robust, economical and provides reasonable accuracy not only for the current problem, but also for a wide range of problems. Therefore, in this paper, we have employed the standard *K*-ε model for both the time-dependent (transient) and steady state analyses in both the separate nozzle and entire turbine models. In the general transport equation for the standard *K*-ε model, the turbulence kinetic energy and the rate of dissipation, k and ε, respectively, are obtained from Equations (7) and (8) [30]. A scalable wall function is selected for the near-wall treatment.

$$\frac{\partial}{\partial t}(\rho k) + \frac{\partial}{\partial x_i}(\rho k V_i) = \frac{\partial}{\partial x_j}\left[\left(\mu + \frac{\mu_t}{\sigma_k}\right)\frac{\partial k}{\partial x_j}\right] + G_k + G_b - \rho\varepsilon - Y_M + S_k \quad (7)$$

$$\frac{\partial}{\partial t}(\rho \varepsilon) + \frac{\partial}{\partial x_i}(\rho \varepsilon V_i) = \frac{\partial}{\partial x_j}\left[\left(\mu + \frac{\mu_t}{\sigma_\varepsilon}\right)\frac{\partial \varepsilon}{\partial x_j}\right] + C_{1\varepsilon}\frac{\varepsilon}{k}(G_k + C_{3\varepsilon}G_b) - C_{2\varepsilon}\rho\frac{\varepsilon^2}{k} + S_\varepsilon \quad (8)$$

where ρ, μ and V_i are density, viscosity and velocity vectors of the flowing fluid, respectively. σ_k and σ_ε are the turbulent Prandtl numbers for k and ε, respectively; whose default values in the tool are used for our analyses. G_k and G_b are the generation turbulence kinetic energy due to the mean velocity gradients and buoyancy, respectively; however, the generation buoyancy is negligible for this problem. Y_M represents the contribution of the fluctuating dilation in compressible turbulence, which is negligible in our analyses. S_k and S_ε are the source terms for kinetic energy and dissipation, which are not applicable for this problem. $C_{1\varepsilon}$, $C_{2\varepsilon}$ and $C_{3\varepsilon}$ are given constant values; $\frac{\partial}{\partial t}$ is the gradient vector with respect to time; $\frac{\partial}{\partial x_i}$ and $\frac{\partial}{\partial x_j}$ are the spatial gradient vectors at the i and j coordinates.

The turbulent viscosity term, μ_t, is computed using Equation (9), where the term C_μ is a constant value. All constants are listed in Table 2 with their corresponding valves.

$$\mu_t = \rho C_\mu \frac{k^2}{\varepsilon} \quad (9)$$

In order to identify an allowable and efficient head for the analyses, an efficiency curve study from steady numerical analyses on the full turbine models is carried out at various flow rate ratios computed from the head ranges from 5–22.2 m. The mass flow rate at each head over the mass flow rate at the maximum head is calculated to find each flow rate ratio. Based on the result, the average allowable head of 12.5 m was maintained for all analyses, as it is where the model provides the maximum computed hydraulic efficiency. In addition, the valve angle position is set at its maximum opening position where the maximum numerical power output is obtained. Moreover, for all simulations on the full turbine model, the rotor speed is maintained at 360 rpm.

Table 2. Given and standard values for constant variables.

Numerical Model Constants	Values
ρ (kg/m^3)	998.2
μ (kg/ms)	0.001003
C_μ (-)	0.09
σ_k (-)	1
σ_ε (-)	1.3
$C_{1\varepsilon}$ (-)	1.44
$C_{2\varepsilon}$ (-)	1.92

5.1. Meshing Qualities and Convergence

After a number of trials and convergence tests, valid mesh sizes of the full turbine model and the separate nozzle model are chosen; see Figure 9. The meshing details and characteristics of the selected meshes of the models (circled in blue in the figures) are shown in Table 3. The total area-weighted average pressure values at the outlets of the models were the convergence test parameters in the test; whereas, built-in mesh quality measures in the meshing tool of ANSYS Fluent,

such as element quality, skewness and orthogonal qualities of the meshes, are checked while maintaining the meshing quality. Moreover, due to the configuration of the problem and the existence of interfacing bodies, the unstructured meshing method is selected, and local meshing techniques are used to refine meshes around the small-sized rotor blades' edges and surfaces. The mesh qualities are then controlled to fall within the recommended range of values of the mesh quality measures.

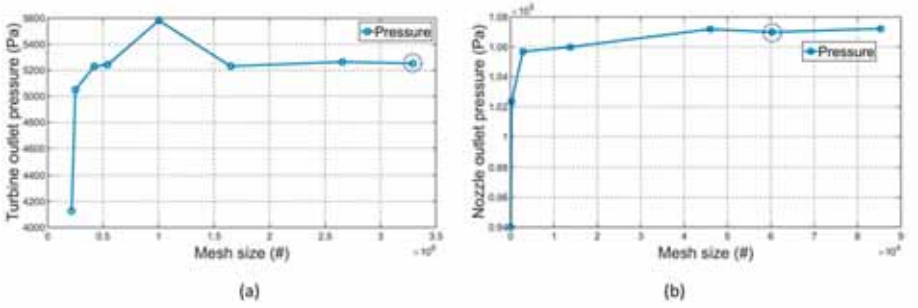

Figure 9. Model mesh validation: (**a**) full turbine model; (**b**) separate nozzle model.

Table 3. Meshing size details of the full turbine geometry and separate nozzle geometry.

Geometries	Housing Elem. Size	Rotor Elem. Size	Total Elem. Size	Mesh Min. Size	Mesh Max. Face size	Max. Tet size
Full turbine geometry	57,662	3,234,243	3,291,905	0.0005	0.0065	0.015
Separate nozzle geometry	60,270	-	60,270	0.00035	0.0045	0.015

Elem. stands for mesh element and Tet stands for tetrahedral.

5.2. Solution Methods

To solve the transport equations for the standard *K*-ε numerical model in CFD tool, the SIMPLE algorithm scheme has been employed to compute the pressure-velocity coupling, and least squares cell-based method has been used to compute the gradient in the spatial discretization. Considering the complex geometry of the rotor and the interface between the housing and rotor domains, the second order method has been employed to compute the pressure and the second order upwind to compute the momentum, turbulent kinetic energy and turbulence dissipation rate equations in the spatial discretization. In both the full turbine and separate nozzle models, all walls are given a no-slip condition, and the outlet surfaces are given pressure-outlets with zero gauge pressure boundary conditions.

After solving the transport equations, the area-weighted average values, which are the valid velocity magnitudes of the numerical fluid flow, are considered to compute the actual velocities at the outlet surfaces of both geometries. In addition, the *x*-components of the combined pressure and viscous forces are used to determine the drag force on the guide valve surface. Pressure and viscous forces ($\overrightarrow{F_p}$ and $\overrightarrow{F_v}$, respectively) are computed based on their computed and user-determined reference values; for instance, the pressure force is computed as Equation (10). On the other hand, the total moment load vector, moment coefficients, output hydraulic power and numerical efficiencies are computed using Equations (11)–(14), respectively.

$$\overrightarrow{F_p} = \sum_{i=1}^{n} (P - P_{ref}) A\hat{\boldsymbol{n}} \quad (10)$$

$$\overrightarrow{M} = \vec{r} \times \overrightarrow{F_p} + \vec{r} \times \overrightarrow{F_v} \quad (11)$$

$$C_m = \frac{M}{\frac{1}{2}\rho_r V_r^2 A_r L_r} \quad (12)$$

$$P_o = M.\omega \quad (13)$$

$$\eta = \frac{M.\omega}{Q_{in}(P_{in} - P_{out})/\rho} \quad (14)$$

where P and P_{ref} are the computed and user-determined reference pressures (Pa), respectively; $\vec{r}$ and $\vec{M}$ are the moment arm and moment vectors. C_m is the unit-less moment coefficient. ρ_r, V_r, A_r and L_r are the reference density (in kg/m^3), velocity (m/s), area (m^2) and length (m) values, respectively, set in the analysis tool. M, Q_{in} and ω are the magnitude values of moment (Joules), mass flow rate (kg/s) and rotational speed of the rotor (rad/s), respectively.

6. Correlation Study between the Separate Nozzle and Full Turbine Models

To identify important output parameters from the separate nozzles that have a direct impact on the performance of the turbine and to understand their trend with the change of the valve design, a correlation study between the separate nozzle and full model was carried out. While conducting this study, several numerical simulations were run on both the separate nozzle and full turbine models at different valve positions, and their results have been analyzed. The valve angle opening position was set to range from 50–100% opening. The other boundary conditions, such as inlet head, rotational speed of the rotor for the full model, numerical model settings and the geometric parameters except valve position, are set constant in all analyses. The output power is computed from the full turbine model, and various output parameters are studied from the nozzle model. The main purpose of this correlation study is to identify the two output parameters from the nozzle model with higher impact on turbine performance and set them as objective parameters.

As depicted in Figure 10a, the results show that the output power increases as expected with the valve opening from 50–100% from the closing position. The simulation results from the separate nozzle model, Figure 10b, reveal that the drag force on the valve profile and the *x*-component of the area-weighted average velocity (X-Velocity) from the nozzle outlet surface have a visible correlation with the output power. The velocity magnitude has a direct relation to the output power, while the drag force has an inverse relation. Therefore, it is valid to set the objectives of the optimization to minimize the *x*-component of the velocity at the nozzle outlet and minimize the drag force on the valve profile.

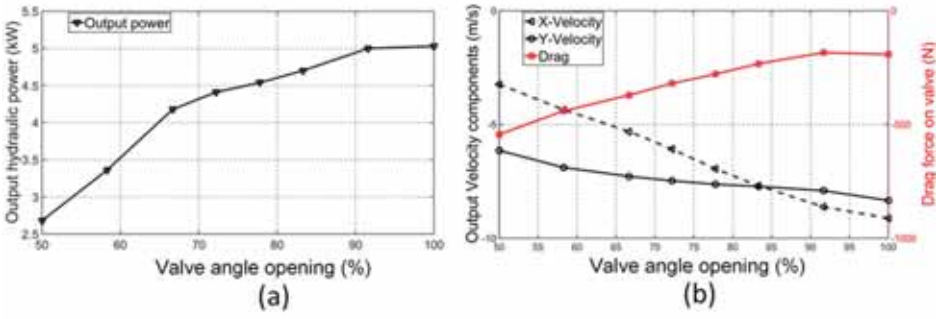

Figure 10. Correlation study between separate nozzle and entire turbine model: (**a**) Output power response; (**b**) Output velocities and drag force responses.

7. Sensitivity Analyses

To assign logical weighting values to the corresponding control points for the NURBS curve, the significance of the optimization parameters for the output objective parameters should be studied.

Such significancy studies (sensitivity analysis) can be achieved by employing the concept of the statistical Design Of Experiment (DOE). The factorial DOE method is a widely-applied method in the scientific community. For this study the fractional factorial design method has been applied to estimate the direct effects of the five optimization parameters (P_i) on the responses of the two objective parameters (*V* and *Dr*) in the separate nozzle model. Unlike the full factorial experimental design, the fractional method does not estimate all the interaction effects of the parameters, but can correctly estimate the main effects with fewer runs, compared to the intensive full factorial.

A three-level five-parameter analysis with two responses was employed. Level 1 is the lower bound; Level 2 is the design point; and Level 3 is the upper bound. The custom optimal factorial design option with random sampling from the Design-Expert tool [32] dictated that 26 combinations of samples should be run. The settings of the other important parameters are carefully controlled based on the standard recommendations of the tool.

According to the sensitivity test results (Figure 11), the first and fifth parameters (P_1 and P_5) are highly sensitive to both objective parameters, compared to the other three, while the second parameter (P_2) is more significant to the second response than the remaining two.

Therefore, the corresponding control points for the first and fifth parameters are given higher weights in the NURBS curve function, so that more construction points will be generated from their surrounding points on the curve, thus generating smooth curves in their vicinity. Note that the total number of construction points in the NURBS curve can be determined in the function's MATLAB script by the user depending on the interest. On the other hand, the two least sensitive parameters (P_3 and P_4) are given only fair weighting values.

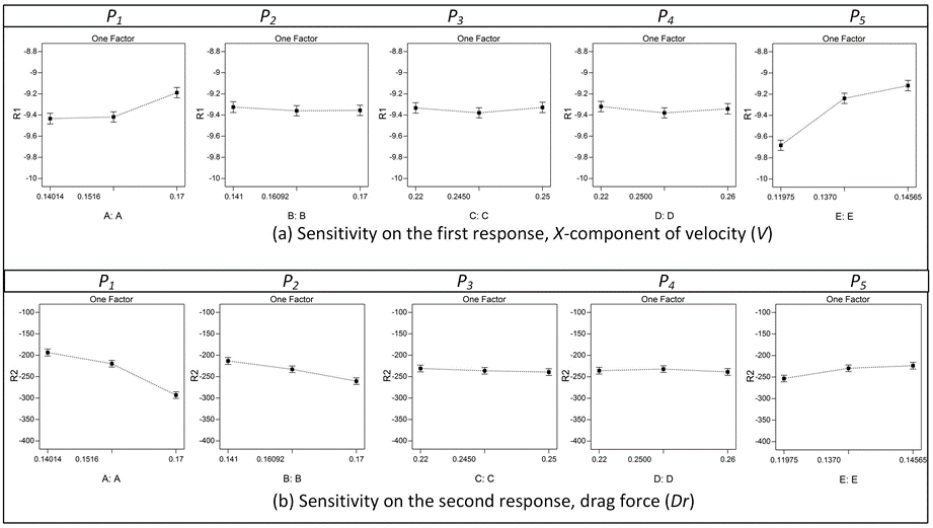

Figure 11. Sensitivity test results of parameters: (**a**) sensitivity on the first objective parameter; (**b**) sensitivity on the second objective parameter.

8. Results and Discussion

The MMAO optimization was performed by setting the OASIS tool to a maximum function evaluation of 100 (based on authors' previous experience on similar problems). Apart from the default convergence tolerance settings, the maximum number of evaluations is used as a stopping criterion for the optimization process in the tool. In the multi-objective GA optimization, the number of generations is set to be six and the stall generation limit of five are set as stopping criteria. The population size is chosen to be 20. This combination gives at least 100 function evaluations in the GA optimization process. The same computational workstation was used for both optimization

processes: HP Z600 of processor Model Intel(R) Xeon(R) X5650 (HP Inc., Palo Alto, CA, USA) with two processors each around 2.67 GHz capacity. The optimization results and the comparative analyses are discussed in detail in Sections 8.1 and 8.2, respectively.

8.1. Optimization Results

Figure 12 shows the convergence plot with the number of function evaluations for the Metamodel-Assisted Optimization (MMAO), i.e., OASIS optimization process; it can be observed that the optimization converged at the 53rd function evaluation count. The total time elapsed was 2 h, 50 min and 26 s. The best Pareto point (with respect to the turbine's performance) from the Pareto frontier points, shown in Figure 13, is taken as the best optimum point (Table 4) for our further comparative analyses.

Unlike the MMAO optimization, the multi-objective GA optimization carried out a total of 121 function evaluation counts, which led to the fact that it took around 3.69 h. Seven (7) Pareto front points are returned from the optimization process (Figure 13); similarly, the best Pareto point (Table 4) is taken as the best optimum point for our further comparative analyses.

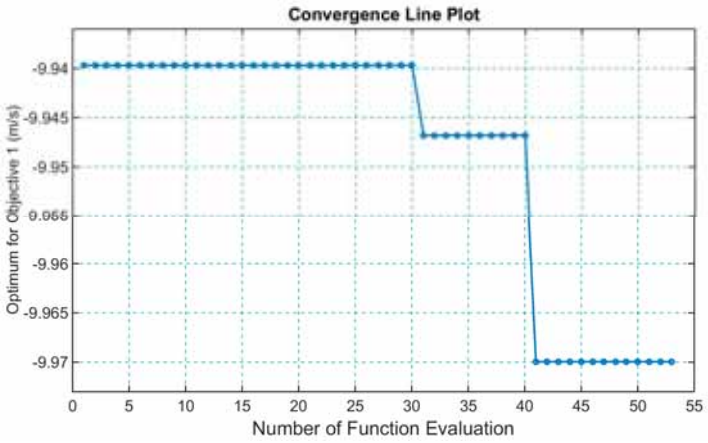

Figure 12. Convergence line plot of the Metamodel-Assisted Optimization (MMAO) optimization tool.

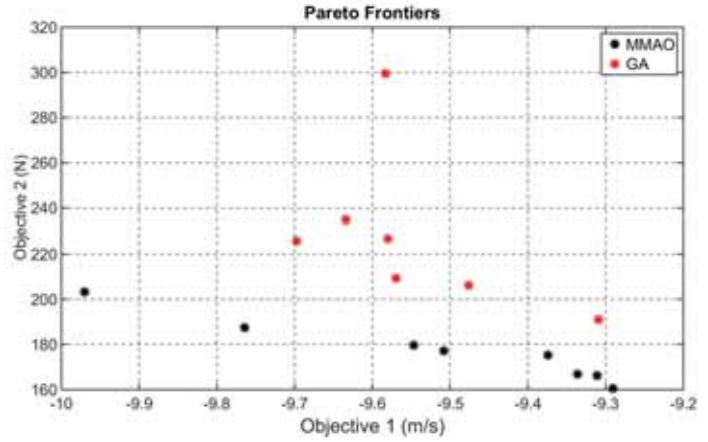

Figure 13. Pareto front plot for MMAO (OASIS) optimization and GA multi-objective optimization.

Apart from the differences in computational time and number of the function evaluations, a difference is also observed in the shape of the optimized valve models (see Figure 14). However, the shapes from both methods are not as complex as one may expect.

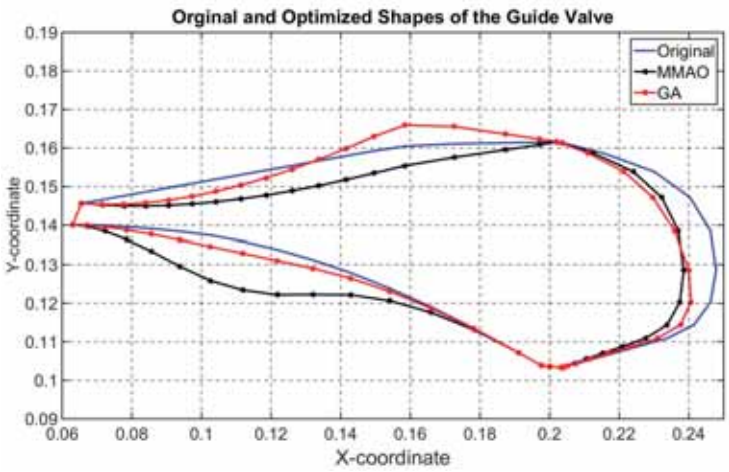

Figure 14. Original and optimized shapes of the guide valve generated from the construction points.

Table 4. Parameter values from the optimization results and steady analyses' results.

Turbine Model	P_1 (m)	P_2 (m)	P_3 (m)	P_4 (m)	P_5 (m)	Power Output (Watt)
Original	0.151600	0.160920	0.24500	0.25000	0.13700	4841.83
GA	0.143077	0.16730	0.23089	0.24575	0.13308	5070.89
MMAO (OASIS)	0.142430	0.15588	0.23567	0.24059	0.12091	5099.85

8.2. Comparative Analyses and Discussions

To see the actual impact of the optimized shapes on the full turbine design, both steady and transient CFD analyses (simulations) have been carried out and the responses collected and compared against the original design. In the transient simulations, the time step size was set at 0.001 and ran for 1000 time steps. Given the rotational speed of the rotor, around 5.83 rotations are expected in one second. An output parameter that has a direct relation to the performance of the turbine, which is the surface moment about the rotational axis of the rotor, has been chosen for comparison. The moment is the result of the effect of the sum of both pressure and viscous forces (Equation (11)). Time-dependent responses of the moments have been collected from the surfaces of the two parts:

(i). From the surfaces of one of the rotors' blade (1); see Figure 4b.
(ii). From the surfaces of the entire set of rotor blades (2).

Note that in order to avoid some irregularities seen on the responses at the beginning of the first cycle, it was decided to consider the data from the second cycle in both cases of the comparative studies.

The moment responses and their peak values of the second rotation (cycle) from the transient analyses are examined using comparative graphs. The comparative graph of the moment responses from the entire set of rotor blade surfaces, depicted in Figure 15, shows that both the optimized designs return better responses than the original design at most of the time steps, except at the beginning of the cycles. On the other hand, the responses from the MMAO optimized design are seen to outperform the GA-optimized design. Therefore, as can be seen from Table 4, the total power output of the MMAO-optimized design from the time-independent (steady) analyses is higher than that of the other two designs.

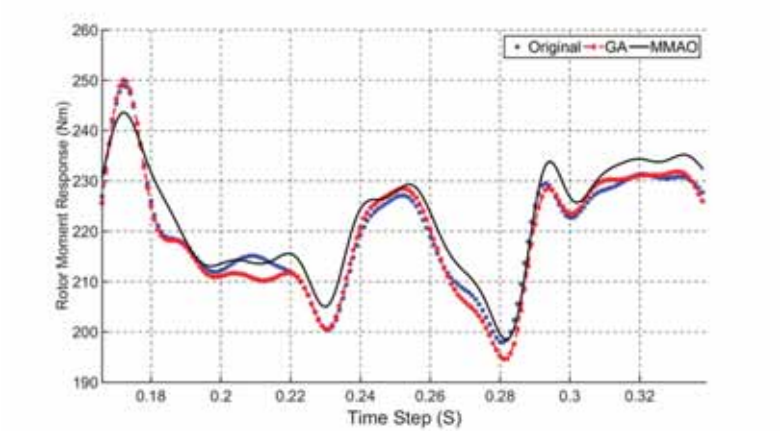

Figure 15. Moment responses from the entire rotor blade surface.

Unlike the responses from the surfaces of the entire set of rotor blade surfaces case, the plot in Figure 16 indicates that the moment responses collected from the single blade (1) show little variation. However, it is clear and possible to deduce that the optimized designs still return better responses in magnitude at most time steps than the original design.

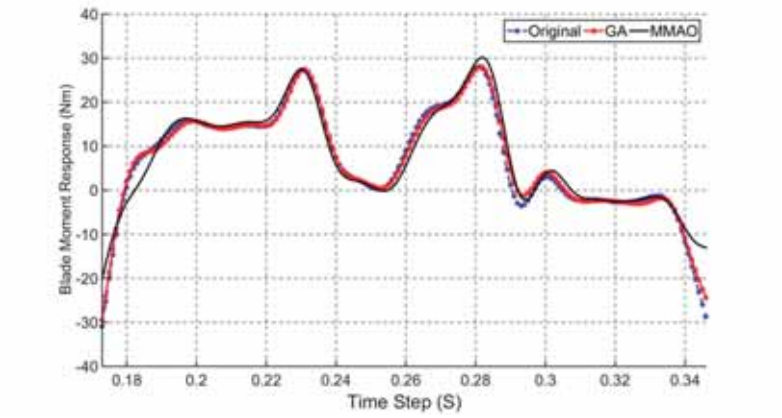

Figure 16. Moment responses from the single blade surfaces (1).

Moreover, the steady analyses' results (Table 3) estimate a power improvement of around 5.33% and 4.73% from the MMAO-optimized design and the GA-optimized design, respectively. On the other hand, from the visual analysis of the fluid stream-band width in the first quarter of the velocity streamline from the steady analyses, Figure 17 illustrates the volumes of the ineffective fluid crossing the rotor in the three models. The optimized models have a thinner fluid stream-band width than that of the original model.

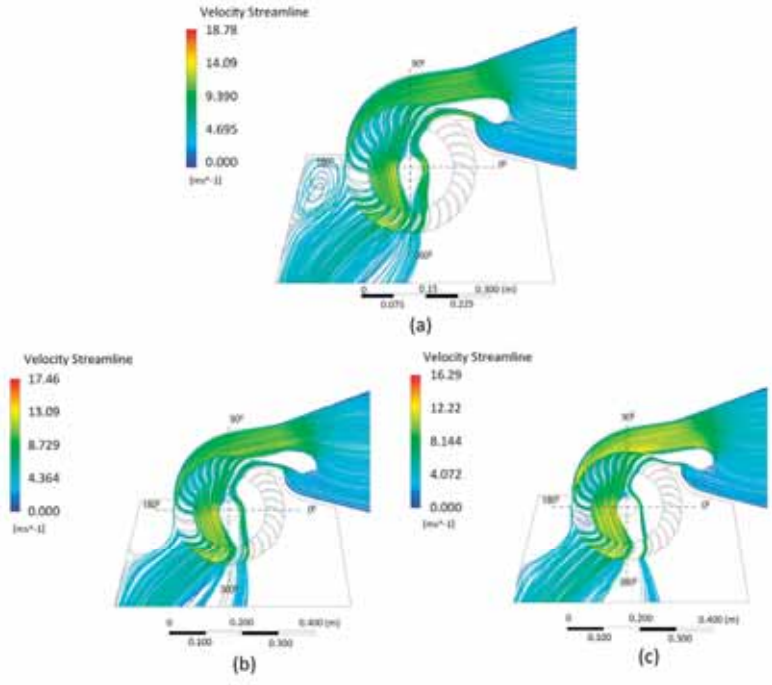

Figure 17. Velocity streamlines from steady analyses: (**a**) original model; (**b**) GA-optimized model; and (**c**) MMAO-optimized model.

In addition, considering the ratio of the sum of all peak moment responses from the three models from the full rotor surface to the single blade surface, we have seen that an estimated average of 8.61 blades contributes to the power generation at each cycle of the rotor.

Moreover, as one can see from both moment response figures, the response curves from all models coincide in some cases, but show a similar trend in all cases, which verifies that the numerical model employed is valid and converging.

9. Conclusions and Recommendations

In this article, CFD-driven shape optimization is performed on the cross-flow turbine design. The approach provided promising results with regard to improving the performance of the cross-flow turbine. The motivation for the study is the fact that, since hydropower is one of the least expensive and most abundant renewable energy sources around the globe, efforts to improve performance by designing optimized critical parts for hydropower facilities are indispensable.

Two different optimization methods have been employed in the approach. One is the widely-applied multi-objective Genetic Algorithm (GA) optimization method, and the second is the Metamodel-Assisted Optimization (MMAO) method from the OASIS tool. Optimized models from both optimization methods showed an estimated 4.73% and 5.33% improvement on the output power, respectively, compared to the original un-optimized design model. Apart from that, the MMAO optimization process converged at fewer function evaluations and lesser processing time than its counterpart. One of the main reasons is that, unlike the GA method, the MMAO method generates samples towards the optimum region to assist the optimization process to converge with fewer function evaluations.

Therefore, we can conclude that the approach we have introduced is effective for such a shape optimization problem to improve the performance of impulse turbines. This approach can be applied to optimize the performance of similar turbines. It is also revealed through the study that the MMAO

method offers a better performance design, and it is more effective than the GA method in identifying the Pareto frontier. The MMAO method has also been shown to be computationally less expensive than GA.

Acknowledgments: The study is funded by the Norwegian Ministry of Education and Research through University of Stavanger (IN-10603). The authors would like to acknowledge both institutions. The authors acknowledge the support from colleagues in the Product Design and Optimization Laboratory at Simon Fraser University, Canada.

Author Contributions: The first author is responsible to develop the framework and the models, to run the analysis and write the paper. The second and the third authors provided valuable advices on the used methodology, evaluated reported results and conducted critical proofreading and review of the paper.

Conflicts of Interest: The authors declare no potential conflict of interest.

References

1. U.S. Energy Information Administration. *International Engergy Outlook 2017*; U.S. Engergy Information Adminstration: Washington, DC, USA, 2017; p. 76.
2. International Renewable Energy Agency (IRENA). *Renewable Power Generation Costs in 2014*; International Renewable Energy Agency: Masdar City, UAE, 2015; p. 164.
3. International Center on Small Hydro Power (ICSHP). What Is SHP? Available online: http://www.inshp.org/detail.asp?RID=8&BID=80 (accessed on 20 August 2017).
4. Koch, F.H. Hydropower—The politics of water and energy: Introduction and overview. *Energy Policy* **2002**, *30*, 1207–1213.
5. International Hydropower Association (IHA). *2017 Hydropower Status Report*; International Hydropower Association: London, UK, 2017; p. 84.
6. United Nations Industrial Development Organization (UNIDO). *World Small Hydropower Development Report 2016*; United Nations Industrial Development Organization: Vienna, Austria, 2016; p. 650.
7. Paish, O. Small hydro power: Technology and current status. *Renew. Sustain. Energy Rev.* **2002**, *6*, 537–556.
8. Dragu, C.; Sels, T.; Belmans, R. *Small Hydro Power: State of the Art and Applications*; ESAT-ELEN Energy Institute: Leuven, Belgium, 2001; pp. 265–270.
9. Zanette, J.; Imbault, D.; Tourabi, A. A design methodology for cross flow water turbines. *Renew. Energy* **2010**, *35*, 997–1009.
10. Sinagra, M.; Sammartano, V.; Aricò, C.; Collura, A.; Tucciarelli, T. Cross-Flow turbine design for variable operating conditions. *Procedia Eng.* **2014**, *70*, 1539–1548.
11. Soenoko, R. Design optimization to increase a cross flow turbine performance: A review. *Int. J. Appl. Eng. Res.* **2015**, *10*, 38885–38890.
12. Sammartano, V.; Aricò, C.; Carravetta, A.; Fecarotta, O.; Tucciarelli, T. Banki-michell optimal design by computational fluid dynamics testing and hydrodynamic analysis. *Energies* **2013**, *6*, 2362–2385.
13. Anagnostopoulos, J.S.; Papantonis, D.E. Optimal sizing of a run-of-river small hydropower plant. *Energy Convers. Manag.* **2007**, *48*, 2663–2670.
14. Pereira, N.H.; Borges, J. A study on the efficiency of a cross-flow turbine based on experimental measurements. In Proceedings of the 5th International Conference on Fluid Mechanics and Heat & Mass Transfer (FLUIDSHEAT'14), Lisbon, Portugal, 30 October–1 November 2014; pp. 63–72.
15. Durgin, W.; Fay, W. Some fluid flow characteristics of a cross-flow type hydraulic turbine. In Proceedings of the American Society of Mechanical Engineers (ASME) Winter Annual Meeting on Small Hydro Power Fluid Machinery, New Orleans, LA, USA, 9–14 December 1984; pp. 77–83.
16. Macmore, C.; Merryfield, F. The Banki water turbine. *Eng. Exp. Station* **1949**, *25*, 3–25.
17. Costa Pereira, N.H.; Borges, J.E. Study of the nozzle flow in a cross-flow turbine. *Int. J. Mech. Sci.* **1996**, *38*, 283–302.
18. Tuhtan, J.A. Cost Optimization of Small Hydropower. Master's Thesis, Universität Stuttgart, Stuttgart, Germany, 2007.
19. Walseth, E.C. Investigation of the Flow through the Runner of a Cross-Flow Turbine. Master's Thesis, Norges Teknisk-Naturvitenskapelige Universitet, Trondheim, Norway, 2009.

20. Choi, Y.; Yoon, H.; Inagaki, M.; Ooike, S.; Kim, Y.; Lee, Y. Performance improvement of a cross-flow hydro turbine by air layer effect. In *IOP Conference Series: Earth and Environmental Science*; IOP Publishing: Bristol, UK, 2010; p. 012030.
21. ENTEC. Entec—Model T-15—High-EFFICIENCY Cross-Flow Turbines. Available online: https://www.energy-xprt.com/downloads/entec-t-15-high-efficiency-cross-flow-turbines-brochure-389094 (accessed on 21 May 2017).
22. Choi, Y.-D.; Lim, J.-I.; Kim, Y.-T.; Lee, Y.-H. Performance and internal flow characteristics of a cross-flow hydro turbine by the shapes of nozzle and runner blade. *J. Fluid Sci. Technol.* **2008**, *3*, 398–409.
23. Chen, Z.; Choi, Y.-D. Performance and internal flow characteristics of a cross-flow turbine by guide vane angle. In *IOP Conference Series: Materials Science and Engineering*; IOP Publishing: Bristol, UK, 2013; p. 052031.
24. Cottrell, J.A.; Hughes, T.J.; Bazilevs, Y. *Isogeometric Analysis: Toward Integration of CAD and FEA*; John Wiley & Sons: Hoboken, NJ, USA, 2009.
25. Empower Operations. Integrate and Optimize. Available online: http://empoweroperations.com/en/oasis/ (accessed on 10 June 2017).
26. Wang, G.G.; Shan, S. Review of metamodeling techniques in support of engineering design optimization. *J. Mech. Des.* **2007**, *129*, 370–380.
27. Gen, M.; Cheng, R. *Genetic Algorithms and Engineering Optimization*; John Wiley & Sons: Hoboken, NJ, USA, 2000; Volume 7.
28. ANSYS. Engineering Simulation Platform. Available online: http://www.ansys.com/products/platform (accessed on 25 June 2017).
29. MathWorks. NURBS Toolbox by D.M. Spike. Available online: https://se.mathworks.com/matlabcentral/fileexchange/26390-nurbs-toolbox-by-d-m-spink (accessed on 10 June 2017).
30. SHARCNet. *ANSYS_Fluent, Standard k-ε Model*; SHARCNet: London, ON, Canada, 2016.
31. Launder, B.E.; Spalding, D.B. *Lectures in Mathematical Models of Turbulence*; Academic Press: London, UK; New York, NY, USA, 1972.
32. Stat-Ease-Inc. *Design-Expert® Software*, version 10; Stat-Ease-Inc.: Minneapolis, MN, USA. Available online: http://www.statease.com/dx10.html (accessed on 15 September 2017).

APPENDIX

Table 7: Nomenclatures and their descriptions of variables used

Nomenclatures		Description	Units
H	-	Head of entering fluid at the inlet	*m*
ρ	-	Density of the fluid	kg/m^3
C_v	-	Constant coefficient to account loss in the nozzle	-
g	-	Gravitational acceleration	m/s^2
$v_{u1}, v_{u2}, v_{u3} and \ v_{u4}$	-	Peripheral velocity components at point 1,2,3 and 4 respectively of the rotor	*m/s*
ω	-	The rotational velocity of the rotor	*rad/s*
ϕ	-	Constant empirical coefficient that accounts loss inside rotor blade	-
R and r	-	Outer and inner radiuses of rotor	*m*
Q	-	Mass flow rate of fluid at inlet	*kg/s*
F and T	-	Force and torques on blades respectively due to hydraulic power	*N and Nm*
P_{in} and P_{out}	-	Output and input theoretical hydraulic powers respectively	*Watt (Nm/s)*
α and β	-	Actual and relative velocities angles from the tangents to the periphery	*rad*